

NASA Contractor Report 3381

Roller Skewing Measurements in Cylindrical Roller Bearings

Lester J. Nypan
California State University, Northridge
Northridge, California

Prepared for
Lewis Research Center
under Grant NSG-3065



Scientific and Technical
Information Branch

1981



Table of Contents

	Page
Summary	1
Introduction	2
Test Bearings	3
Lubrication	3
Method of Approach	3
Film Measurement and Error Estimation	5
Load and Bearing Misalignment	6
Test Program and Data Organization	7
Results and Discussion	7
Conclusion	12
References	13

PRECEDING PAGE BLANK NOT FILMED

Summary

Measurements of roller skewing in a 118 mm bore roller bearing operating at shaft speeds to 12000 rpm are reported.

High speed motion pictures of a modified roller were taken through a derotation prism to record skewing as the roller moved through loaded and unloaded regions of the bearing. Subsequent frame by frame measurement of the photographic film provided information on roller skewing. Radial and tangential skew amplitudes of .4 to .5 degrees were observed with .5 degree misalignment.

Introduction

Rollers in roller bearings may misalign or skew as they roll between the raceways (1)¹. This is controlled by small clearances between race shoulders and the roller which provide a restoring moment at the ends of the roller to restrain the roller from further skewing. In high speed turbine bearings the skewing and associated rubbing contact can lead to wear on the roller ends, increased skewing, and eventual failure (2). In some instances skewing and wear can be so severe that the roller turns and lodges within the separator pocket (3). This investigation was undertaken to gather experimental data for comparison with theoretical predictions of skewing magnitudes, and also for comparison of one roller bearing design with future improved designs. The investigation reports skewing behavior of a 1.15 length to diameter ratio roller in 118 mm bore roller bearings of 0.18 and 0.21 mm (0.0073 and 0.0083 in.) clearance operating with a 4450 N (1000 lb) radial load at shaft speeds of 4000, 8000, and 12000 rpm with outer race misalignment of 0, 0.25, 0.5, -0.5 degree.

ORIGINAL PAGE IS
OF POOR QUALITY

¹Numbers in brackets designate References at end of paper.

Test Bearings

Two test bearings were used in the investigation. They were representative of aircraft gas turbine engine roller bearings and had PWA 541043D markings. The bearings' original out-of-round outer rings were replaced with cylindrical rings having radial clearances of 0.18 and 0.21 mm (0.0073 and 0.0083 in). These radial clearances were calculated as the difference between the average of the outer race measured maximum and minimum inner diameters and the inner race nominal raceway diameter plus two roller diameters. Table I gives dimensions of the bearings used.

Lubrication

While the inner race had grooves for under race cooling and drilled passages for cage and roller lubrication, these were not used. Oil was sprayed onto the rollers through two jet pipes at a total flow rate of $1.8 \times 10^{-3} \text{ m}^3/\text{min}$ (0.47 gpm). The oil used was a 5-centistoke neopentylpolyol (tetra) ester. This is a type II oil which conforms to specification MIL-L-23699. Test bearing inlet oil was heated and controlled to 339°K (150°F).

Method of Approach

Roller skewing was measured from photographs of a modified roller in a bearing operating at shaft speeds to 12000 rpm. Figure 1a is a schematic of the test shaft assembly. A 16 mm Fastax WF4 camera was used with synchronized Xenon flash tube illumination to photograph a 32 x 24 mm (1.25 x .94 in) area of the bearing at up to 8000 frames per second. The derotation prism apparatus described in ref. (4-7) was used to maintain this area centered on the modified roller and to follow this roller as it orbited through 360 degrees within the bearing. The

32 x 24 mm (1.25 x .94 in) area photographed in 16 mm format included a segment of a fixed outer race protractor, a segment of an inner race protractor, a segment of the roller bearing separator, the modified roller and portions of adjacent rollers. Figure 1b is an enlargement of a data photograph. At the 12000 rpm shaft speed photographs of the modified roller were obtained at 4 to 5 degree intervals as observed on the outer race protractor. The inner race protractor permitted cage to shaft speed ratio determinations. Two to three hundred photographs could usually be obtained before the energy storage capacitors discharged. This permitted photographs of three to four revolutions of the separator and roller orbit to be obtained.

Camera speeds of 6000 frames per second were often used for the 8000 and 4000 rpm bearing speeds with proportionate adjustments to photographic intervals within the bearing and number of separator revolutions available for analysis.

The roller modification to permit frame by frame roller orientation measurements incorporated a 3.18 mm (0.125 in) diameter x 1.59 mm (0.626 in) deep counterbore recess to help to identify the roller center in the photographs. A pin 1.27 mm (0.050 in) in diameter by 6.35 mm (0.250 in) in length is extended out along the roller axis from the roller end. Figure 2 is a photograph of a modified roller.

In the data photographs, the end of the pin appeared superimposed on the image of the counterbore. By measuring radial and tangential distances from the counterbore image center to the pin image center and dividing by the pin length the tangents of the roller orientation angles are obtained. Measurements were made so that the roller orientation angles are radially outward from the bearing center and tangent to the roller path. As the camera axis was oriented along the bearing center line the pin image center is always offset radially on the counterbore image by the "camera angle". The radial roller skew angle appears superimposed on the constant camera angle. Radial and tangential roller skew

angles are thus obtained as a function of roller location within the bearing.

Film Measurement and Error Estimation

A Vanguard Instrument Corporation Motion Analyzer was used to project the films for frame by frame measurement. A template with concentric circles was used to align a Gerber Scientific Instruments measuring and digitizing instrument first on the image of the pin end, and then on the image of the counterbore. Four digit measurements of the tangential and radial coordinates of the circle centers were automatically punched on computer cards at each alignment. A computer program calculated differences, applied scale factors and prepared output to drive a Calcomp 936 plotter to graph the data.

An estimate of the uncertainty and possible errors inherent in the measurement system was obtained by repeatedly measuring the same film frame. These measurements were then processed in the same manner as regular data measurements made on frames taken at 5 degree increments of roller orbit within the bearing. Figure 3 shows the apparent variation in skew angles due solely to the film measurement system. The test indicates that the maximum deviation from the mean of 72 readings was 0.42 degrees. The standard deviation from the mean was 0.028 degrees in radial skew and 0.037 degrees in tangential skew. When the test measurements were subjected to the Fourier analysis described under Results and Discussion, Figure 3F resulted. It may be observed that amplitudes of up to 0.12 degrees are present. The limitations of the measurement system should be considered in evaluating the roller skew data presented in this report.

Load and Bearing Misalignment

A 4450 N (1000 lb) load was used throughout most of the investigation. This was applied to the test bearing by a cable loop over the test bearing as may be seen in Fig. 1a. The outer race protractor was positioned so that 0 (360) degrees was centered under the cable loop. As the derotation prism and camera viewed the protractors and bearing the protractor degree scale increased in a clockwise direction. Due to bearing clearance rollers entered the loaded zone at about 340° and left it at about 20°.

The misalignment of the outer race relative to the inner race was measured with a dial indicator on a bar bolted to the end of the test shaft. The bar was perpendicular to the shaft center line. Measurements were made by indicating on a machined surface of the test bearing housing. This machined surface of the housing was also perpendicular to the shaft center line when the zero misalignment cases were set up. What is referred to as positive misalignment in this report was produced by forcing the housing at 90° towards the prism and camera while simultaneously forcing the housing at 270° away from the prism and camera by turning nuts on studs extending from the test machine frame. Back-up nuts were kept tight to keep the housing positively positioned. The shaft was turned over by hand and indicator readings written down at 45° intervals over a shaft revolution. Nuts forcing misalignment and back-up nuts were readjusted until the desired misalignment condition was attained. Negative misalignment was produced in a similar fashion by using the nuts and studs at 90° and 270° to force the 90° housing location away from the prism and camera while forcing the 270° housing location towards the prism and camera.

By adjusting the nuts constraining the housing at 90 and 270 degrees the outer race was pivoted about an axis through 0 and 180 degrees on the outer race protractor. Misalignment was maximum at 90 and 270 degrees and minimum at 0 and 180 degrees. Rollers entered the loaded zone at

about 340 degrees with the misalignment decreasing, passed the most heavily loaded point at 0 degrees with the raceway surfaces most nearly parallel, and exited with roller to raceway contact force decreasing as the roller encountered increasingly non-parallel raceway surfaces.

While it had originally been proposed to study misalignment of 0, 0.25 and 0.50 degrees, a reversed misalignment of -0.50 degrees was added to the test program to determine the effect of a reversal of misalignment on roller skewing behavior and the measurement system.

Test Program and Data Organization

The chronological sequence of tests may be followed through the dates and film sequence numbers identifying films and data obtained from the films. Testing began with the 0.21 mm (0.0083 in.) clearance bearing with 0 degree misalignment with films being taken at 4000, 8000, and 12,000 rpm under the 4,450 N (1,000 lb) load. Table 2 lists data presented in the report, and summarizes the organization and figure identification system for the bearing clearance, misalignment, and speed cases studied.

As indicated in Table 2, Figures 4 through 7 are results obtained with the 0.18 mm (0.0073 in.) clearance bearing. Figures 4a, b, c are data at 0 degree misalignment and 4000, 8000, and 12,000 rpm. Figures 5a, b, c; 6a, b, c; and 7a, b, c are results at 0.25, 0.50, and -0.50 misalignment. As more than one roller orbit or revolution of the roller through the bearing could sometimes be read from the film taken for each of these figures a further number is added as 5b-1, 5b-2, to identify the revolution or reading of the film. Figures 8 through 11 show similar information for the 0.21 mm (0.0083 in.) clearance bearing.

Results and Discussion

To plot radial and tangential roller skew angle simultaneously on the same axes without overlap, the camera angle

of about 4.7 degrees was plotted along with the radial skew angle. The camera angle appears in the data photographs because the roller center is radially distant from the bearing-camera center line by the bearing pitch radius. Radial roller skew motions are superimposed on the camera angle.

A fast Fourier transform (FFT) program was used to estimate the frequency components of the data. The FFT program requires N equally spaced data points and N must be a power of 2. These data points were obtained by linearly interpolating 128 points over the 360 degrees of roller orbit measured in each film. Plots of tangential and radial skew angle amplitude absolute value (degrees) as a function of frequency are presented on pages facing the original data figures and are numbered with the original figure number followed by F. Phase (degrees) is also plotted.

Output from the FFT program was manipulated so that the amplitudes are the square root of the sum of the squares of the a_i and b_i coefficients of the Fourier series sine and cosine terms for each frequency. The phase angles are the arc tangent of the a_i/b_i coefficients. Fourier analysis figures are plotted so the first amplitude is the average value of the data in the original figure, the second amplitude is the amplitude of a sine function of 360 degree roller orbit period, the third amplitude is the amplitude of a sinusoid of two cycles in the 360 degrees of roller orbit, etc.

The average value of the radial skew data includes the camera angle. In order to make this point plot together with the other roller skew amplitudes of 0.4 degree or less, this first point was plotted at a tenth of its true value so that the first radial skew amplitude plotted at 0.47 degrees indicates an average radial skew plus camera angle of 4.7 degrees.

Figure 4a shows a result obtained with the 0.18 mm (0.0073 in.) clearance bearing at 0° misalignment and 4000 rpm. It was plotted from 202 frames taken every

1.8 degrees of roller position within its orbit. While any reading could be in error by as much as 0.4 degrees, the errors are probably of the order of 0.04 degrees as indicated in the paragraphs on Film Measurement and Error Estimate. An average skew angle is evidently present along with amplitudes associated with a number of frequencies. Figure 4a and 4aF together indicate a tangential skew averaging -0.33° over the roller orbit, a one-cycle-per-orbit skew amplitude of 0.05° , a 2-cycle-per-orbit skew amplitude of 0.02° , a 3-cycle-per-orbit skew amplitude of 0.05° , a 4-cycle-per-orbit skew amplitude of 0.13° , an 8-cycle-per-orbit skew amplitude of 0.08° , and a 12-cycle-per-orbit skew amplitude of 0.28° . The radial skew plots indicate a camera angle plus average radial skew angle of 10 times 0.47 or 4.7° ; 2, 3, 4, and 12-cycle-per-orbit amplitudes of 0.04 , 0.03 , 0.02 , and 0.31° . In view of the 0.12° amplitude noted in repeated measurements on the same film frame described under Film Measurement and Error Estimation amplitudes less than 0.12 may not be significant.

The 12-cycle-per-roller-orbit frequency which appears strongly in all the data corresponds to the roller frequency as the ratio of outer raceway circumference to roller circumference is 12.42. This is the roller to cage speed ratio. This investigator has not been able to make use of information in the phase angle data.

Figures 4b, and 4c show the effect of increasing speed at 0° misalignment. The amplitude at 4 cycles per orbit continues to be evident in the tangential skew, and the sharp peak at 12 cycles that was evident in Figure 4a broadens to include 11 and 14 cycles.

Figures 5a, 5b-1, 5b-2, 5c-1, and 5c-2 are results at 0.25° misalignment. A radial skew amplitude of about 0.18° with a 1-cycle-per-roller-orbit frequency is evident in all of these Figures. Figures 5b-1, 5b-2, 5c-1 and 5c-2 show differences in consecutive revolutions. The amplitude associated with the roller frequency is up to 0.39° in

Figure 5a and extends from 11 to 15 cycles-per-roller-orbit with smaller amplitude in Fig. 5c-2.

Figures 6a, 6b, 6b-2, 6c-1, 6c-2, and 6c-3 show results with the bearing misaligned by 0.5° . The radial skew amplitude is 0.33 to 0.43° at one cycle per orbit. The original data plots resemble a negative sine function. Radial and tangential skew amplitudes associated with the roller frequency again appear to broaden in frequency extent as speed increases. It was not possible to read data beyond 320° in the second roller orbit for Fig. 6b-2, and a Fourier analysis was not obtained for this figure. Some lower frequency components appear consistently in the 3 roller orbits through the bearing that are followed through Figures 6c-1, -2, and -3.

Figures 7a-1, 7a-2, 7b-1, 7b-2, 7c-1, and 7c-2 show the result of a reversed misalignment of 0.5° . Radial skew amplitude are typically 0.47° at one cycle per orbit, and the original data plots resemble a positive sine function of one period per orbit. Comparing this one cycle per orbit information with the one cycle per orbit radial skew information in Figures 5 and 6, it seems that the one cycle per orbit radial skew is the misalignment of the outer race which is being followed by the roller. A noticeable amplitude in both radial and tangential skew at 4 cycles per orbit is present in a number of these figures. It was possible to follow 2 orbits at each of the 8000 and 12,000 rpm speed cases. There appear to be differences in roller behavior from orbit to orbit. Successive revolutions in Figure 7a-1 and 7a-2 differ as the amplitude of one cycle per orbit radial skew is more apparent in Figure 7a-2. As the outer ring circumference is not an integer multiple of the roller circumference, the roller may not enter the loaded zone with the same skew angles on successive revolutions.

Figure 8a, 8b, and 8c show results for the 0.21 mm (0.0083 in.) clearance bearing with 0° misalignment at the 4000, 8000, and 12,000 rpm speeds. There appears to be no significant amplitude at low frequencies, but a skewing amplitude of 0.19 to 0.26° at the 12 cycle per roller orbit frequency.

Figures 9a, 9b, and 9c show results for the larger clearance bearing with 0.25° misalignment. There is radial skew amplitude of 0.1 to 0.23° at one-cycle-per-roller orbit. Both tangential and radial skew amplitudes of 0.18 to 0.26° are present at the 12 cycles-per-roller orbit frequency. Some broadening of the 12 cycle appears as speed increases.

Figures 10a, 10b-1, 10b-2, 10c-1, 10c-2, 10c-3, and 10c-4 show the effect of 0.5° misalignment. A one-cycle-per-orbit amplitude ranging from 0.18 to 0.45° is present in radial skew angle with the original data again resembling minus sine function. A 12-cycle-per-orbit amplitude ranging from 0.12 to 0.36° is present. The 4000 rpm speed case has the highest amplitude and most sharply defined 12 cycle frequency. As speed increases the 12 cycle amplitude seems to decrease, and broadens to extend to lower frequencies. Figures 10b-1 and 10b-2 at 8000 rpm show some variation in consecutive revolutions. Figures 10c-1, 10c-2, 10c-3, 10c-4, 10c-5, and 10c-6 at 12,000 rpm further indicate differences from revolution to revolution.

Figures 11a, 11b-1, 11b-2, 11c-1, 11c-2, and 11c-3 show the result of a reversal of the 0.5° misalignment. Radial skew amplitudes of 0.39 to 0.55° appear at one-cycle-per-roller orbit with the original data again resembling a positive sine function. Tangential and radial skew amplitudes of 0.12 to 0.32° appear to be associated with the roller frequency. Figure 11a appears to indicate there may be a tangential and radial skew amplitude of 0.12° at 20-to 24-cycle-per-roller orbit frequency. This may be a 2 times a roller revolution skewing behavior that could be seen only in 4000 rpm speed studies as the camera frame rate gives data at about 2, 4, and 6 degrees of roller orbit at 4000, 8000, and 12,000 rpm shaft speeds. This limits the frequencies

observable in the data. This frequency does not appear as prominently in other 4000 rpm speed cases. Data from consecutive revolutions again appears to differ slightly. Figures 11c-2, and 11c-3 show the effect of missing frames over 90 to 160° of roller orbit. The film was not measureable over this sector of the bearing, but could provide information over the rest of the roller orbit. The missing frames are interpolated as a straight line in the FFT program which makes the frequency analysis information difficult to evaluate.

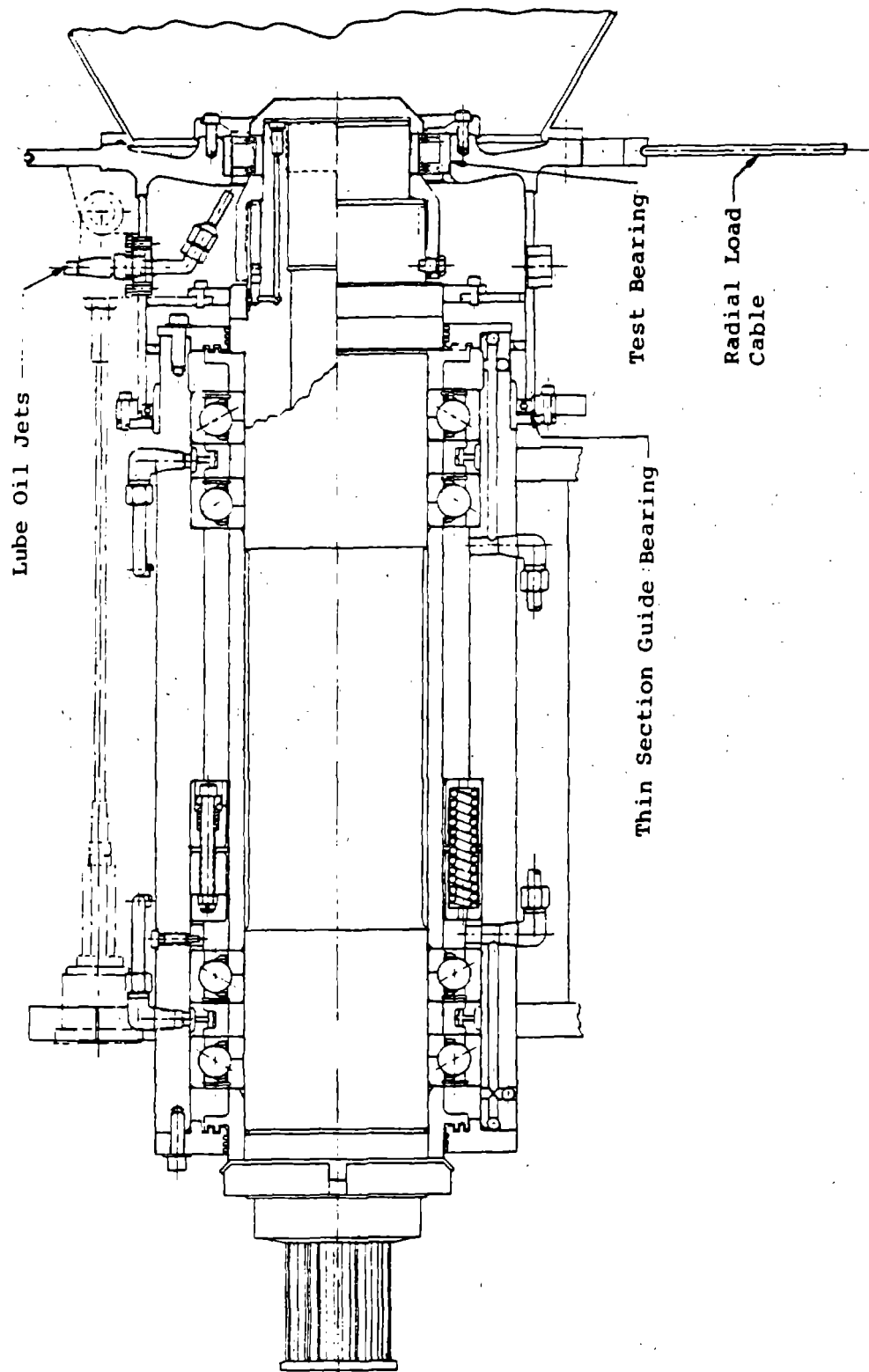
Conclusion

Radial skew amplitudes of 0.4 to 0.5° at the roller orbit frequency were observed with 0.5° bearing misalignment. Radial and tangential skew amplitudes of 0.4° associated with the roller frequency were observed. These generally decreased in amplitude and extended in frequency at higher speeds. The 0.21 mm (0.0083 in.) larger clearance bearing generally had slightly smaller roller skew amplitudes than the 0.18 mm (0.0073 in.) clearance bearing. Differences in roller skewing are apparent in successive orbits of the roller.

Further work which should be undertaken is the investigation of roller skewing with misalignment oriented so that the loaded zone of the bearing includes raceway surfaces of maximum misalignment.

References

1. Savage, M. and Loewenthal, S.H., "Kinematic Stability of Roller Pairs in Free-Rolling Contact", NASA Technical Note D-8146, 1976.
2. Savage, M. and Pinkston, B.H., "Roller Bearing Geometry Design", NASA CR-135082, October 1976.
3. Greby, D.F., "What Turbine Technology Is Teaching Us About High-Speed Roller Bearings", Machine Design, April 30, 1970, pp 229-234.
4. Signer, H.R., "Experimental Ball Bearing Dynamics Study", NASA CR-134528, October 1973.
5. Nypan, L.J., "Ball to Separator Contact Forces in Angular Contact Ball Bearings Under Thrust and Radial Loads", NASA CR-2976, April 1978.
6. Nypan, L.J., "Roller to Separator Contact Forces and Cage to Shaft Speed Ratios in Roller Bearings", NASA CR-3048, September 1978.
7. Nypan, L.J., "Measurement of Separator Contact Forces in Ball Bearings Using a Derotation Prism", Journal of Lubrication Technology, Trans. ASME, Series F, Vol. 101, No. 2, April 1979, pp. 180-189.



ORIGINAL PAGE IS
OF POOR QUALITY

Figure 1a Schematic of Shaft Assembly

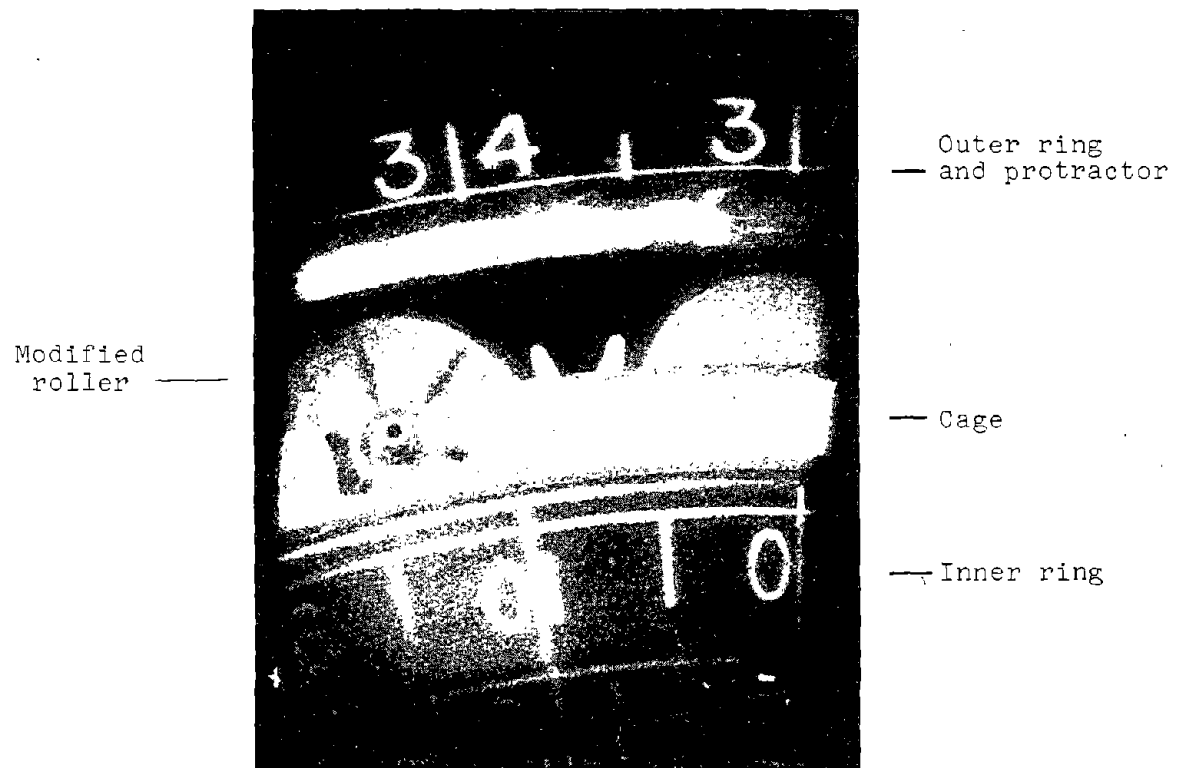


Figure 1b Enlargement of Data Photograph



Figure 2 Modified Roller

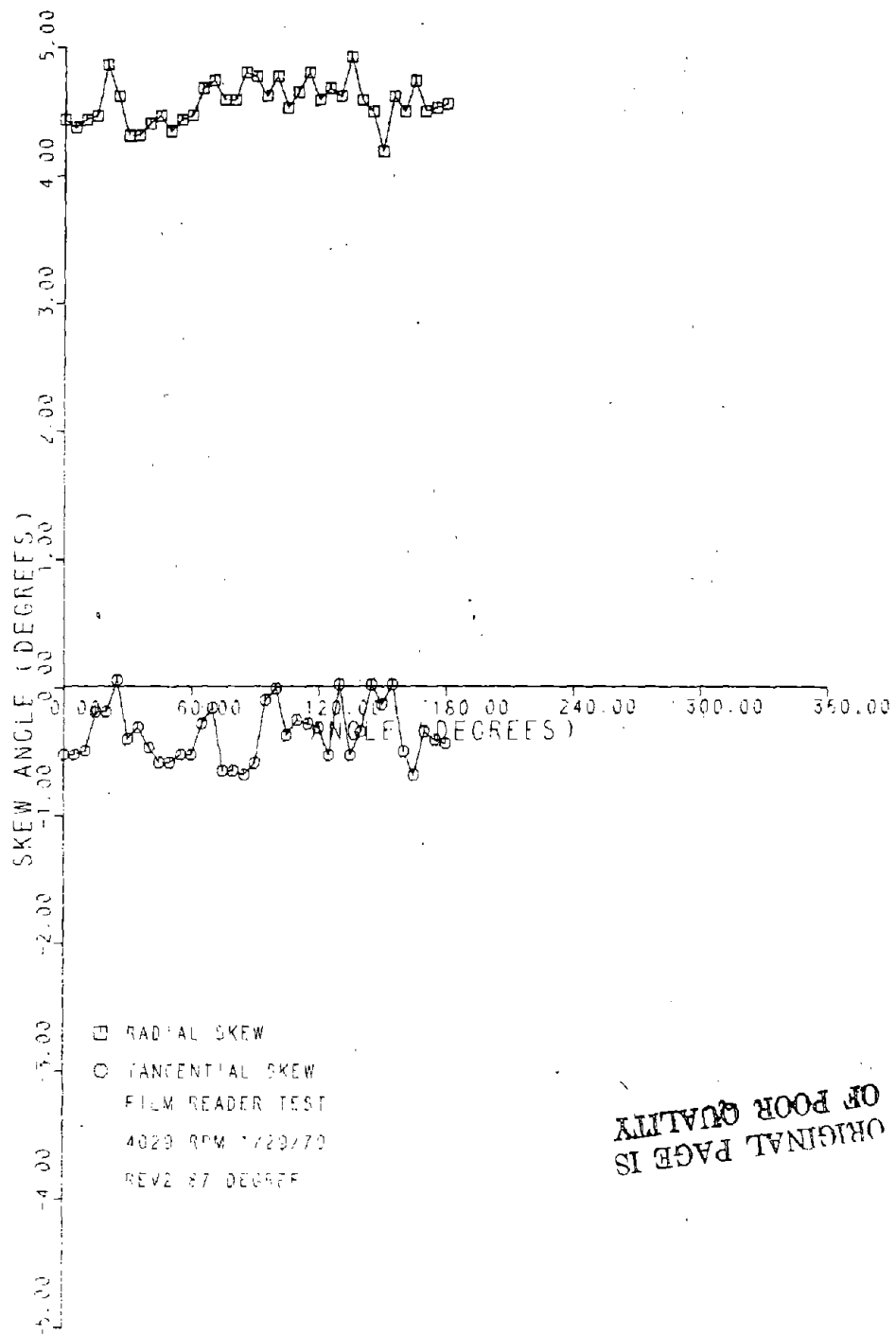


Figure 3 Variability in Skew Angle
Due to Film Measurement

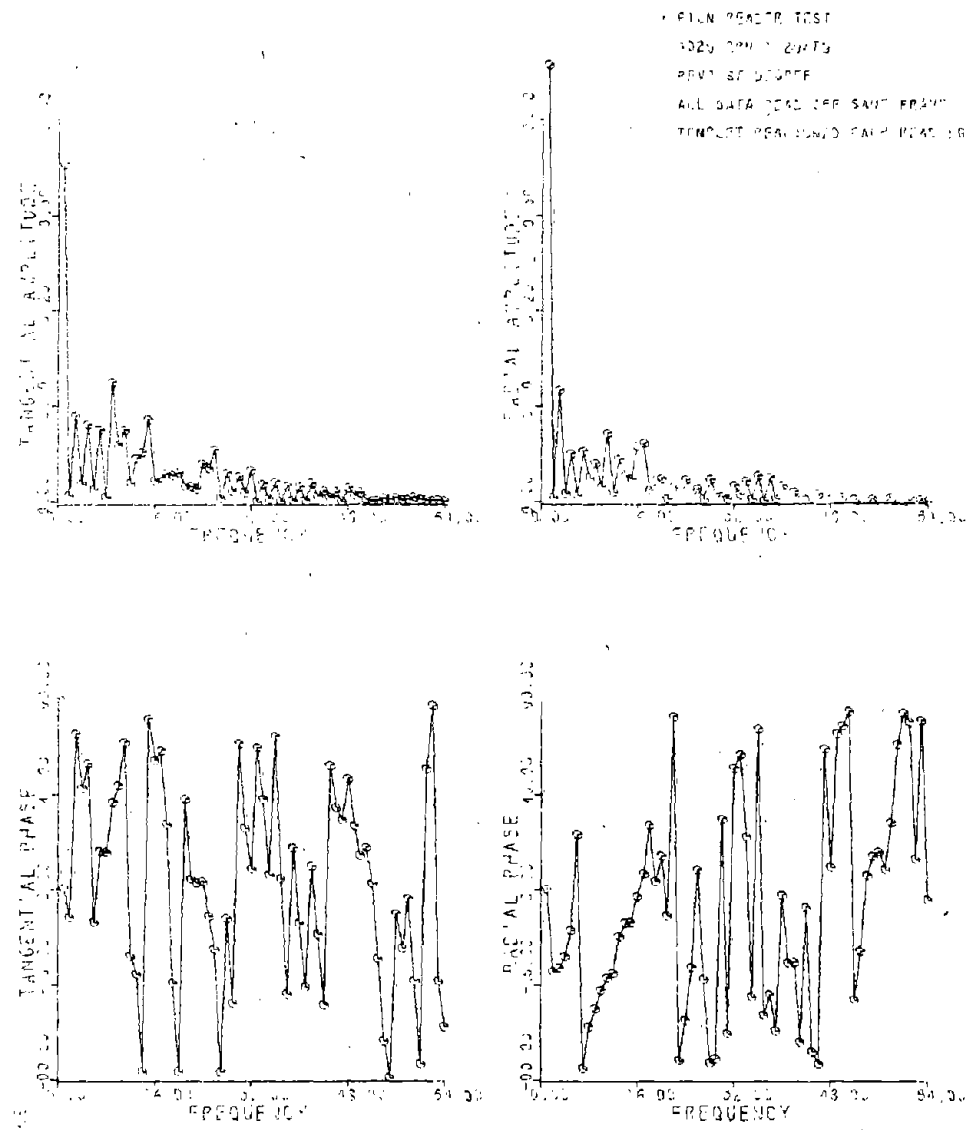


Figure 3F Fast Fourier Transform of Data in Figure 3

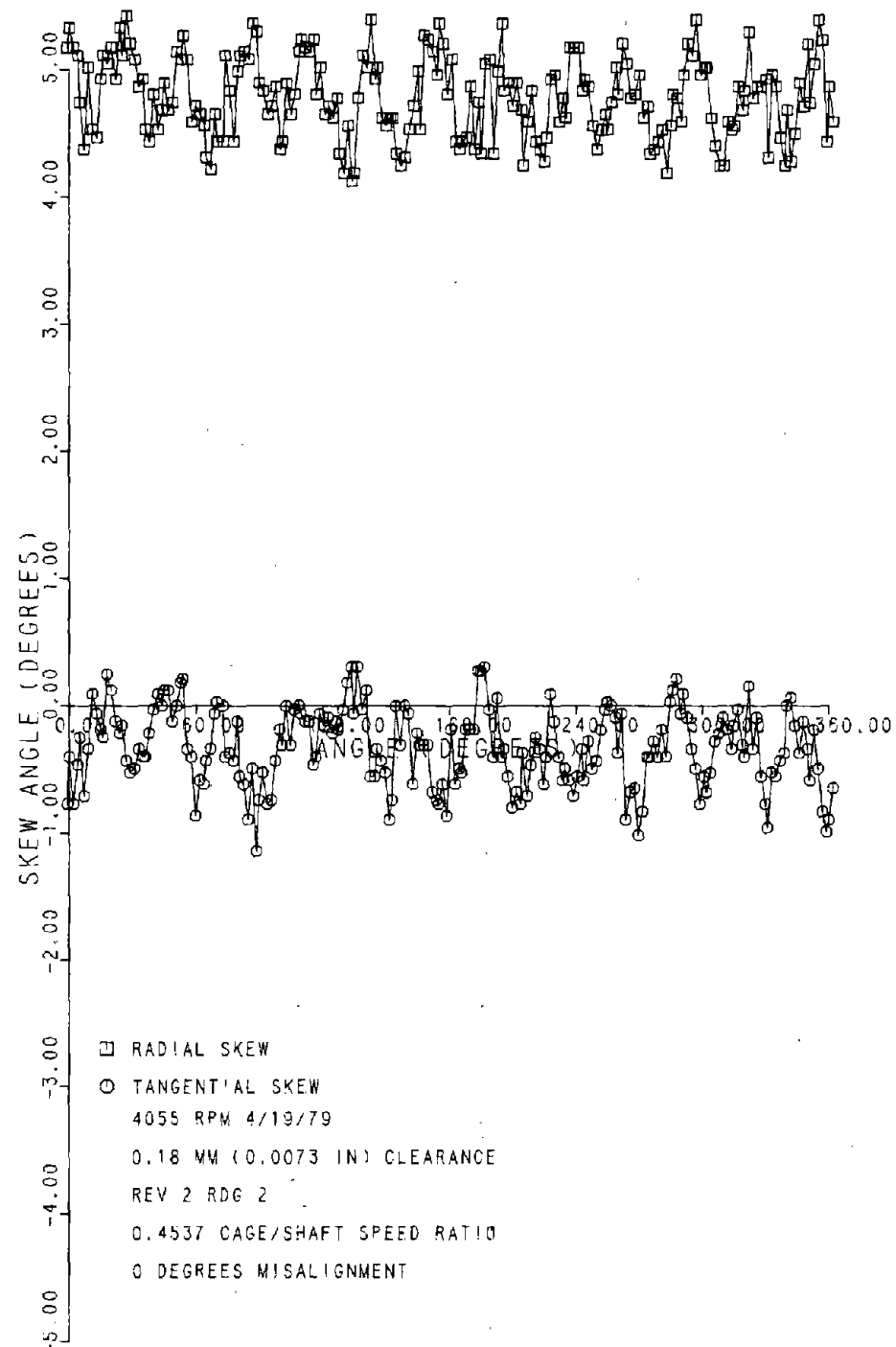
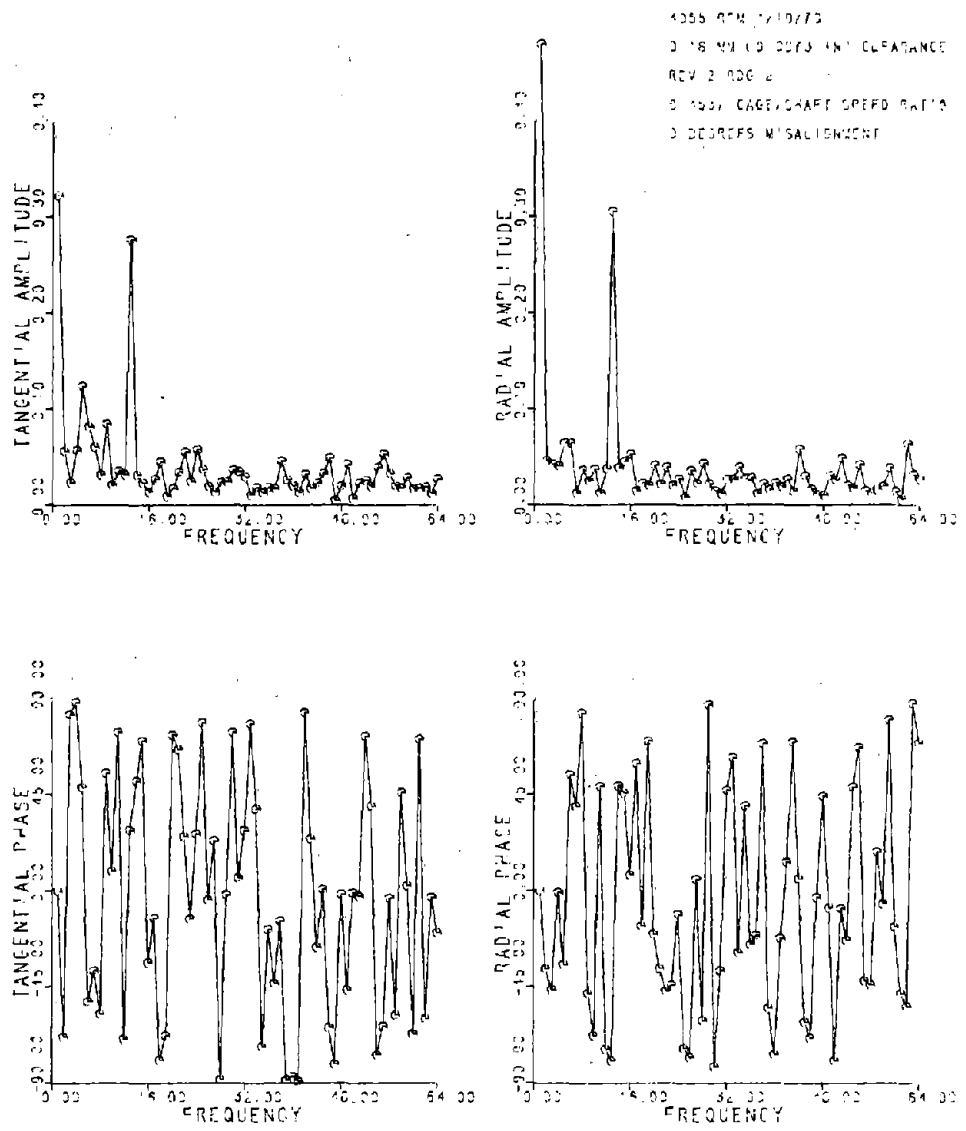


Figure 4a Roller Skew, 0.18 mm Clearance
Bearing, 0° Misalignment



ORIGINAL PAGE IS
 OF POOR QUALITY

Figure 4aF Fast Fourier Transform of
 Data in Figure 4a

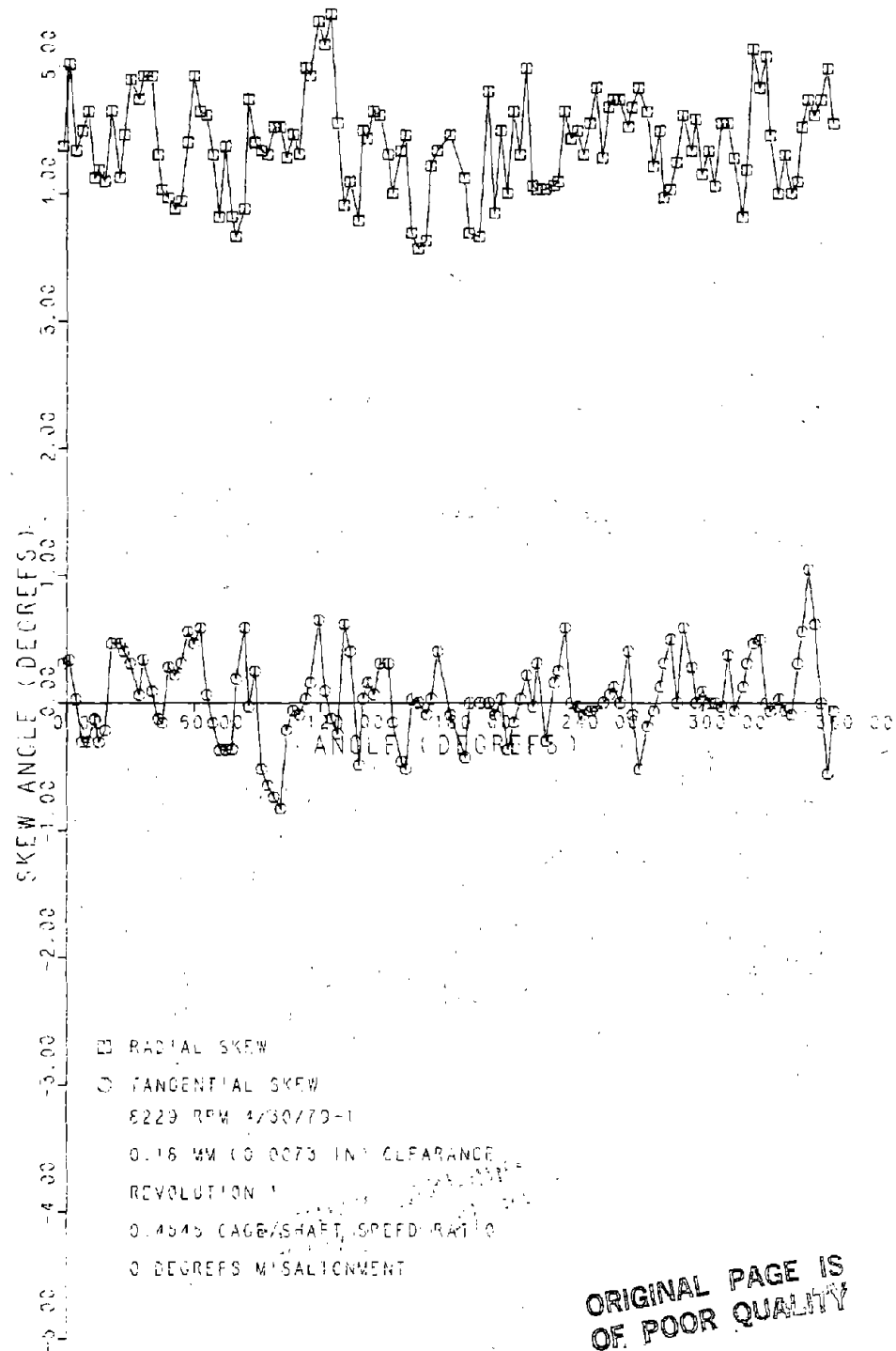


Figure 4b. Roller Skew, 0.18 mm Clearance
Bearing 0° Misalignment

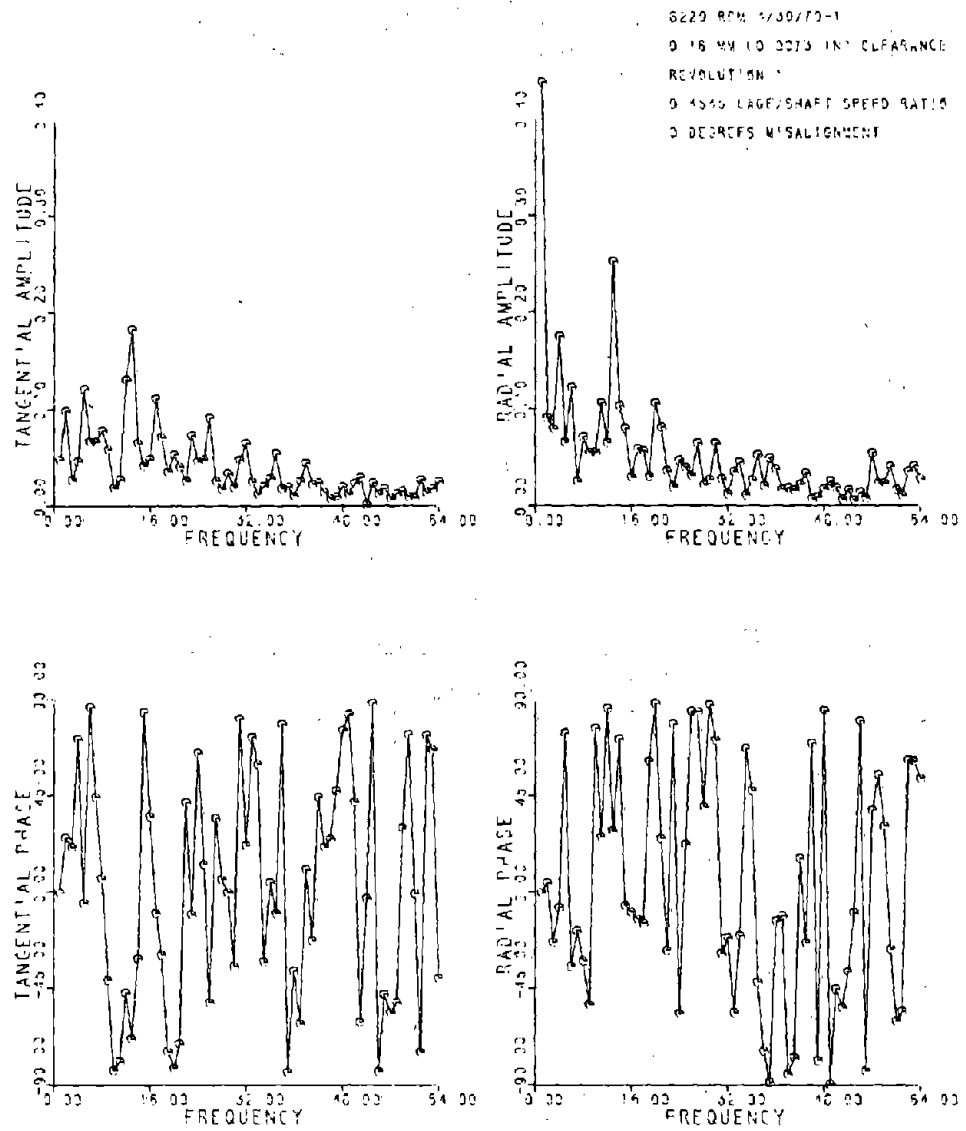


Figure 4bF Fast Fourier Transform of Data in Figure 4b

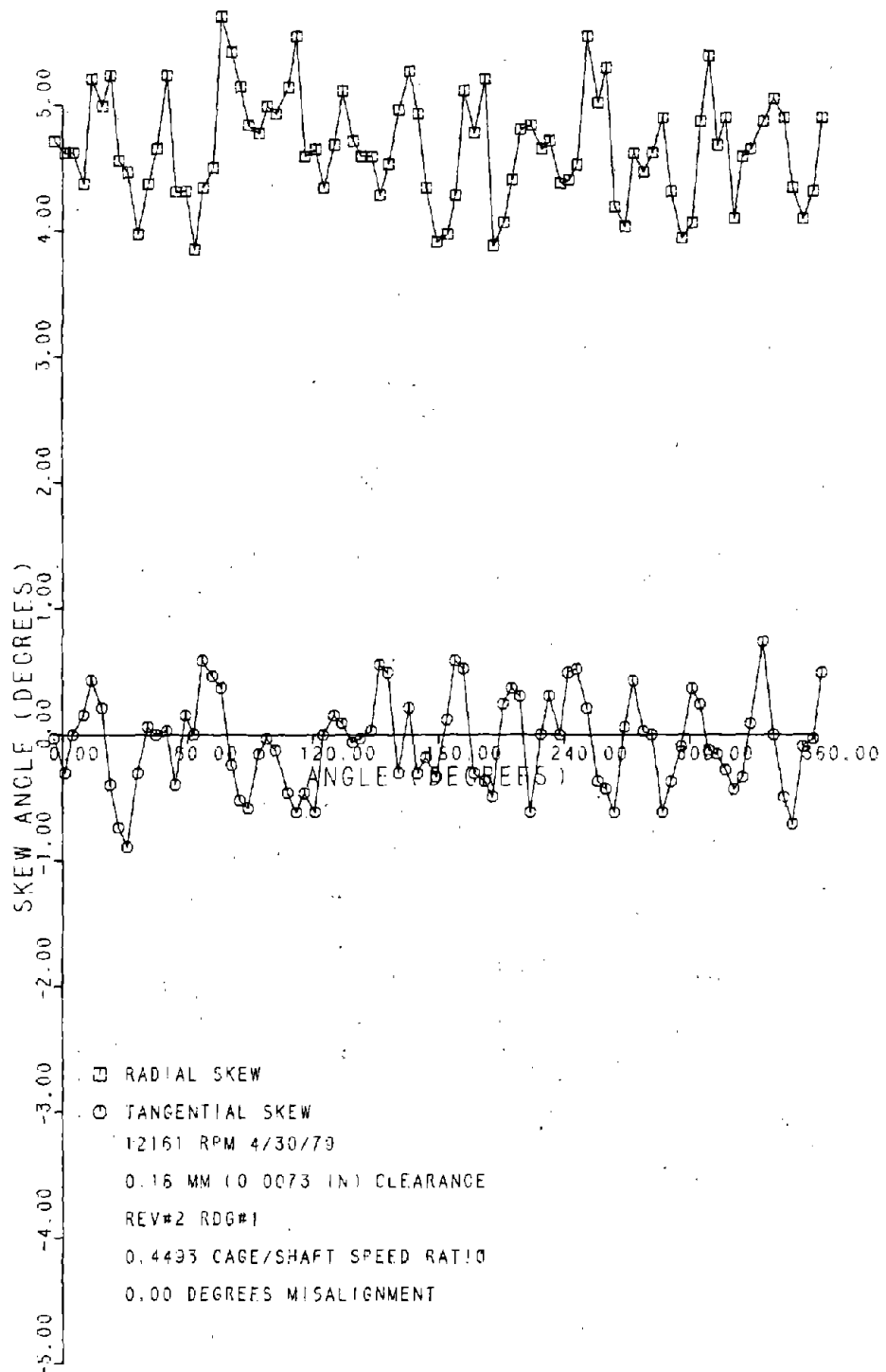


Figure 4c Roller Skew, 0.18 mm Clearance
Bearing, 0° Misalignment

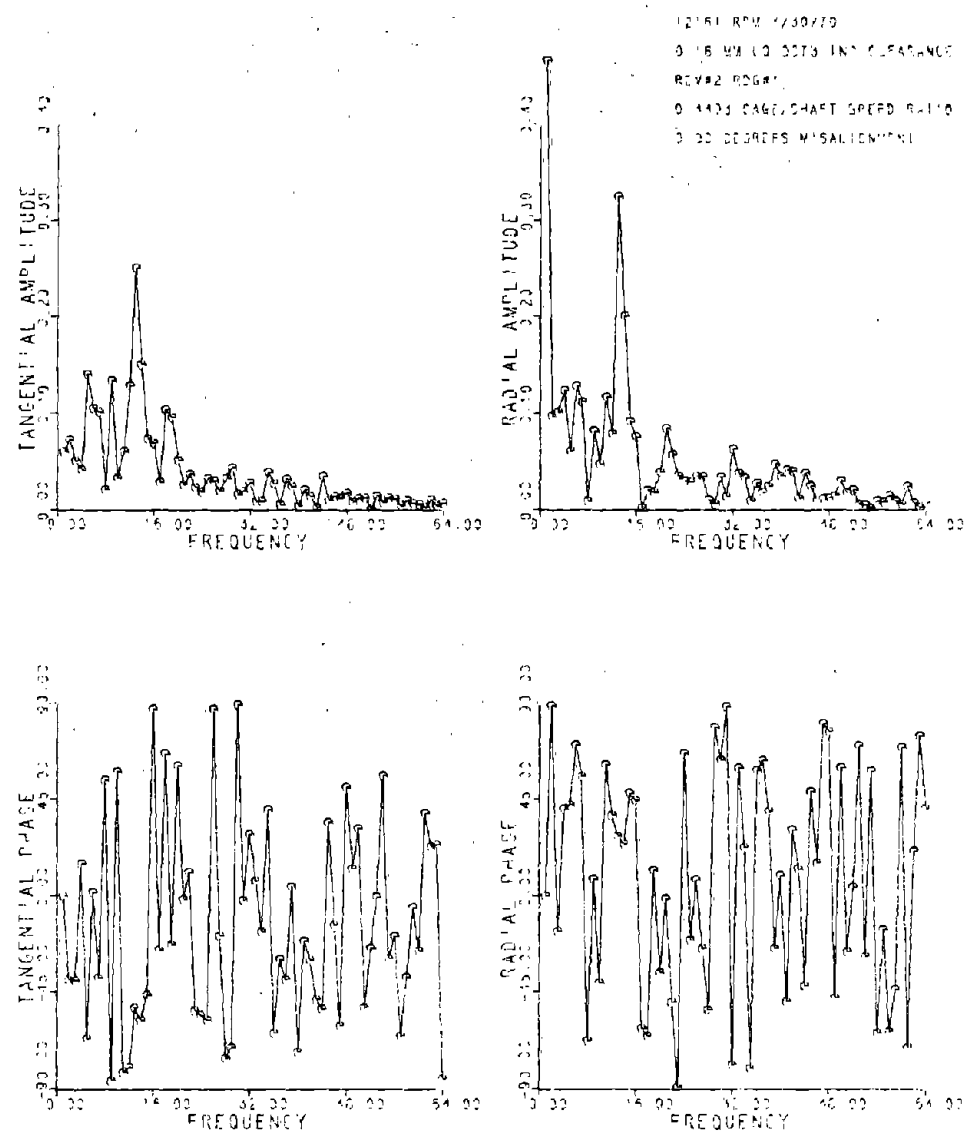


Figure 4cF Fast Fourier Transform of Data in Figure 4c

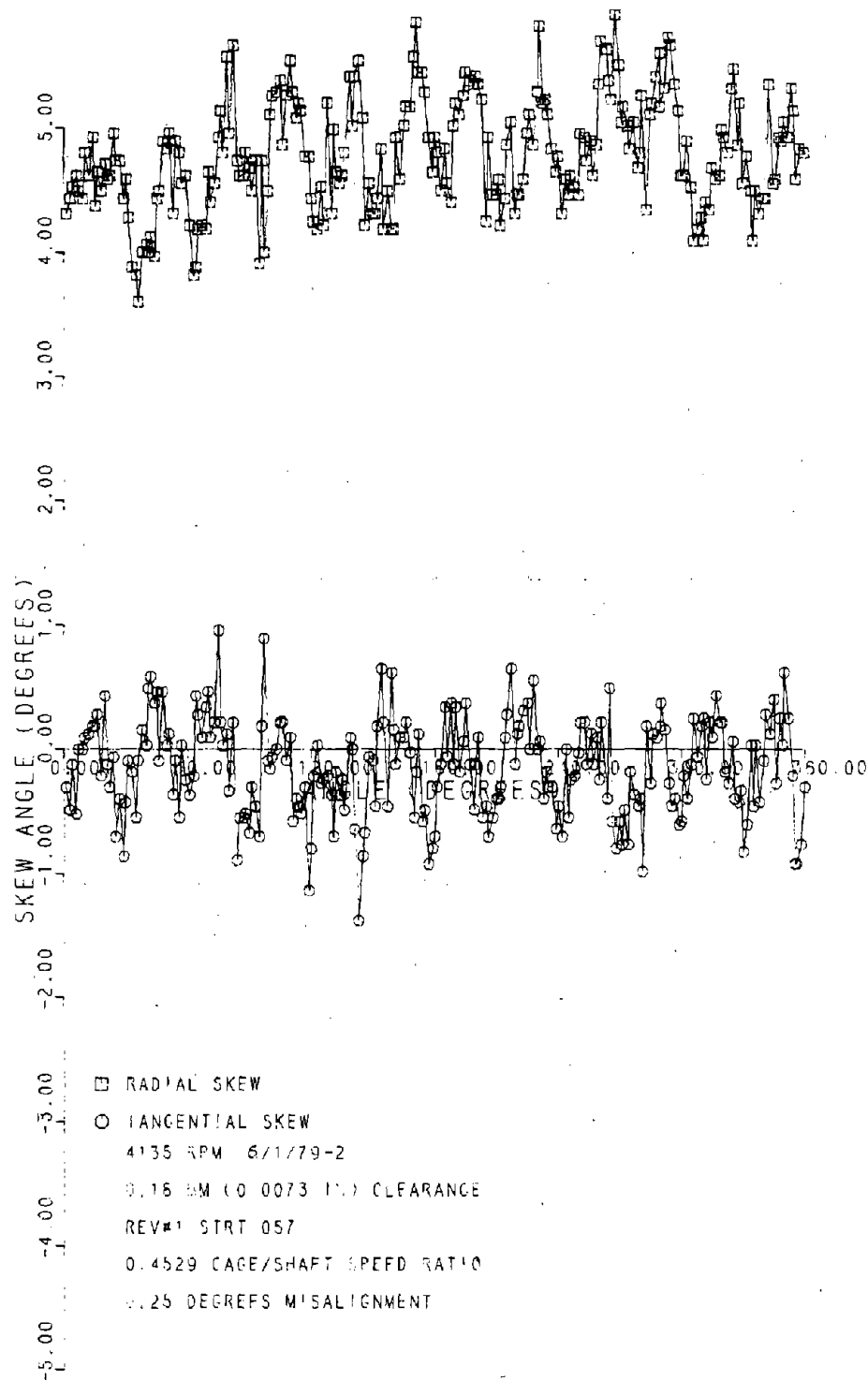


Figure 5a Roller Skew; 0.18 mm Clearance
Bearing, 0.25° Misalignment

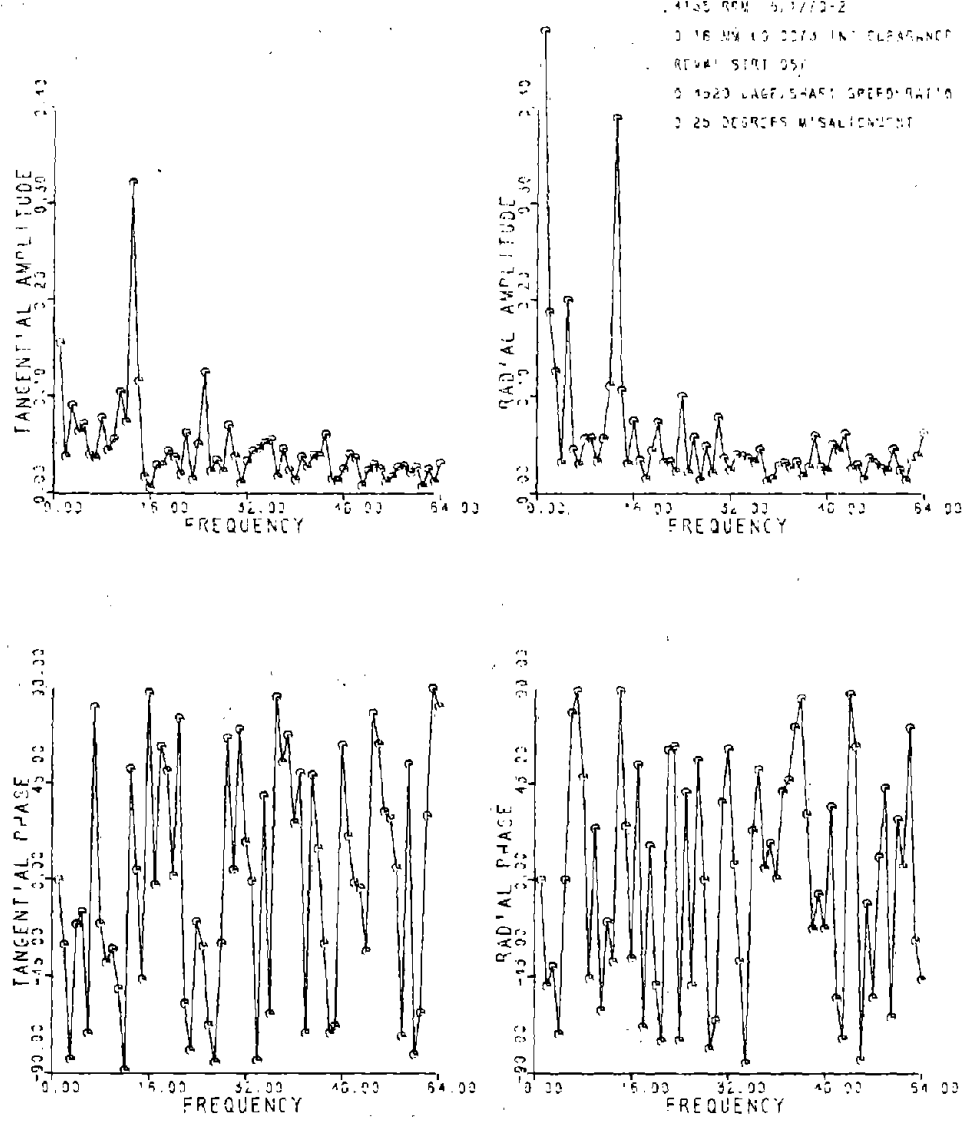


Figure 5aF Fast Fourier Transform of Data in Figure 5a

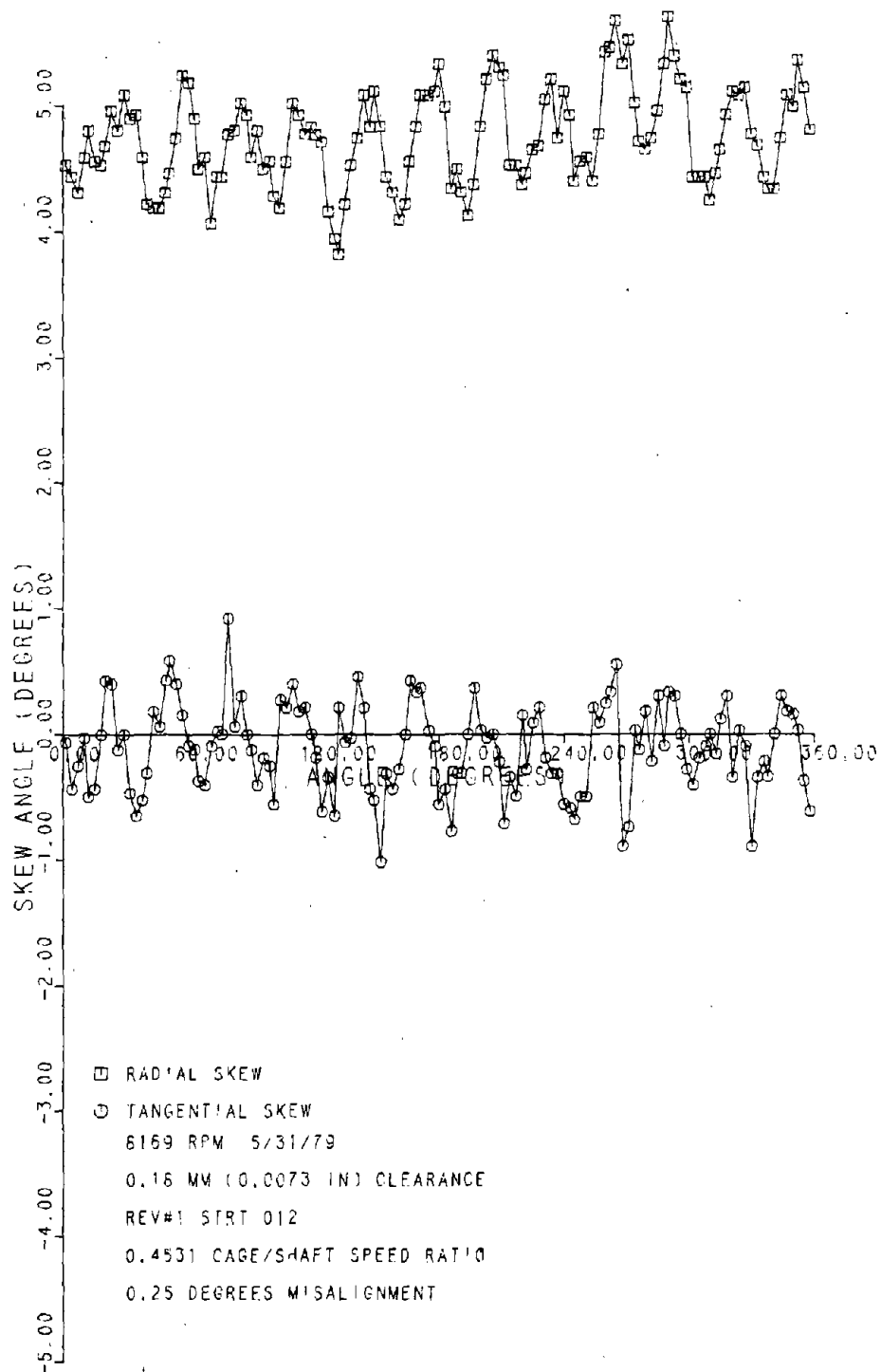


Figure 5b-1 Roller Skew, 0.18 mm Clearance
Bearing, 0.25° Misalignment

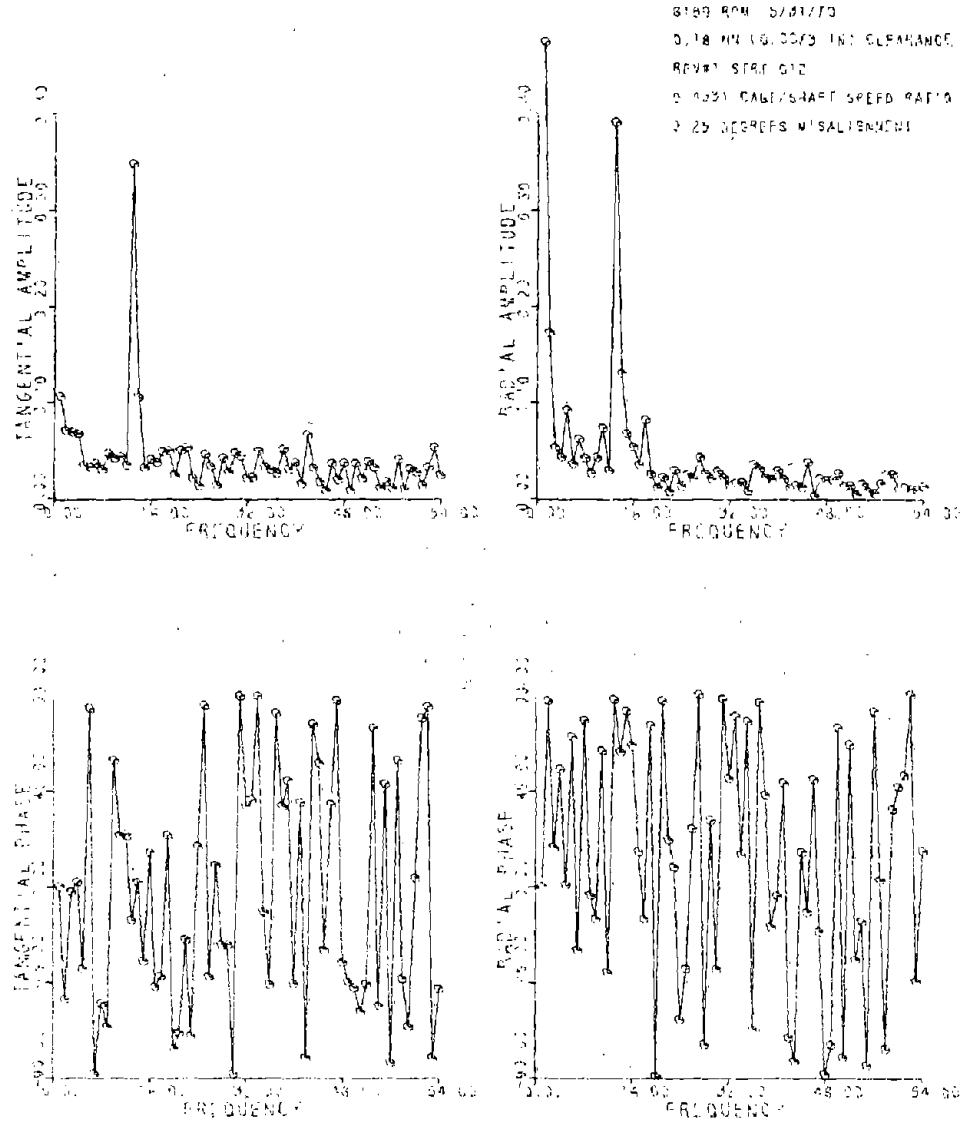


Figure 5b-1F Fast Fourier Transform of Data in Figure 5b-1

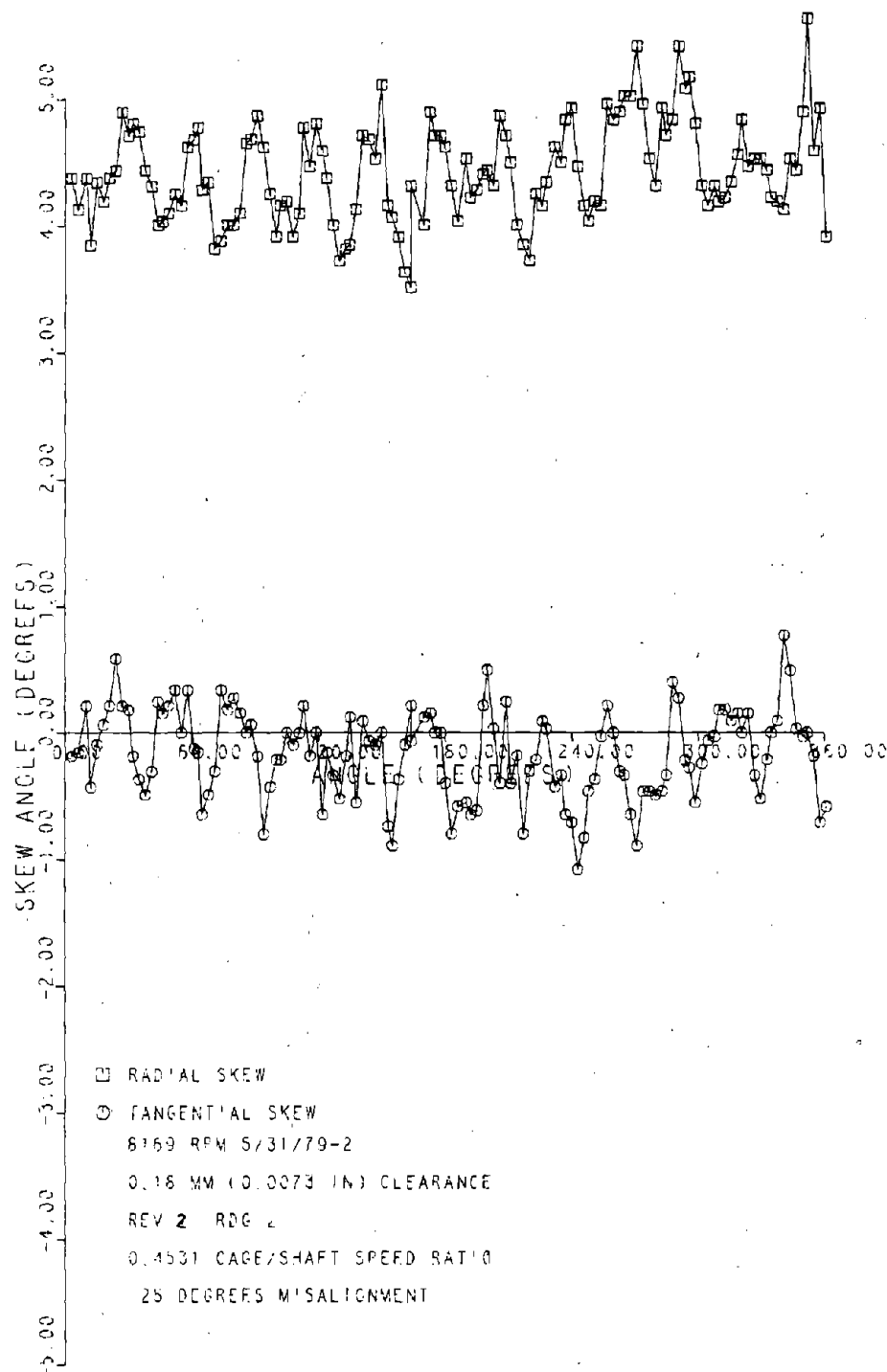
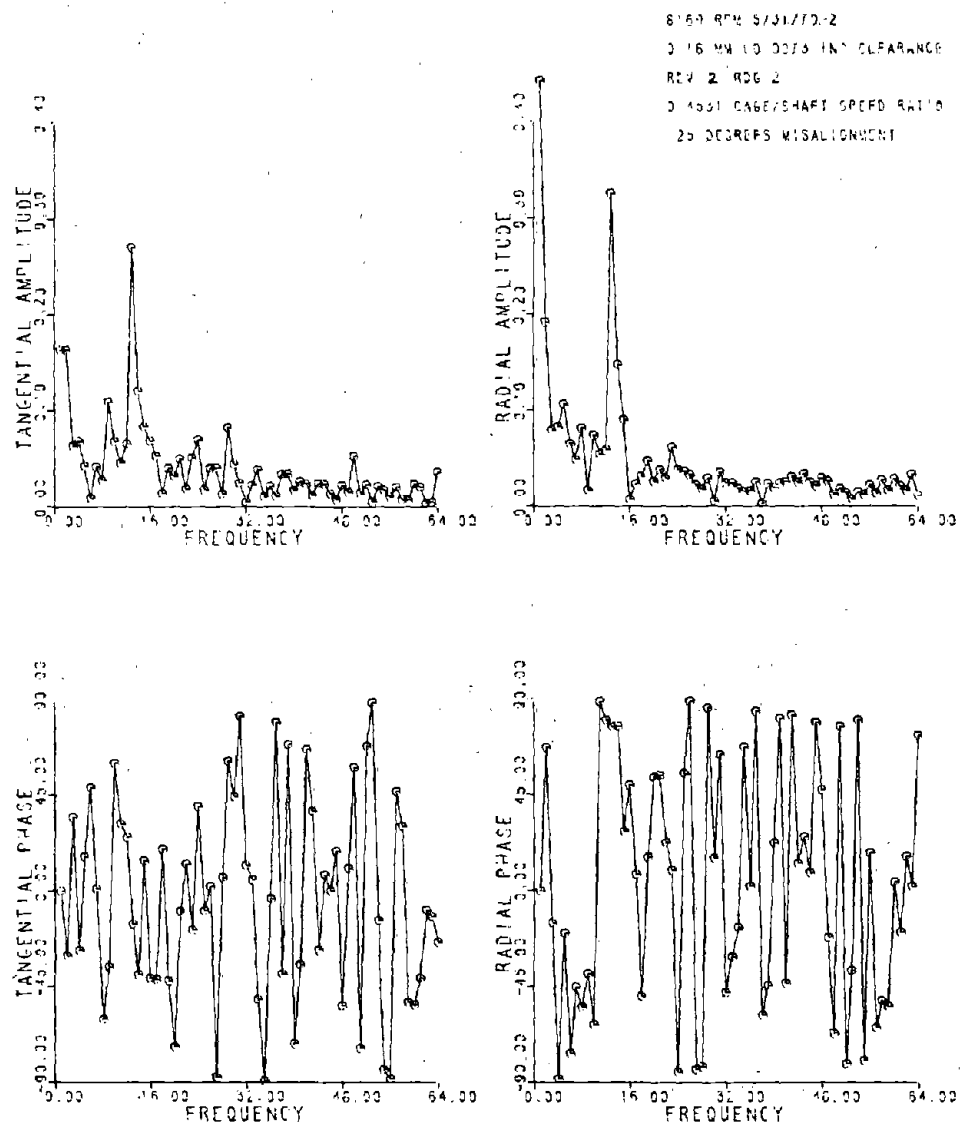


Figure 5b-2 Roller Skew, 0.18 mm Clearance
 Bearing, 0.25° Misalignment



ORIGINAL PAGE IS
 OF POOR QUALITY

Figure 5b-2F Fast Fourier Transform of
 Data in Figure 5b-2

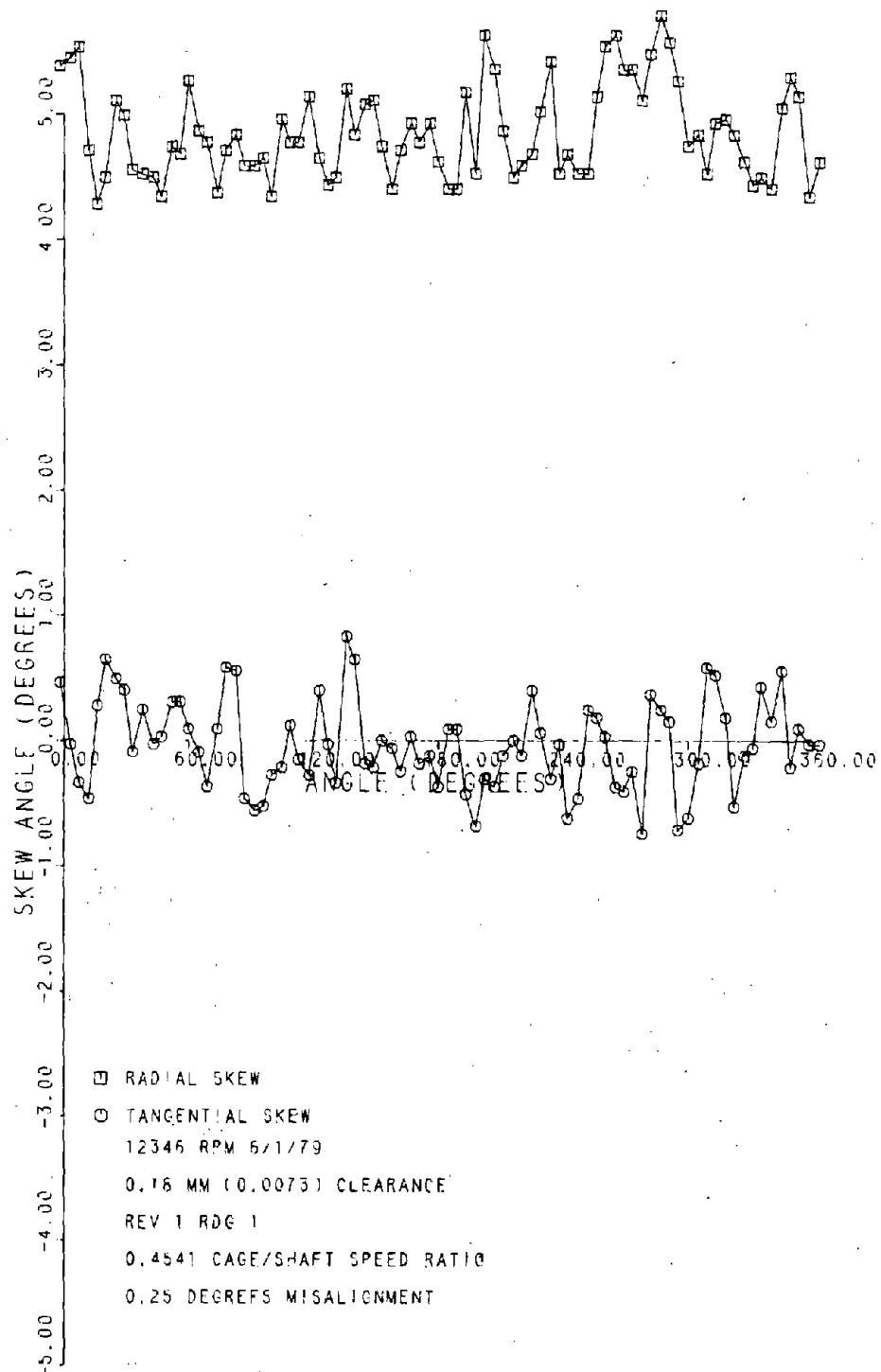


Figure 5c-1 Roller Skew, 0.18 mm Clearance
Bearing, 0.25° Misalignment

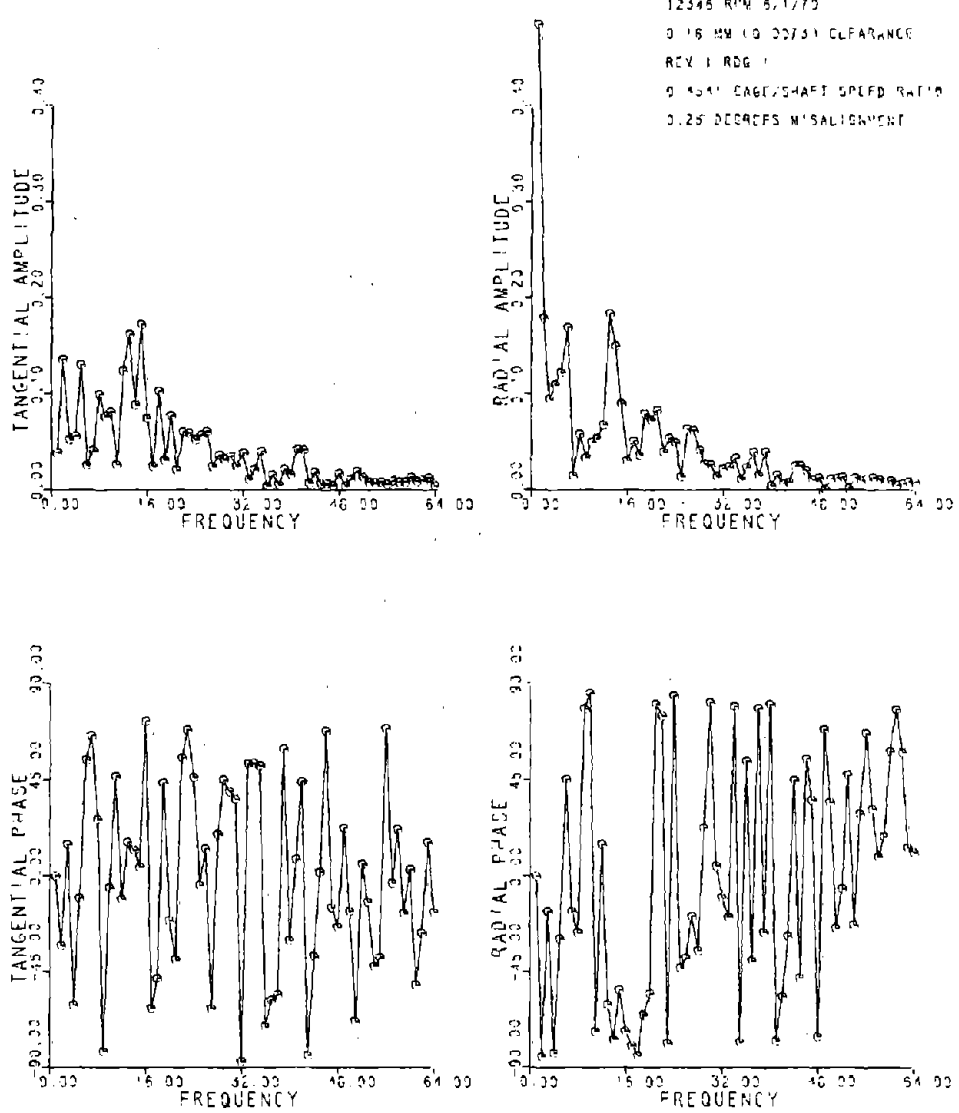


Figure 5c-1F Fast Fourier Transform of Data in Figure 5c-1

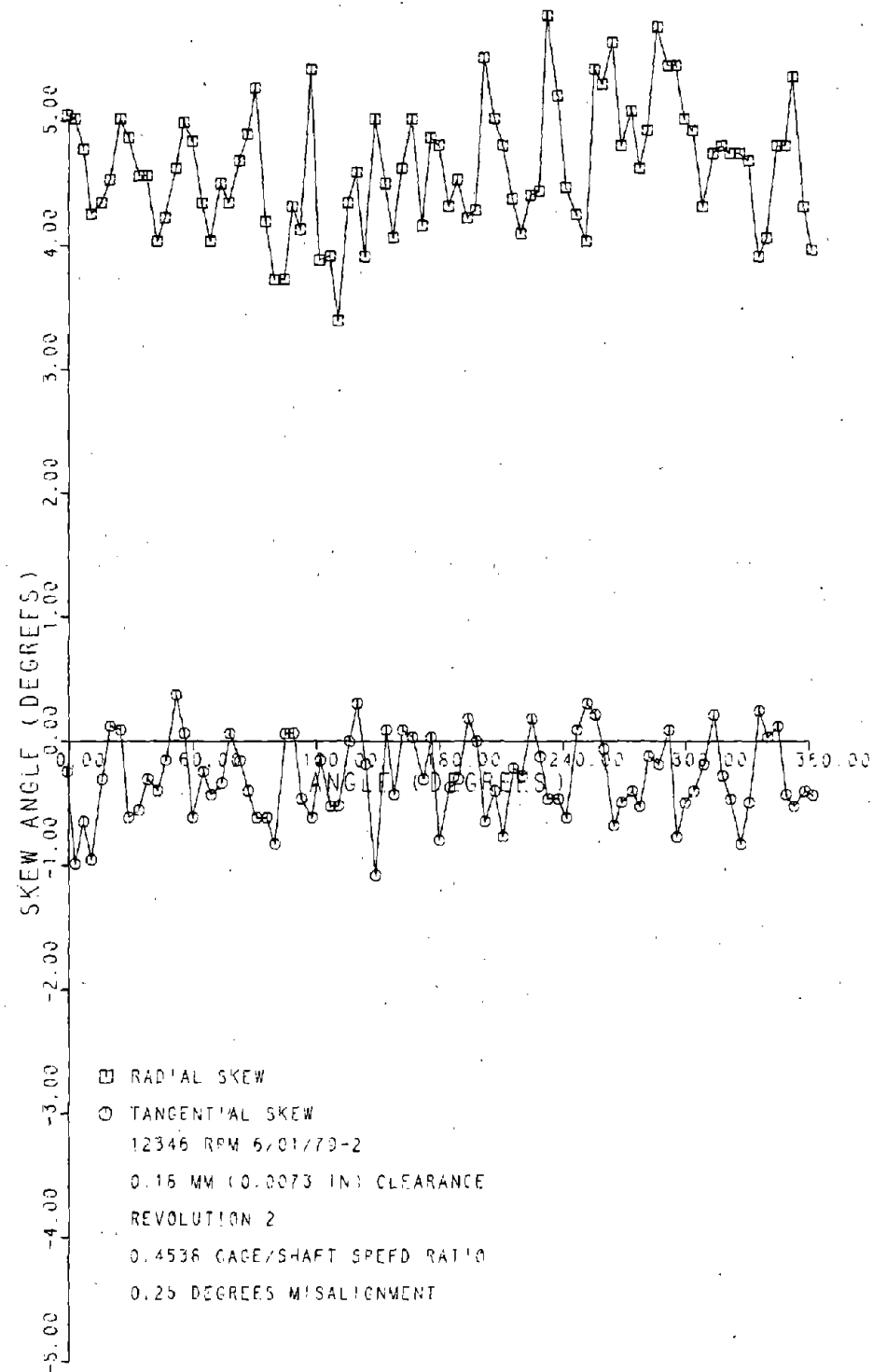


Figure 5c-2 Roller Skew, 0.18 mm Clearance
Bearing, 0.25° Misalignment

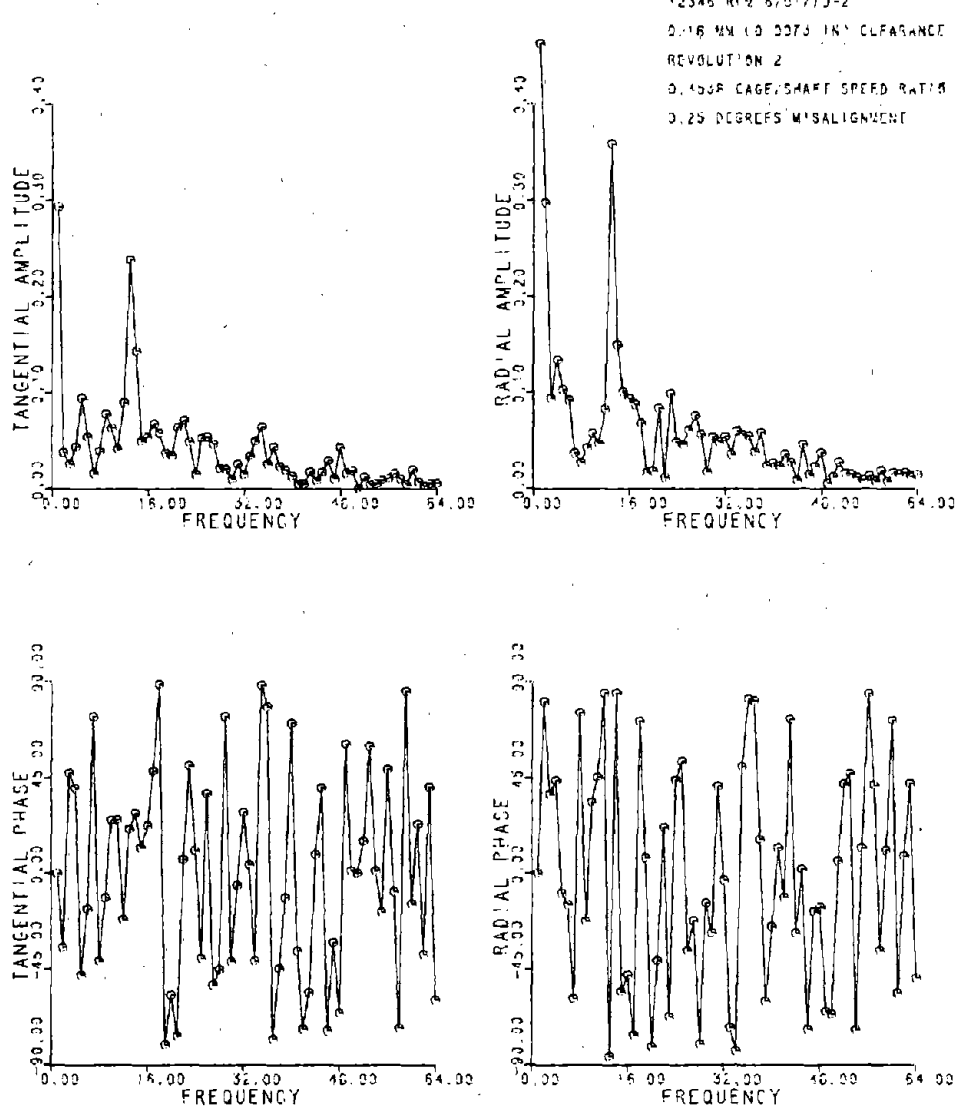


Figure 5c-2F Fast Fourier Transform of Data in Figure 5c-2

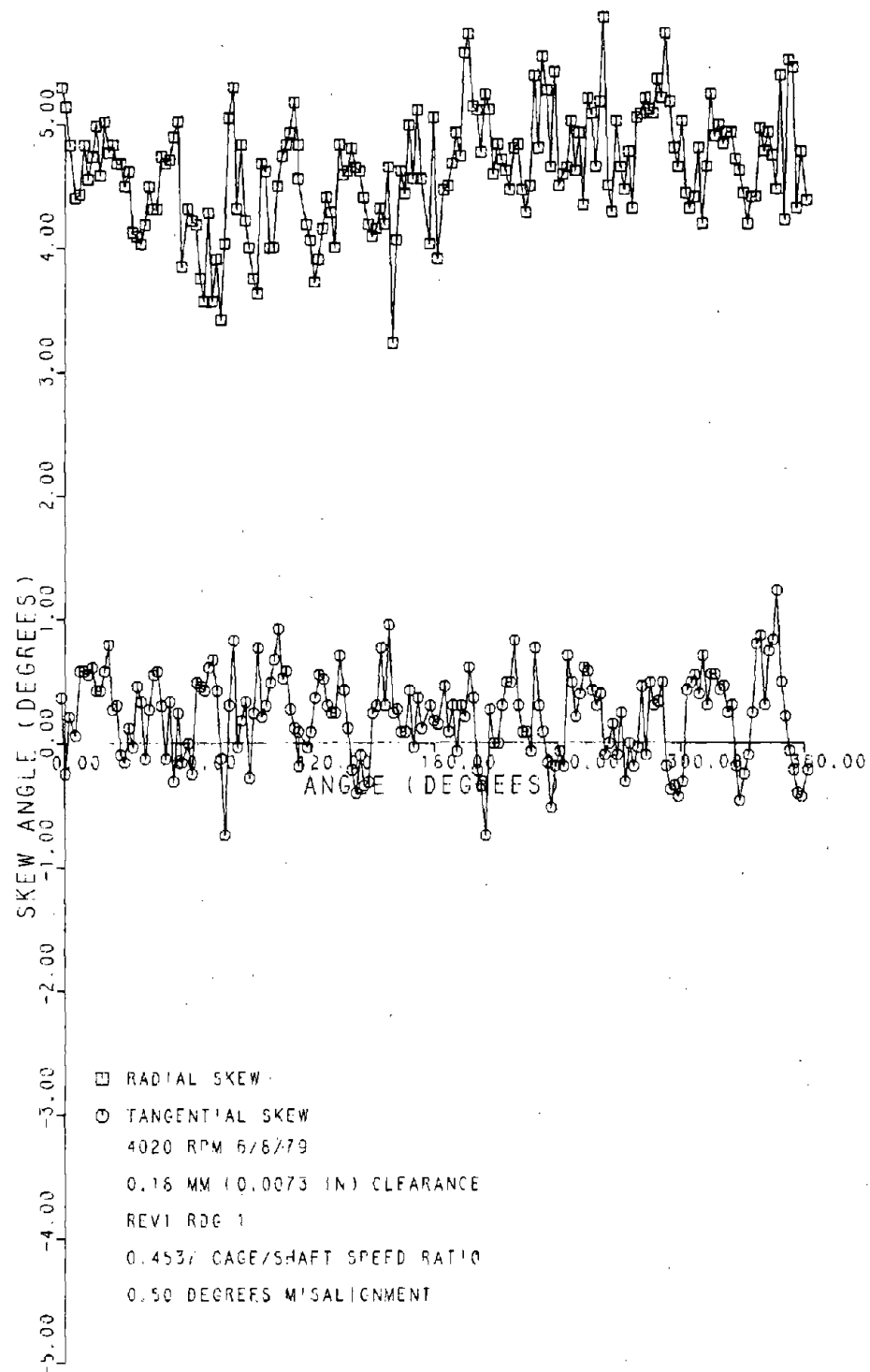
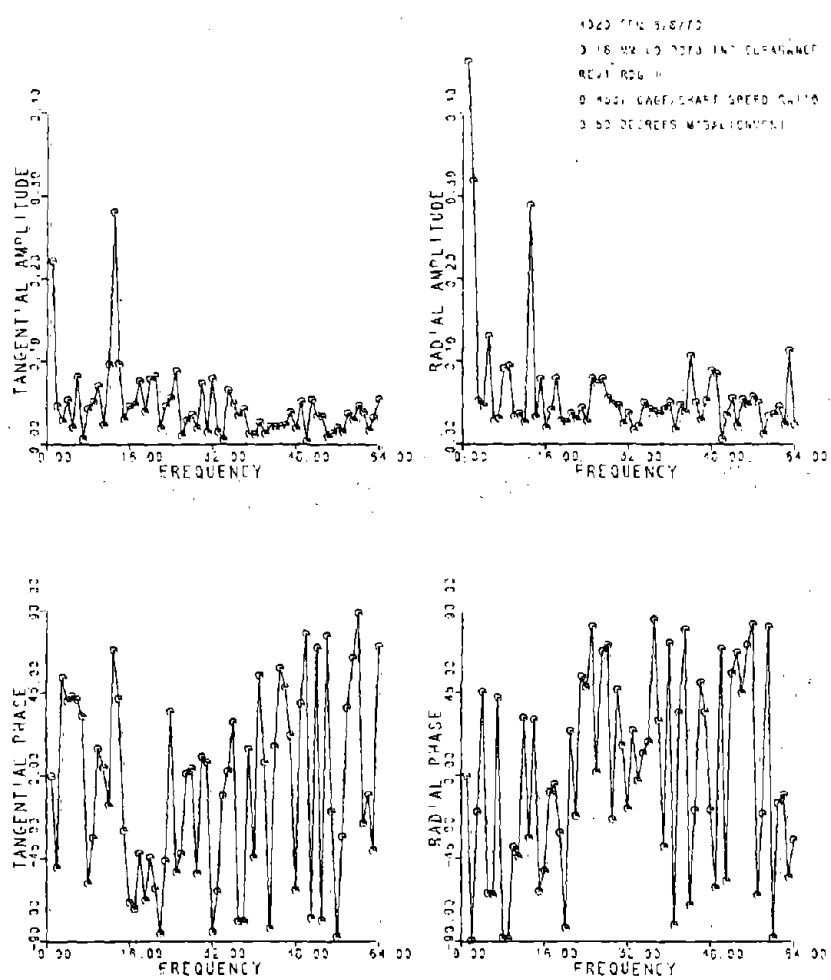


Figure 6a Roller Skew, 0.18 mm Clearance
Bearing, 0.50° Misalignment



ORIGINAL PAGE IS
 OF POOR QUALITY

Figure 6aF Fast Fourier Transform of
 Data in Figure 6a

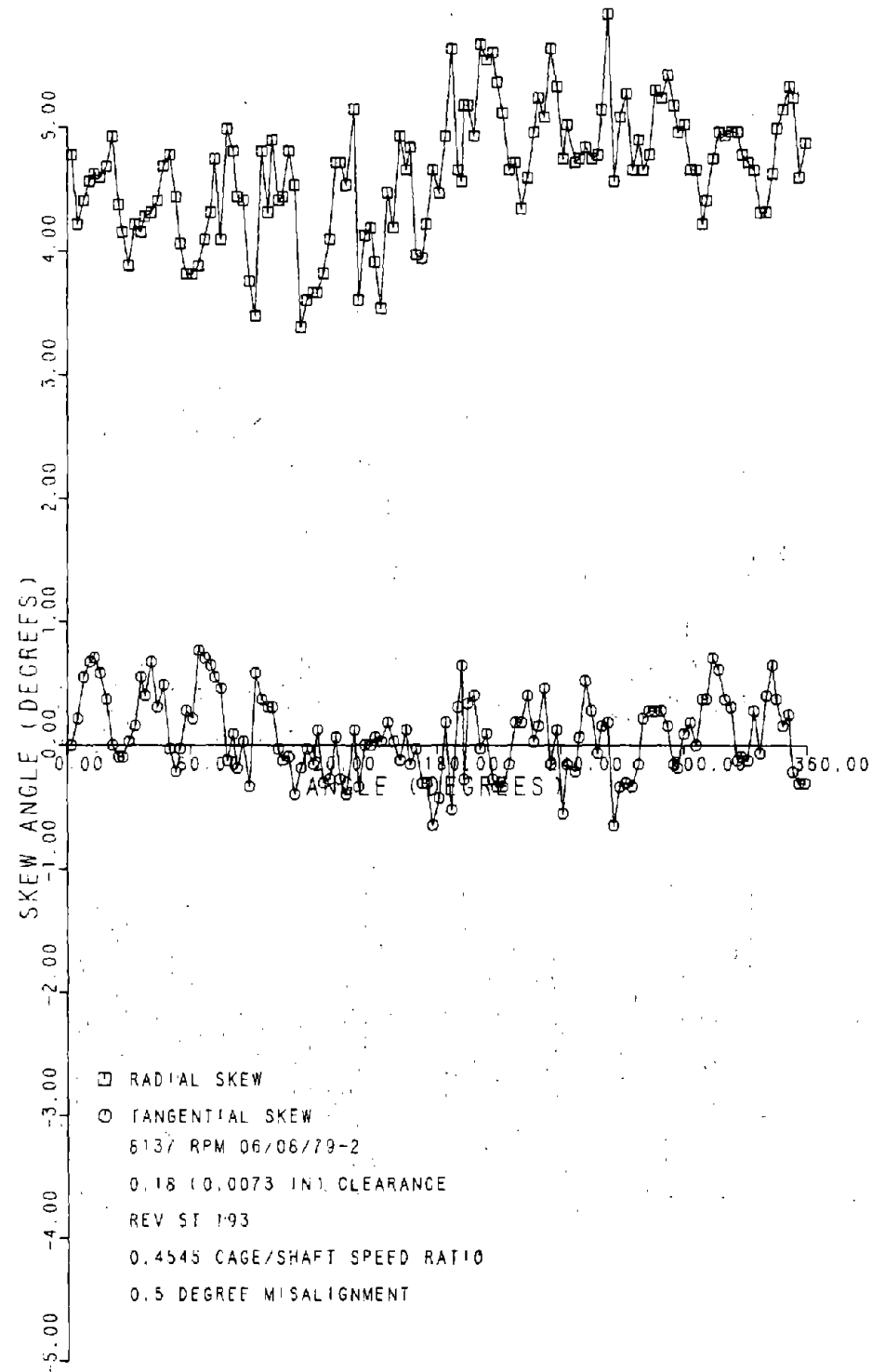


Figure 6b-1 Roller Skew, 0.18 mm Clearance
Bearing, 0.50° Misalignment

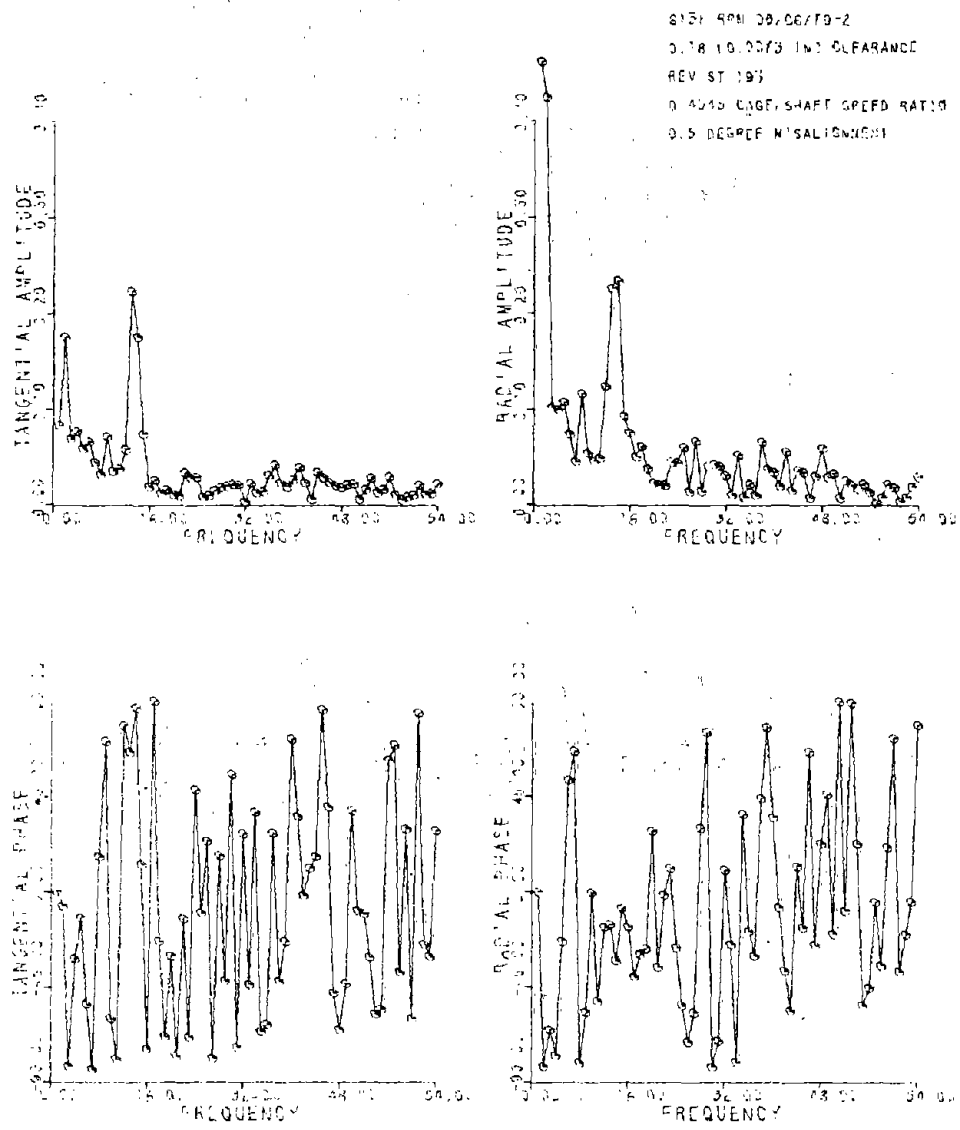


Figure 6b-1F Fast Fourier Transform of Data in Figure 6b-1

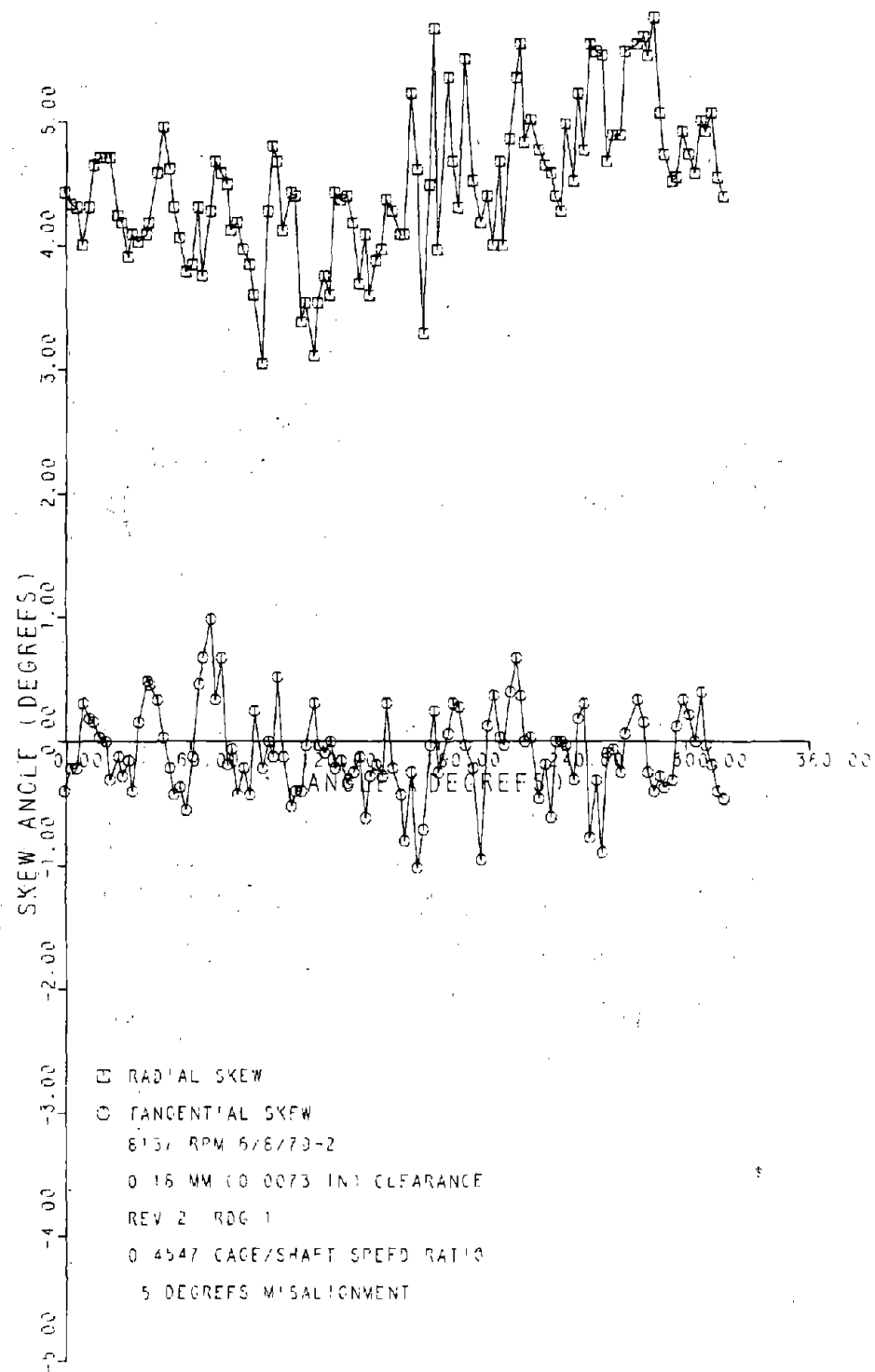


Figure 6b-2. Roller Skew, 0.18 mm Clearance
Bearing, 0.50° Misalignment

Fourier Plot not possible as data
does not cover 360°

Figure 6b-2F

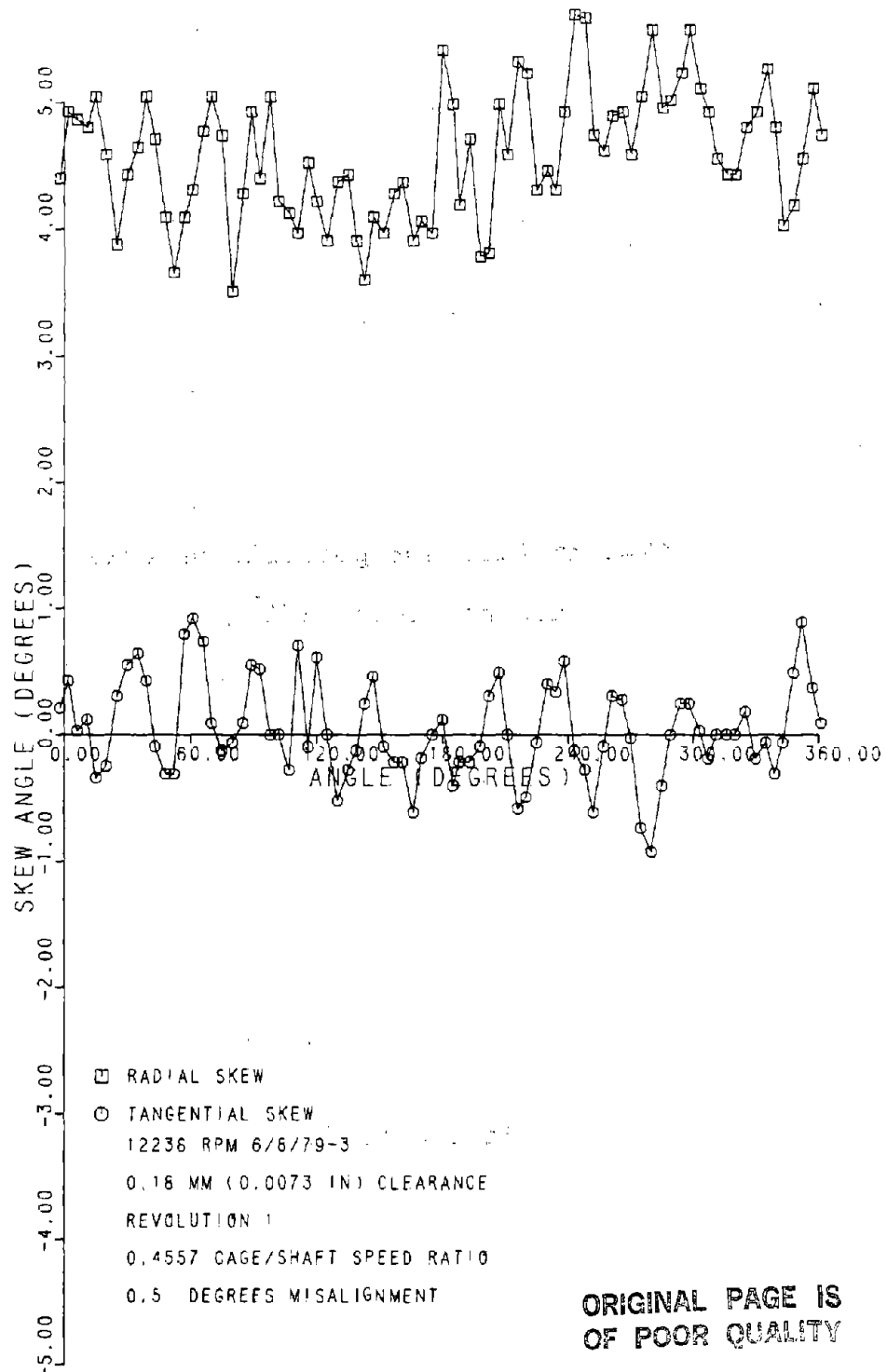


Figure 6c-1 Roller Skew, 0.18 mm Clearance
Bearing, 0.50° Misalignment

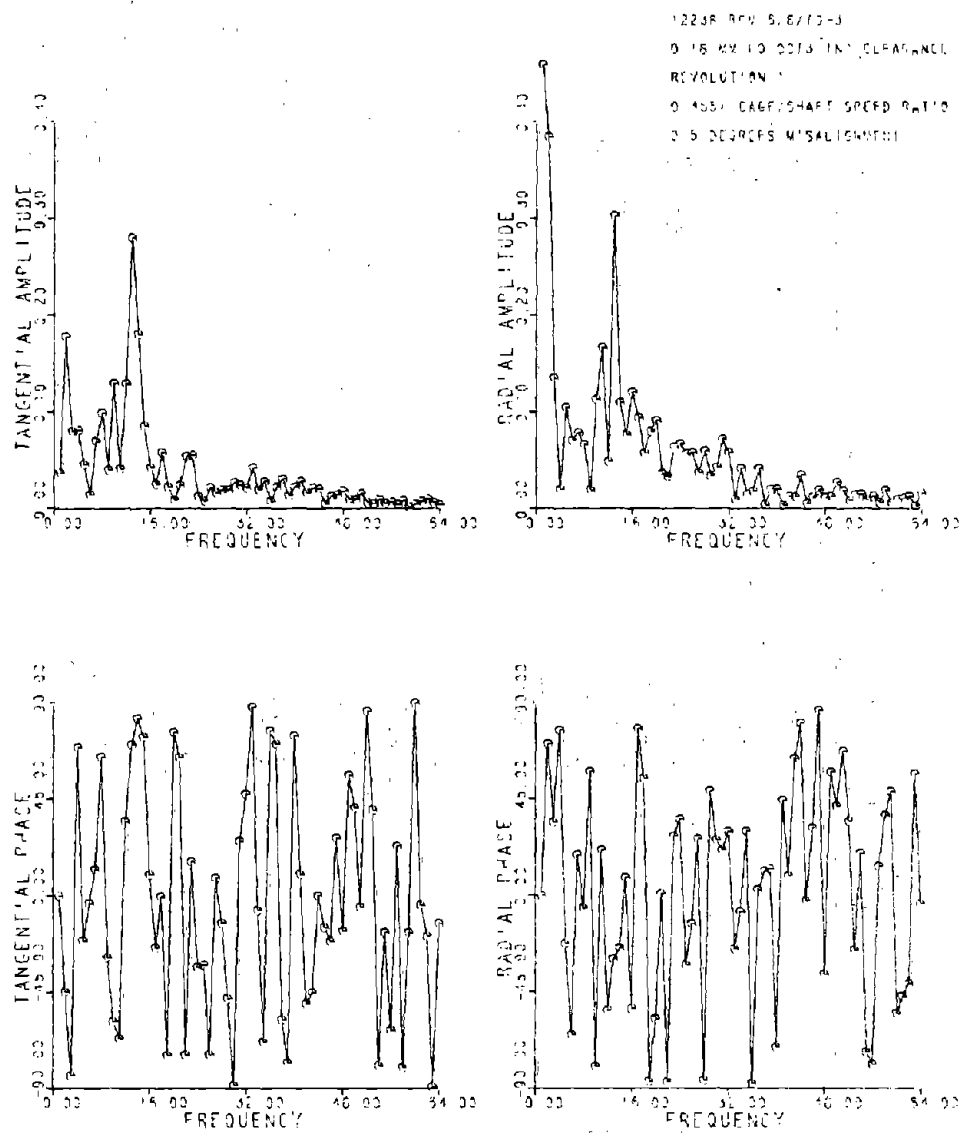


Figure 6c-1F Fast Fourier Transform of Data in Figure 6c-1

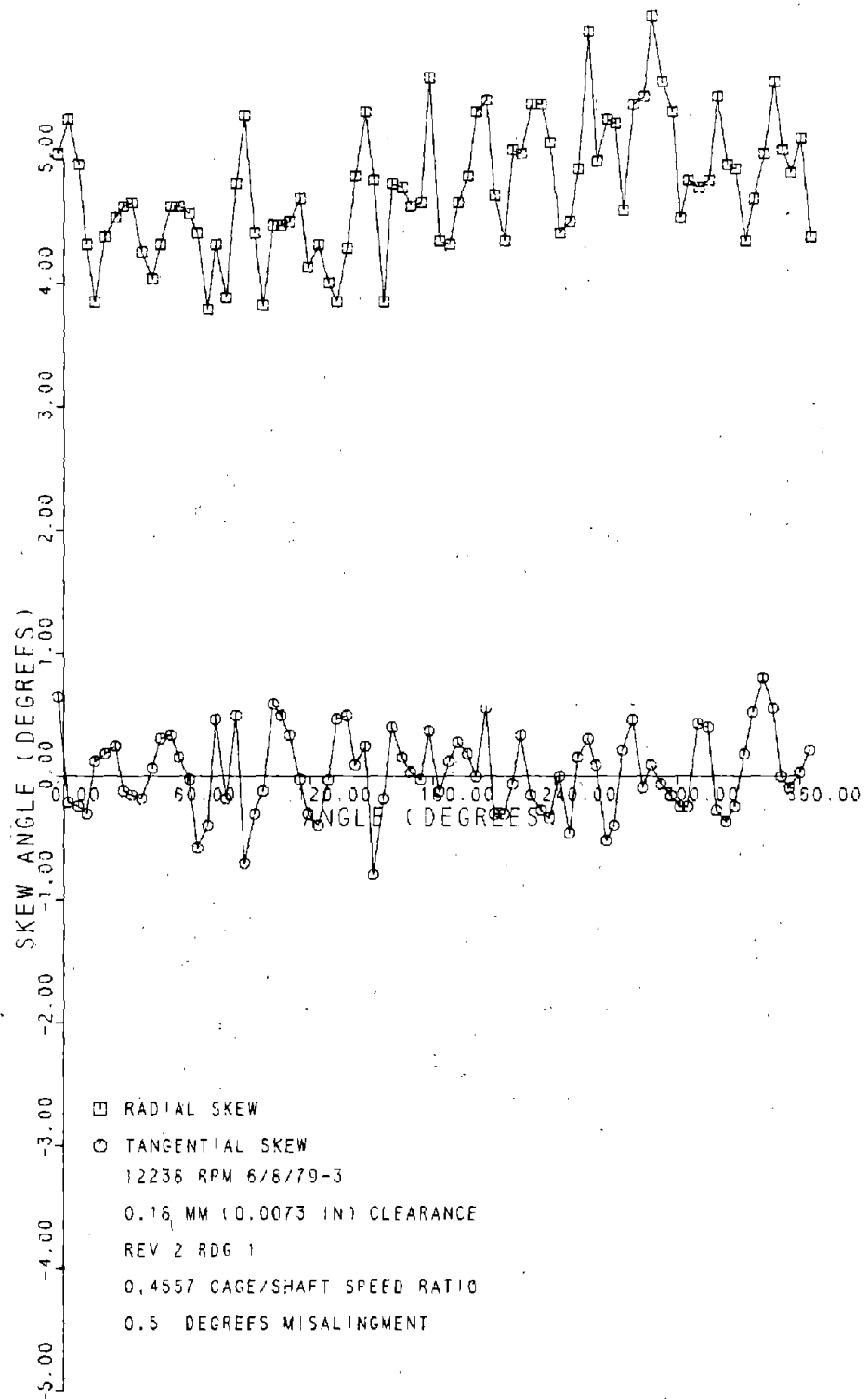


Figure 6c-2 Roller Skew, 0.18 mm Clearance
Bearing, 0.50° Misalignment

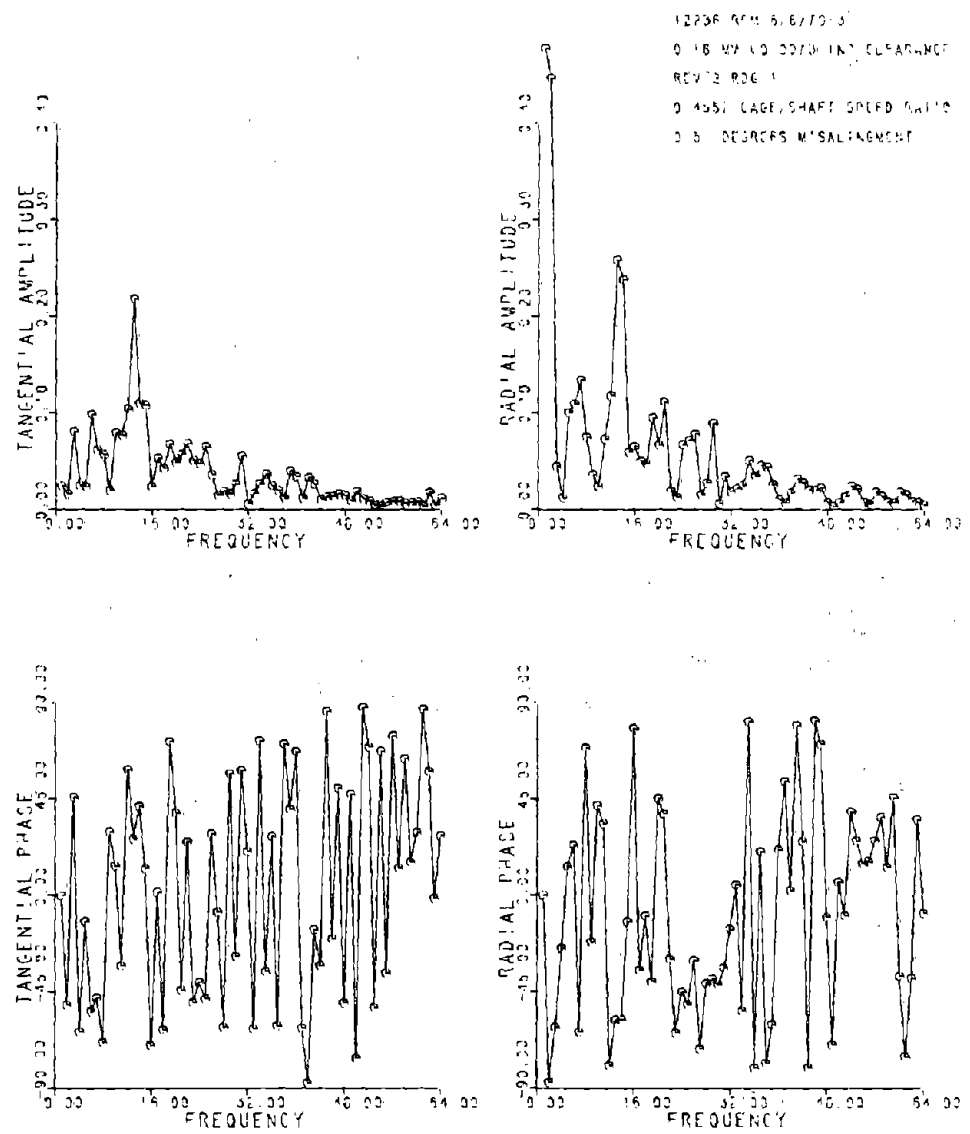


Figure 6c-2F. Fast Fourier Transform of Data in Figure 6c-2

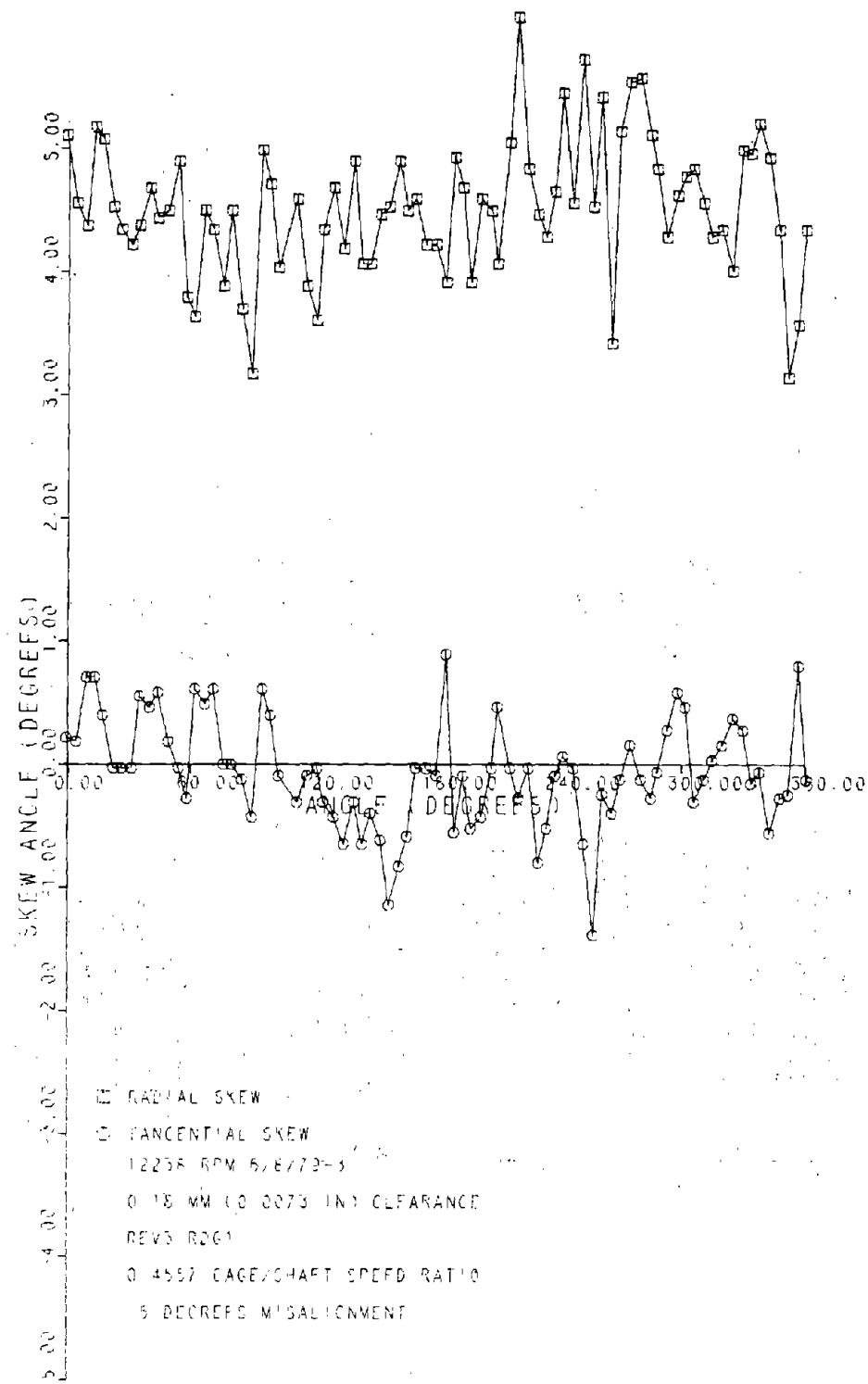
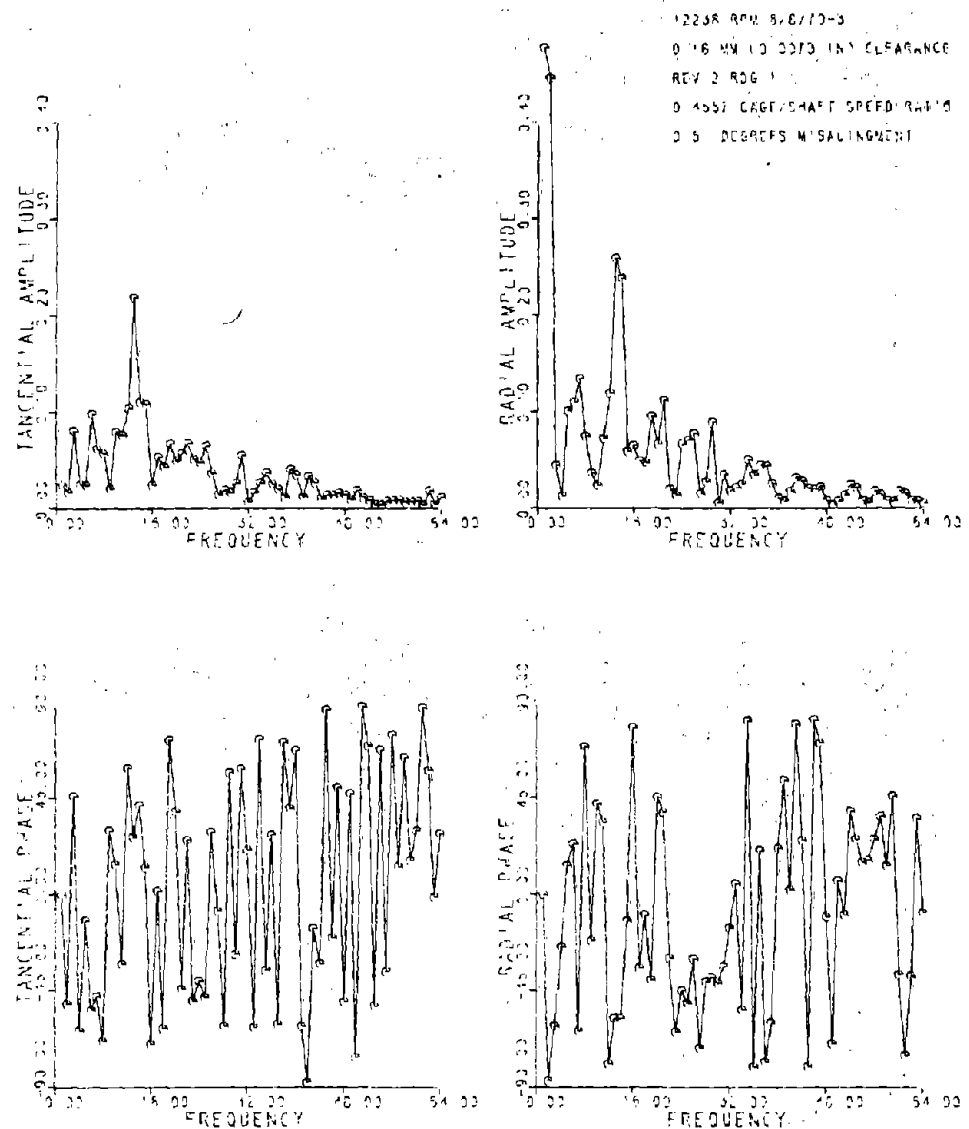


Figure 6c-3 Roller Skew, 0.18 mm Clearance
Bearing, 0.50° Misalignment



ORIGINAL PAGE IS
OF POOR QUALITY

Figure 6c-3F : Fast Fourier Transform of
Data in Figure 6c-3

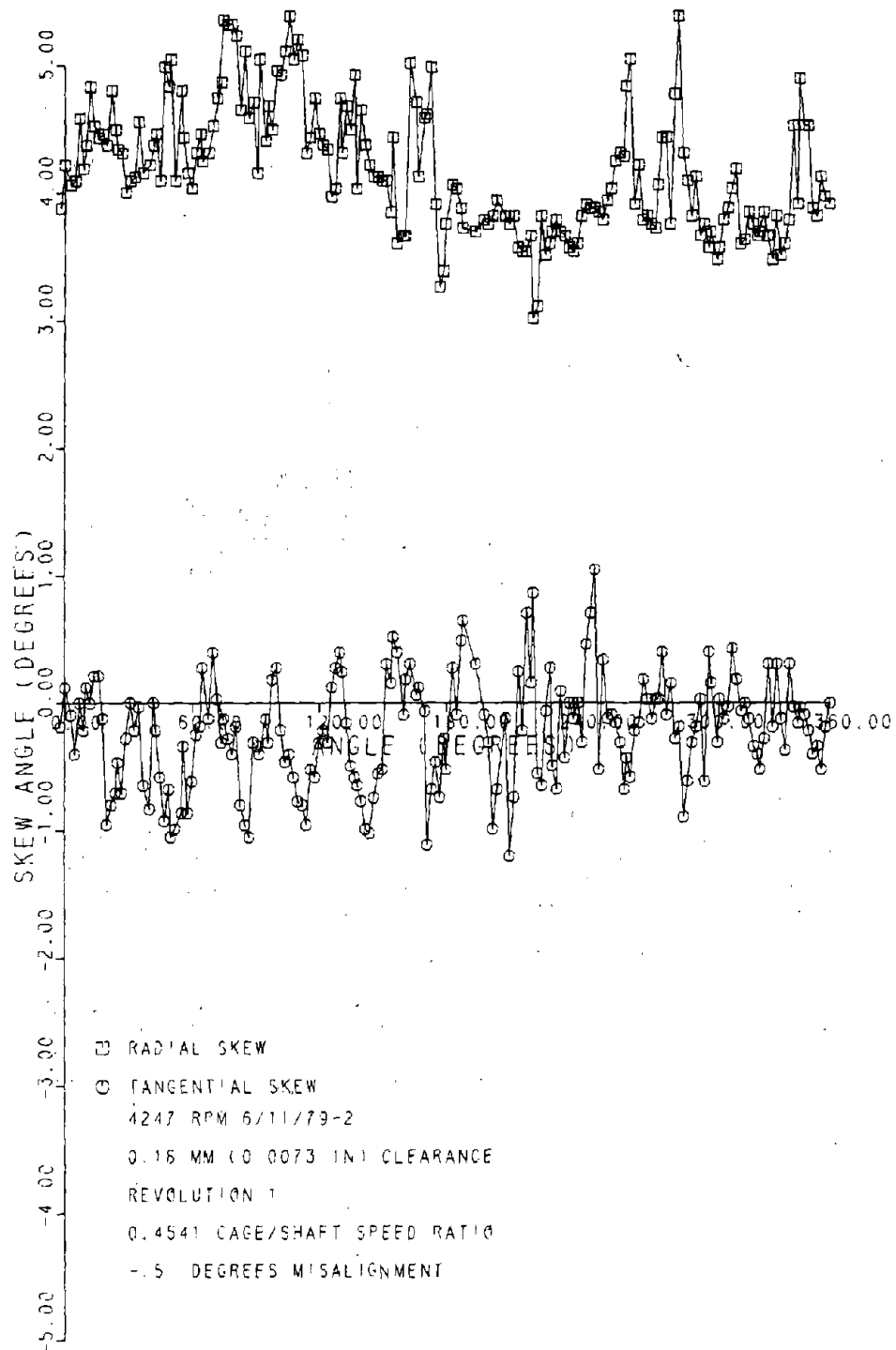
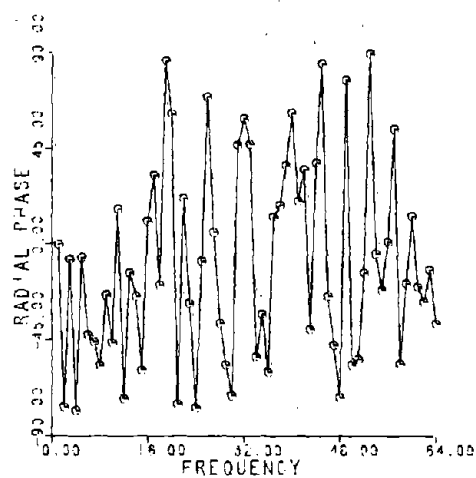
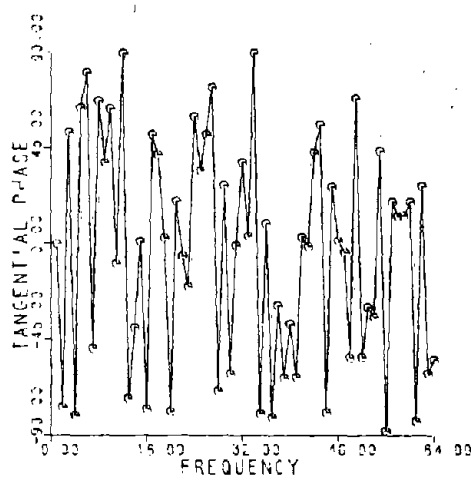
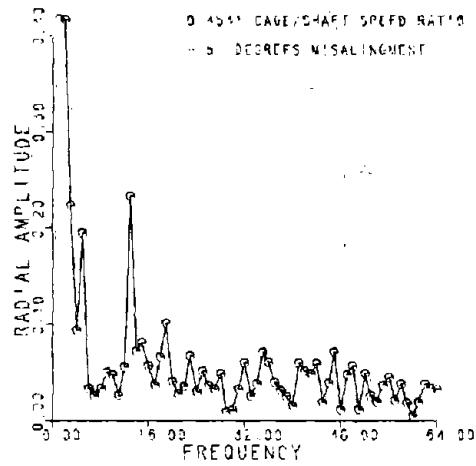
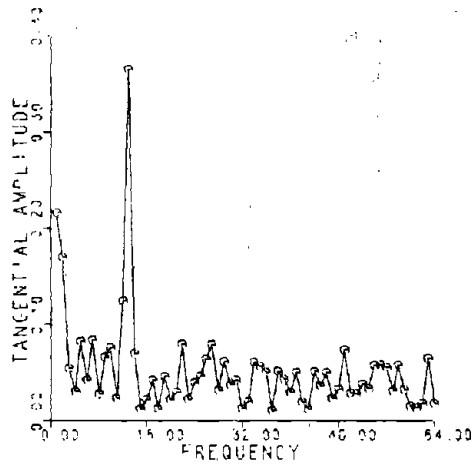


Figure 7a-1 Roller Skew, 0.18 mm Clearance
Bearing, -0.50 Misalignment



4217 ACM 8/11/72-2
 0.18 INCH ID DOTS 1IN² CLEARANCE
 REVOLUTION 1
 0.151² CAGE/SHAFT SPEED RATIO
 5 DEGREES MISALIGNMENT

Figure 7a-1F Fast Fourier Transform of Data in Figure 7a-1

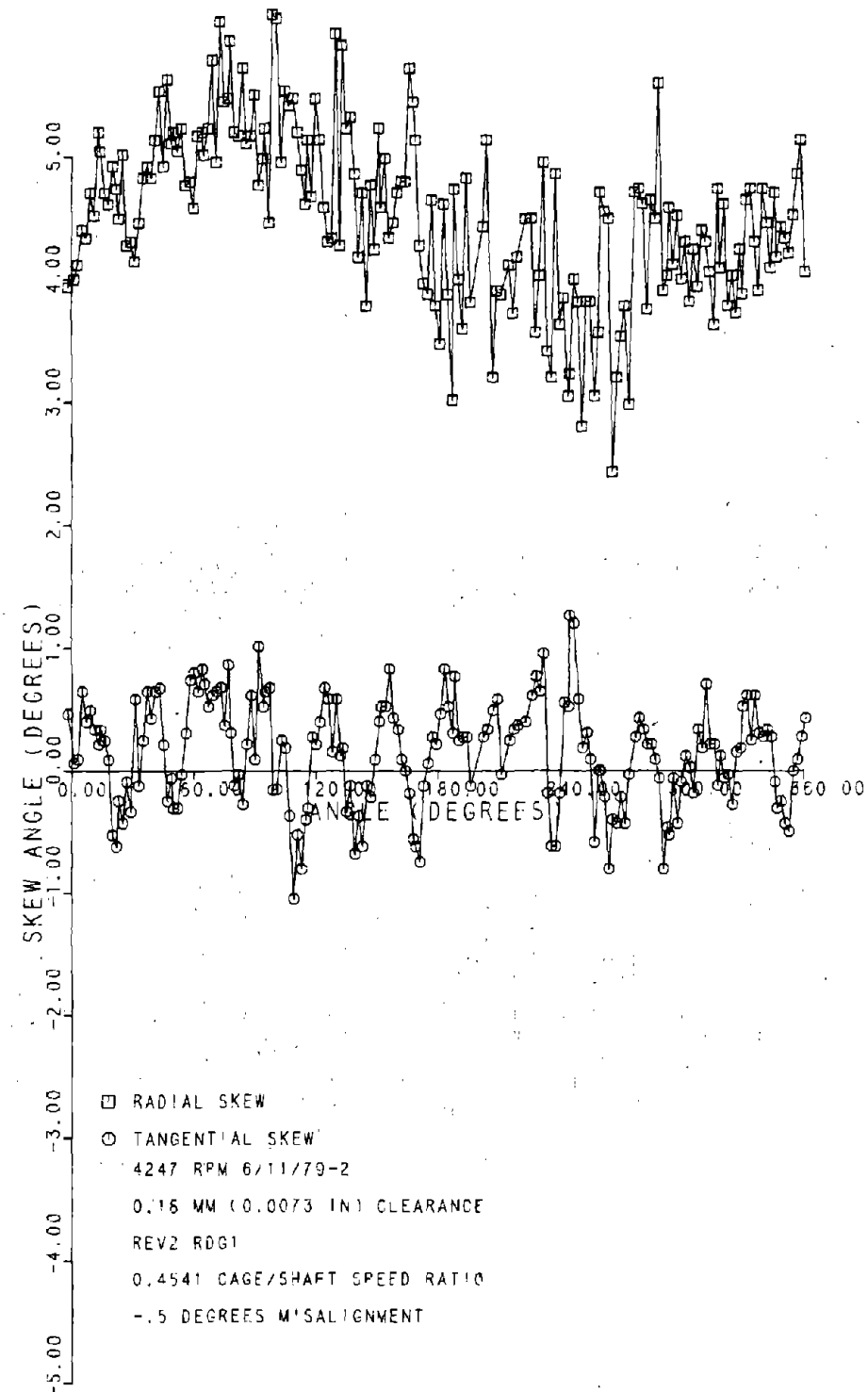


Figure 7a-2 Roller Skew, 0.18 mm Clearance
Bearing, -0.50 Misalignment

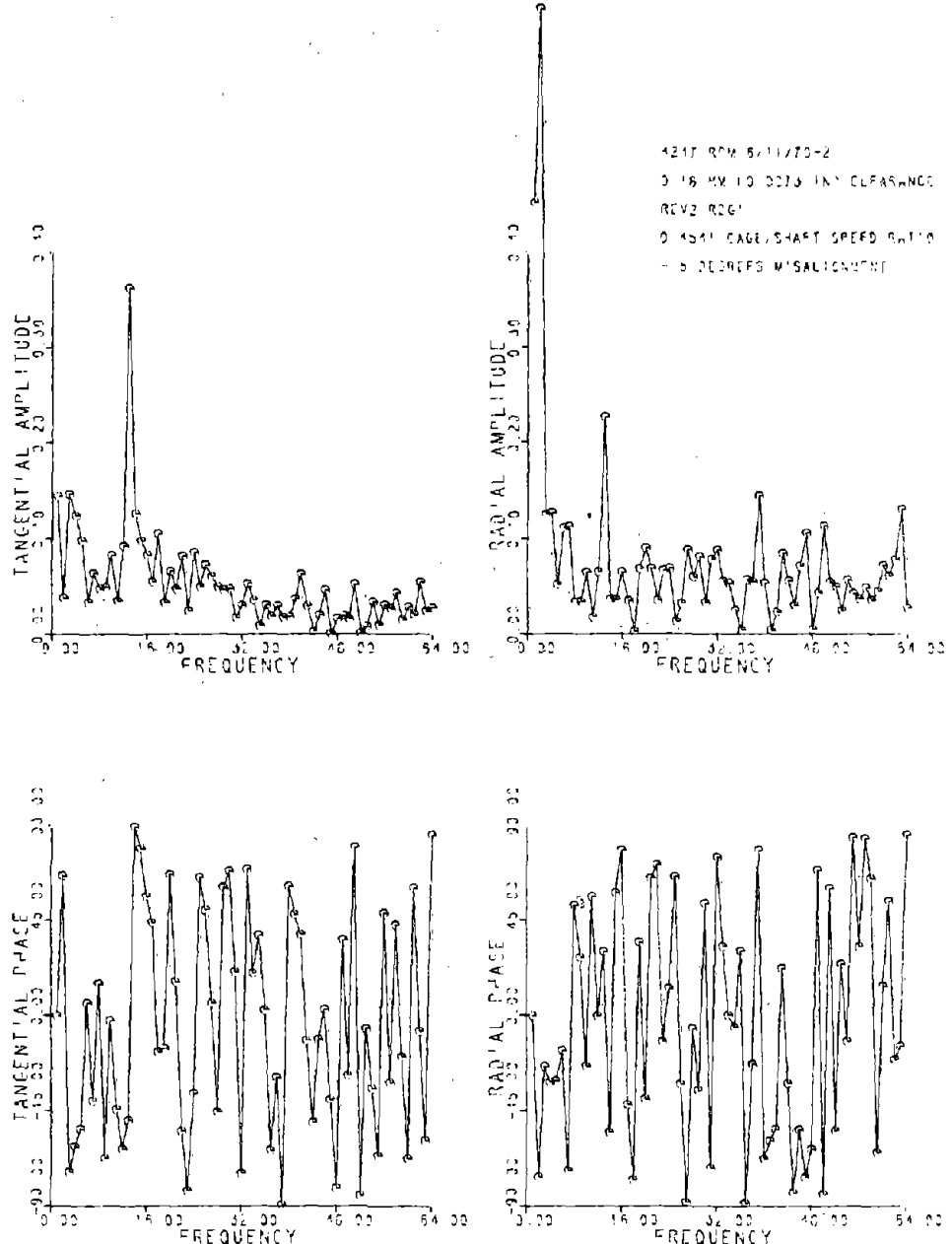


Figure 7a-2F Fast Fourier Transform of Data in Figure 7a-2

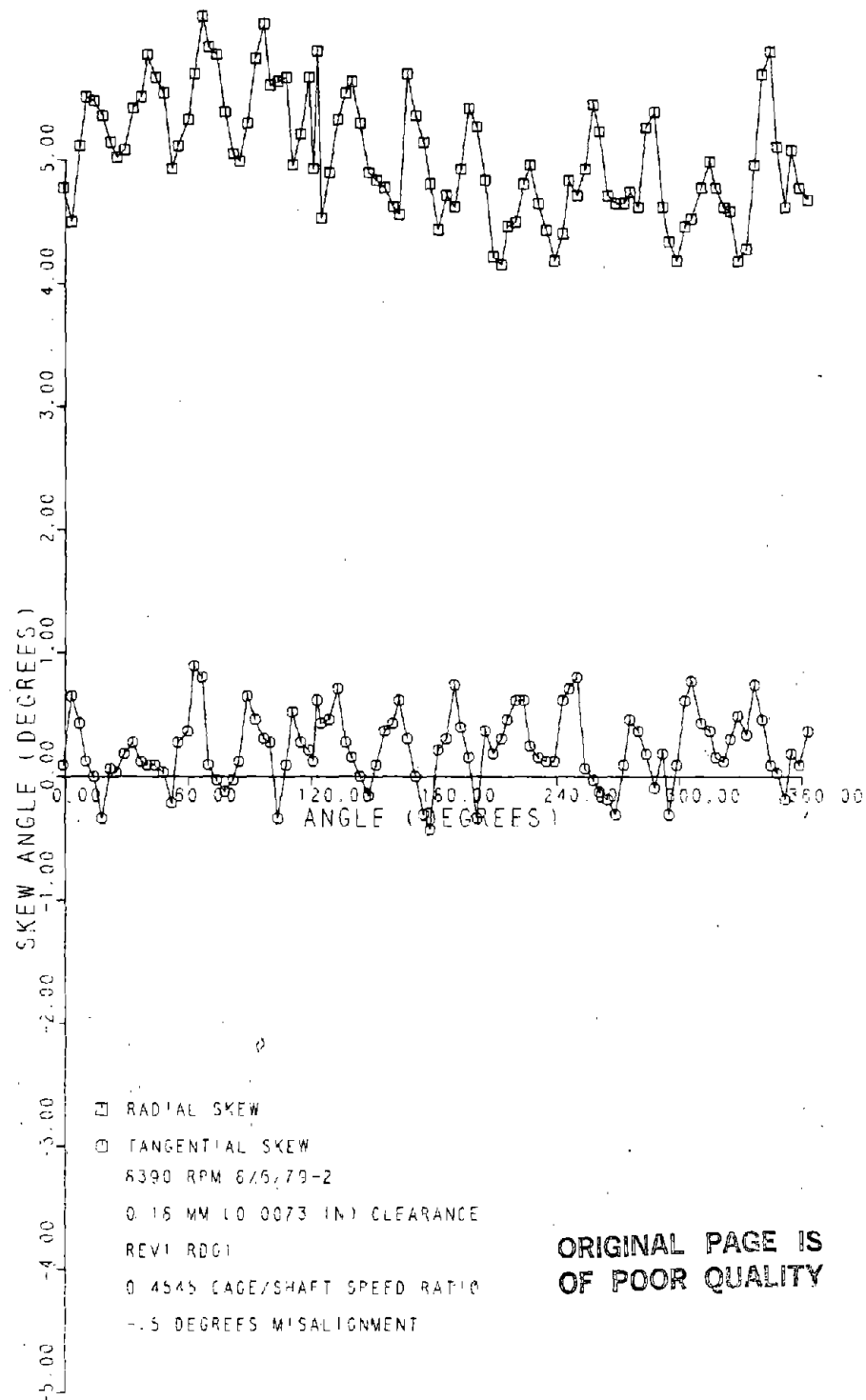


Figure 7b-1 Roller Skew, 0.18 mm Clearance
Bearing, -0.50 Misalignment

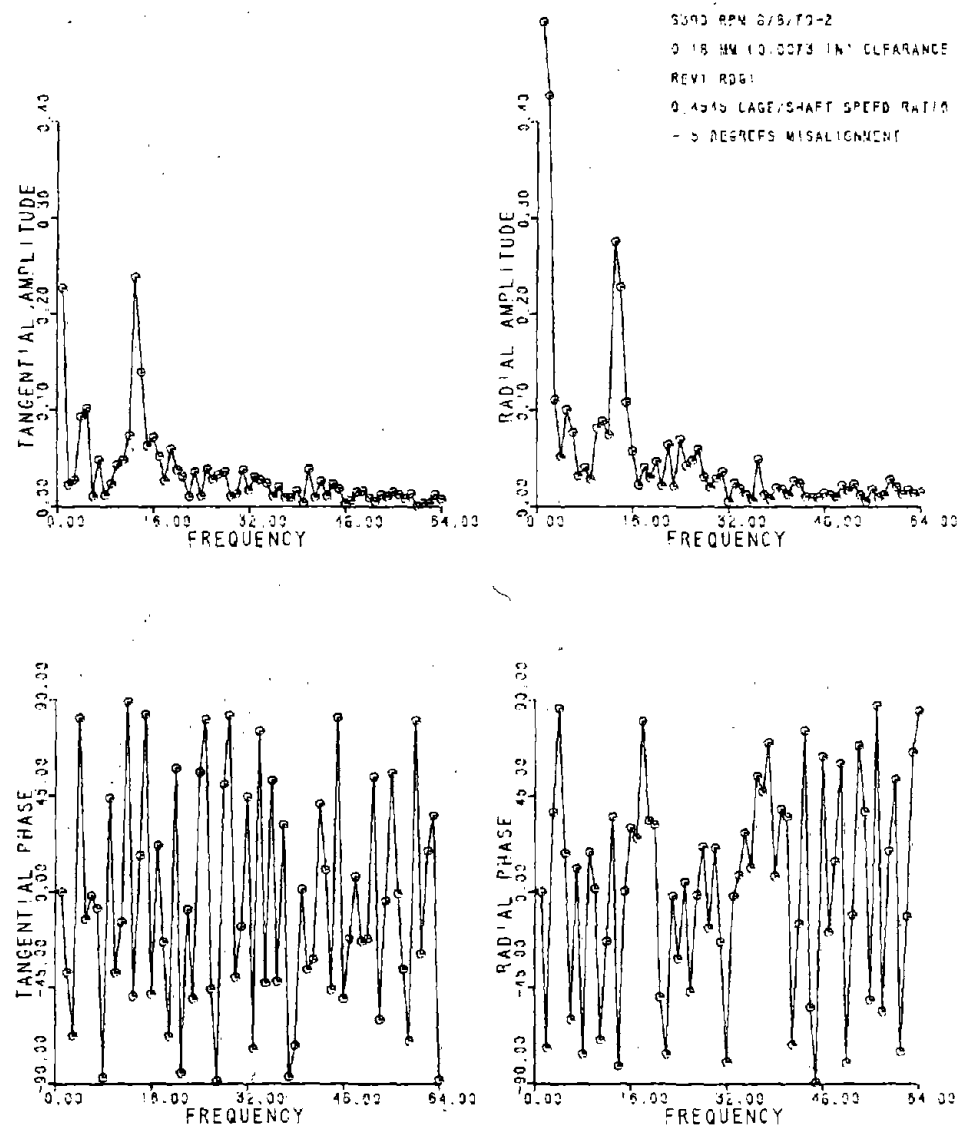


Figure 7b-1F Fast Fourier Transform of Data in Figure 7b-1

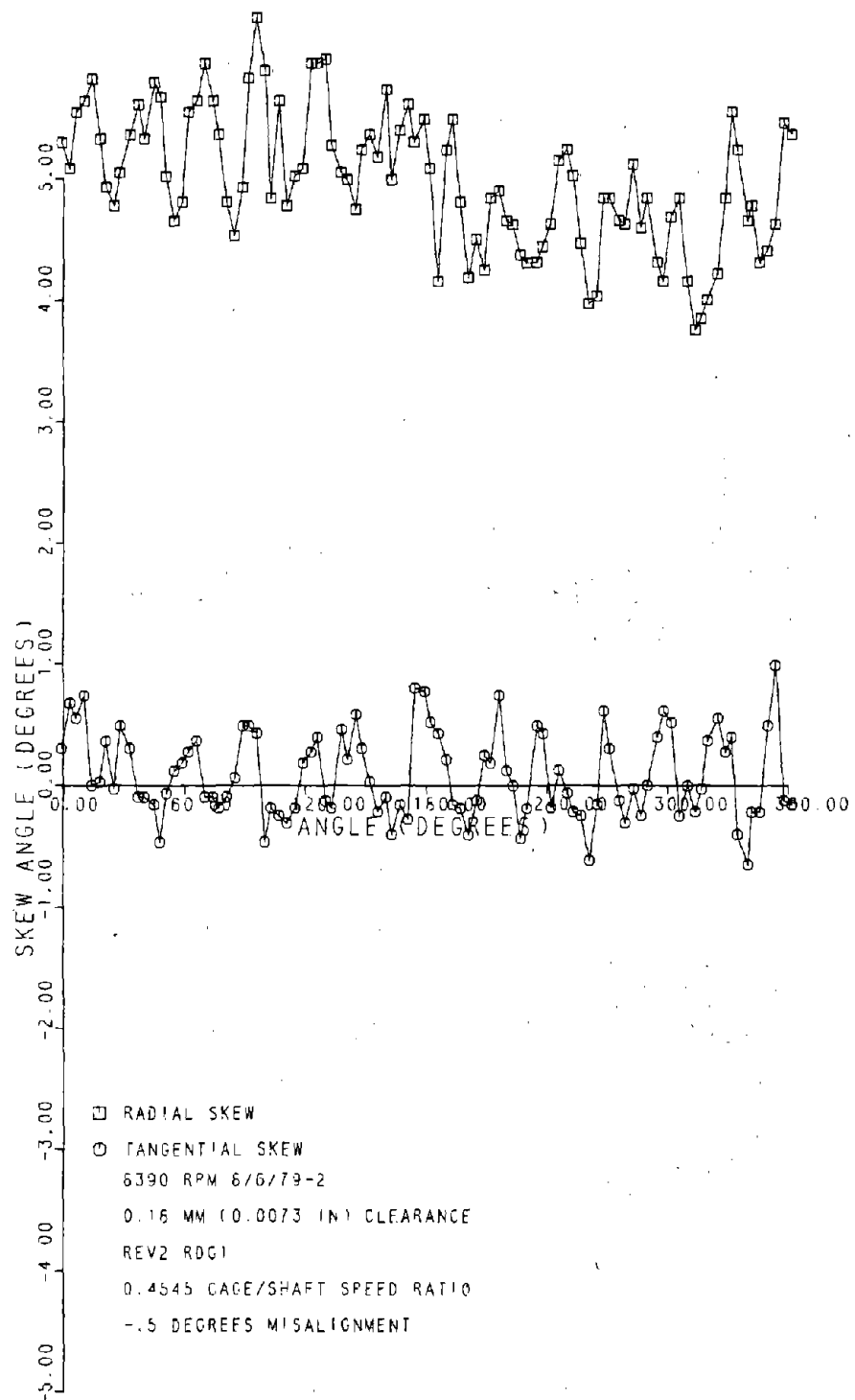


Figure 7b-2 Roller Skew, 0.18 mm Clearance
Bearing, -0.50 Misalignment

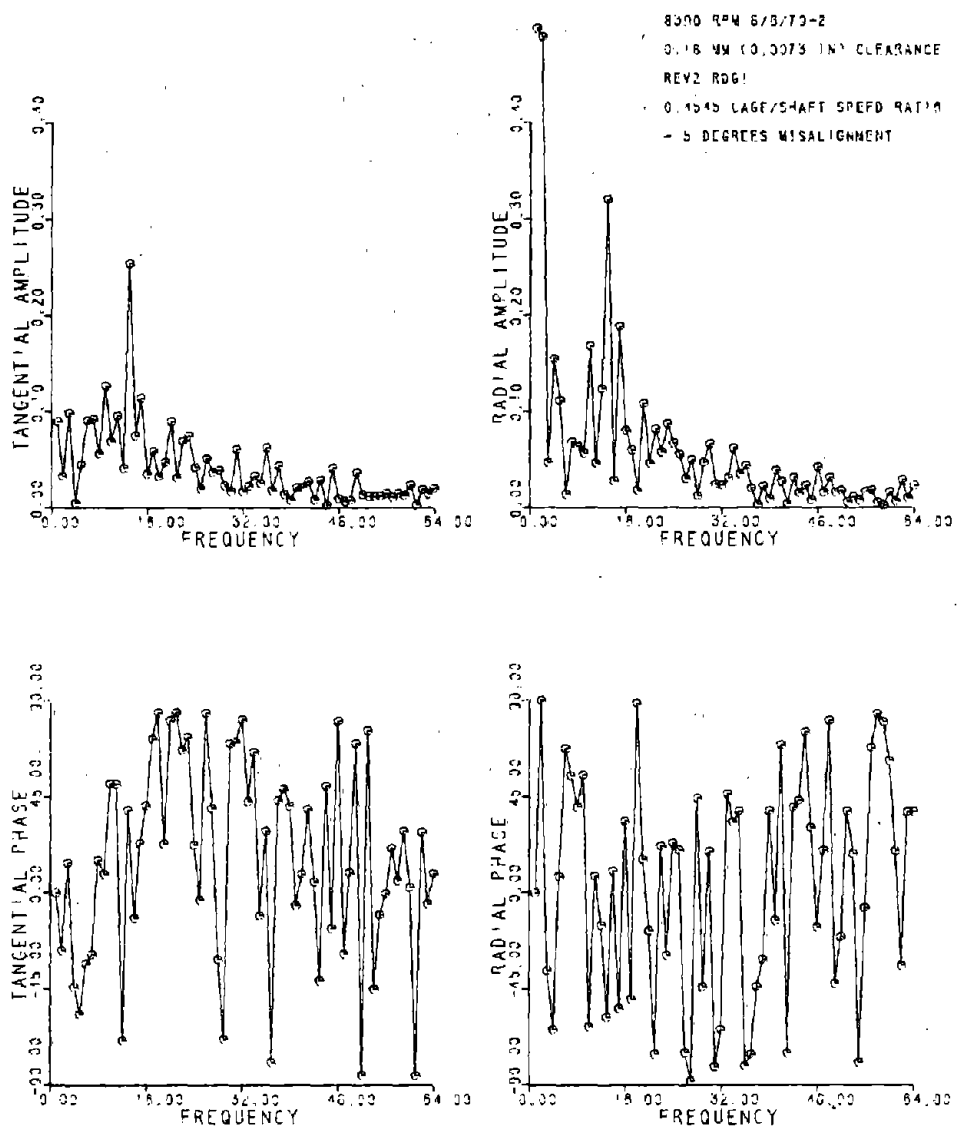


Figure 7b-2F Fast Fourier Transform of Data in Figure 7b-2

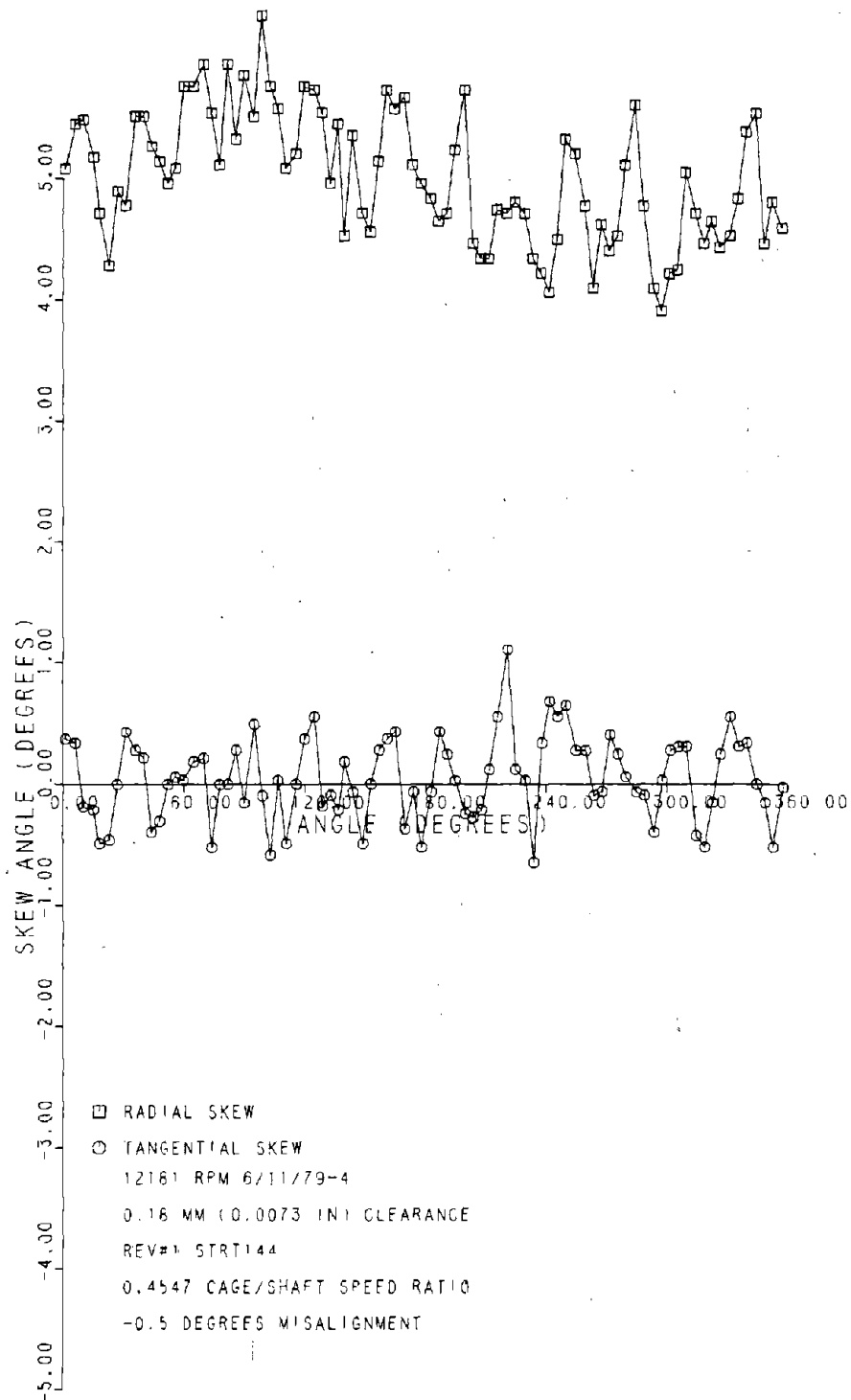
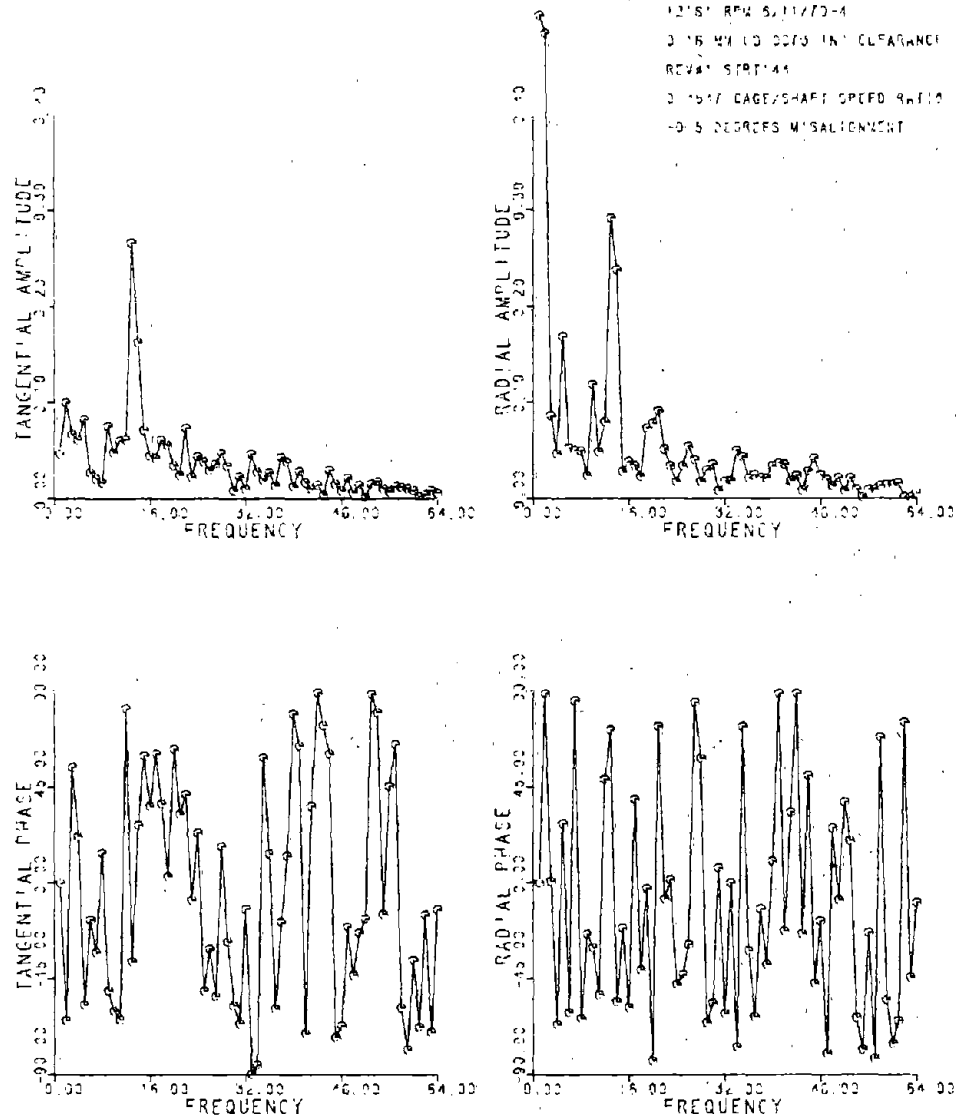


Figure 7c-1 Roller Skew, 0.18 mm Clearance
Bearing, -0.50 Misalignment



ORIGINAL PAGE IS
 OF POOR QUALITY

Figure 7c-1F Fast Fourier Transform of
 Data in Figure 7c-1

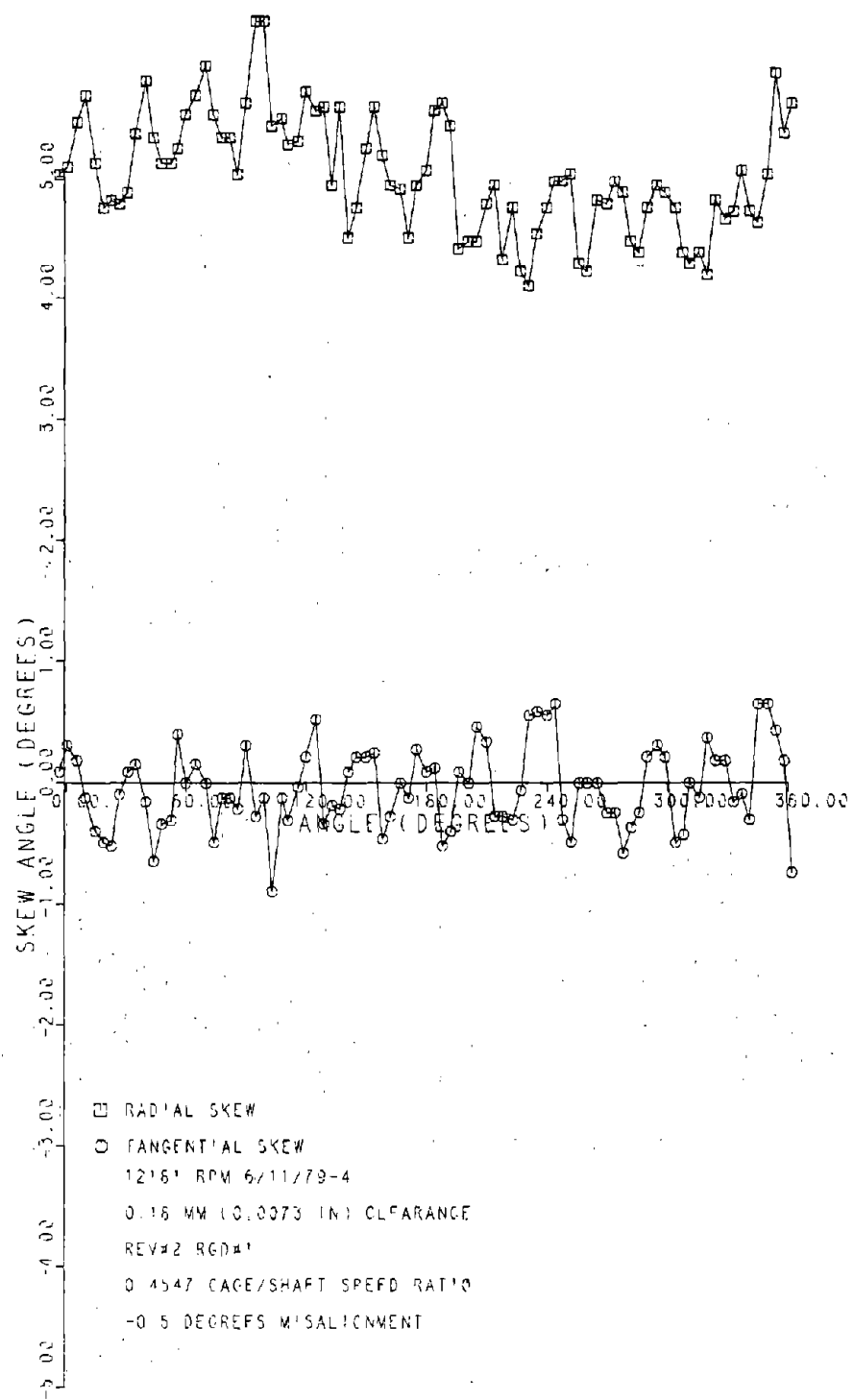


Figure 7c-2 Roller Skew, 0.18 mm Clearance
Bearing, -0.50 Misalignment

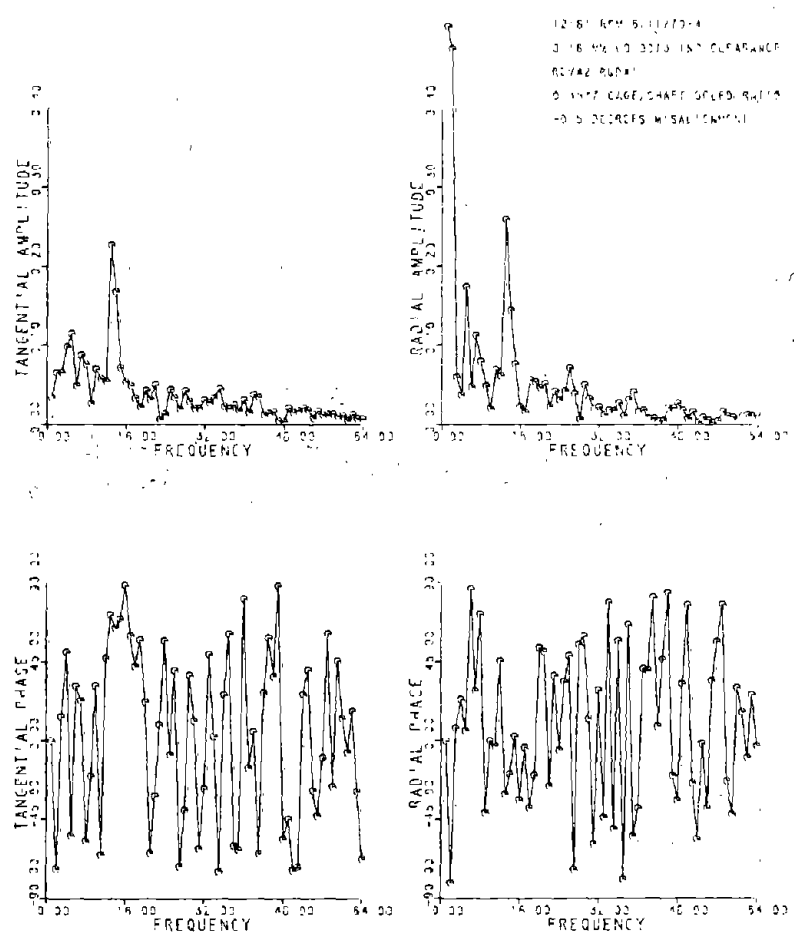


Figure 7c-2F Fast Fourier Transform of Data in Figure 7c-2

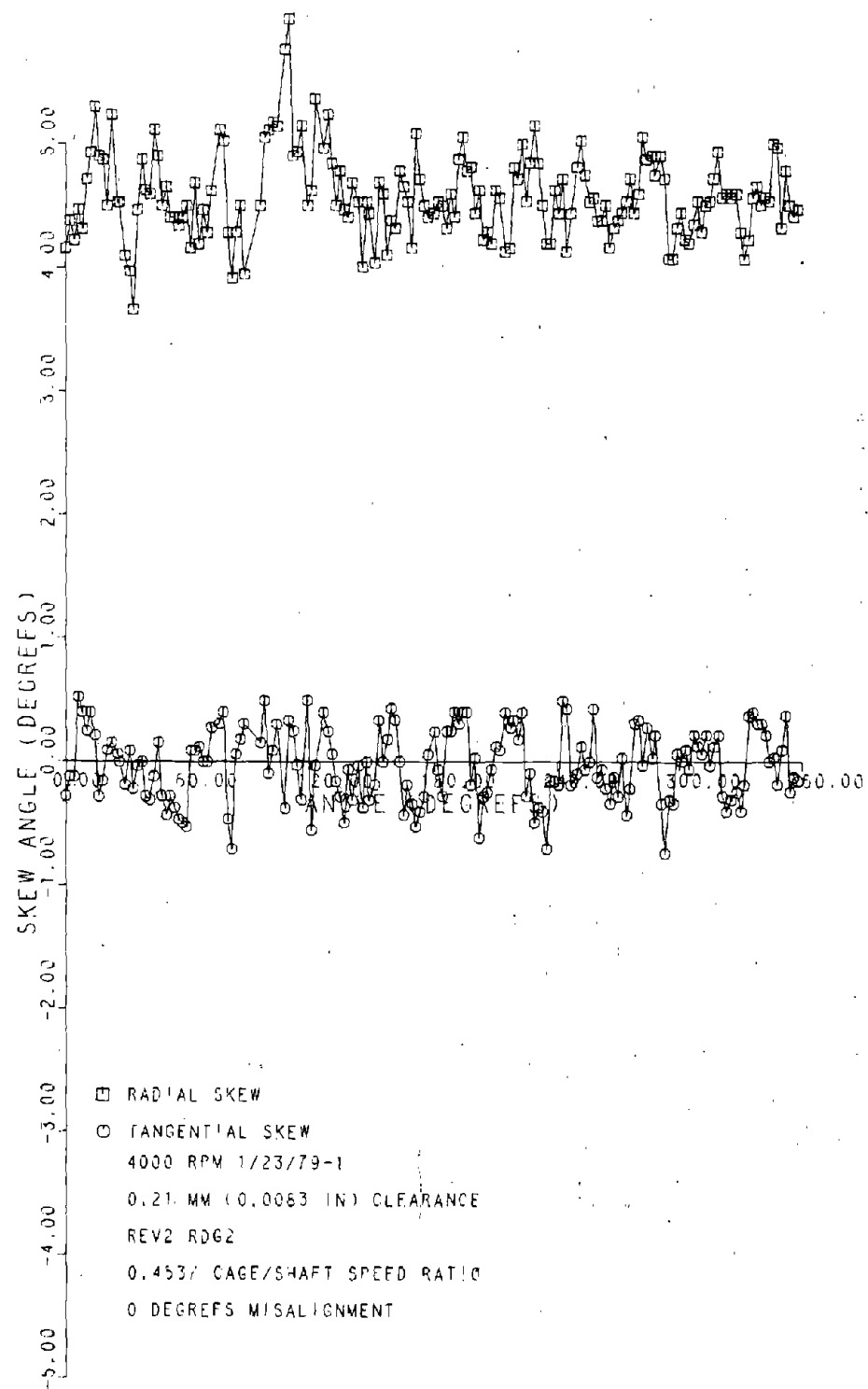


Figure 8a Roller Skew, 0.21 mm Clearance
Bearing, 0° Misalignment

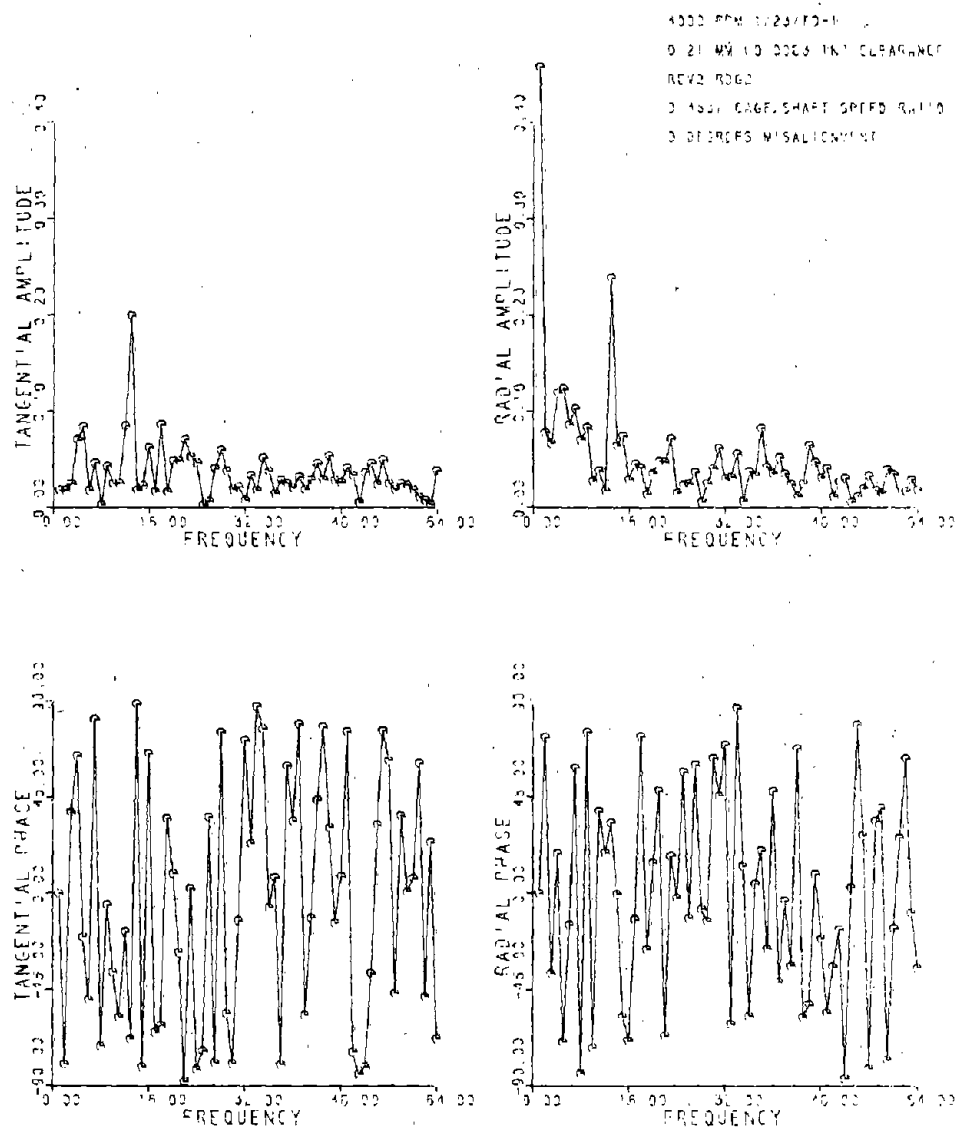


Figure 8aF Fast Fourier Transform of Data in Figure 8a

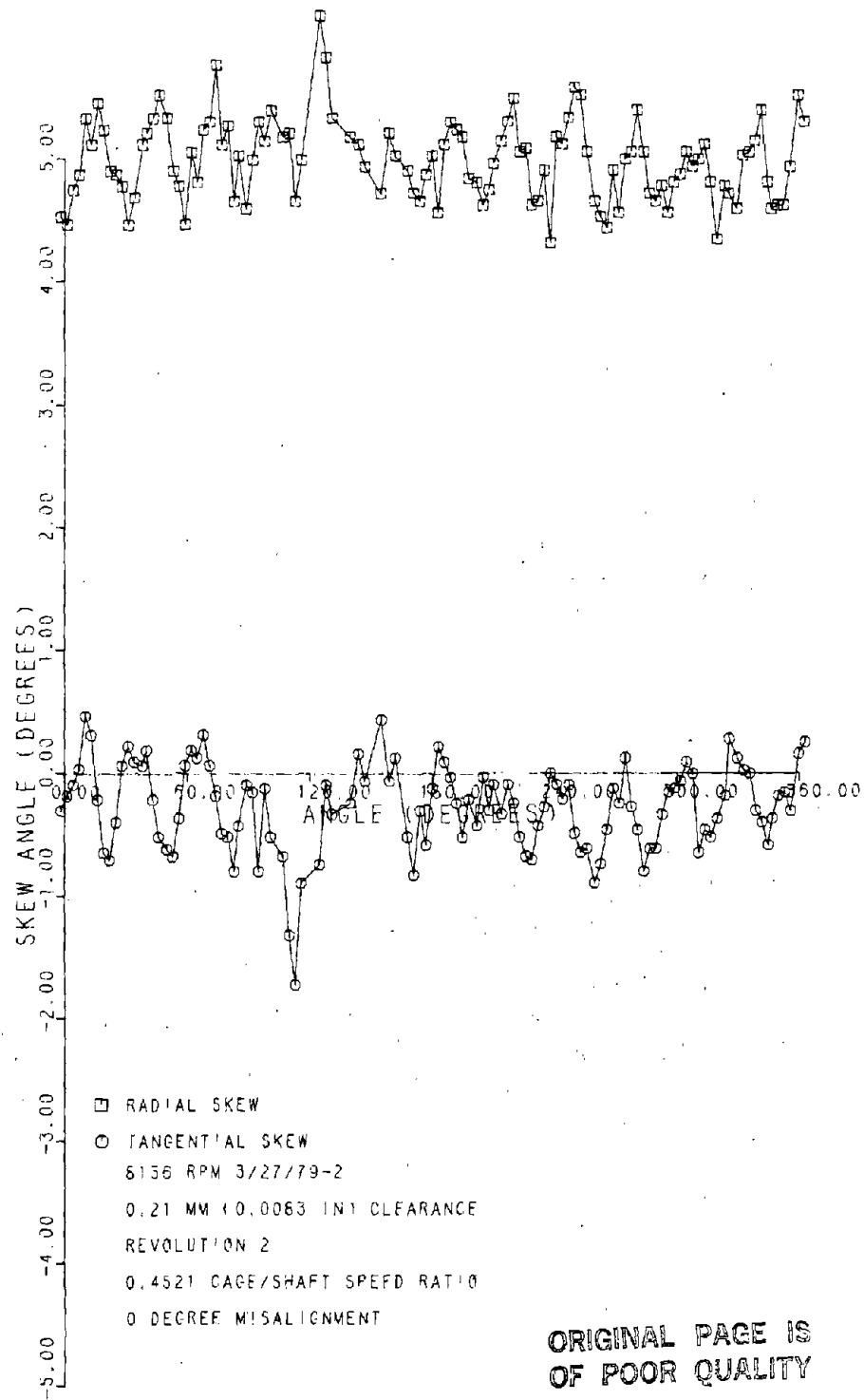


Figure 8b Roller Skew, 0.21 mm Clearance
Bearing, 0° Misalignment

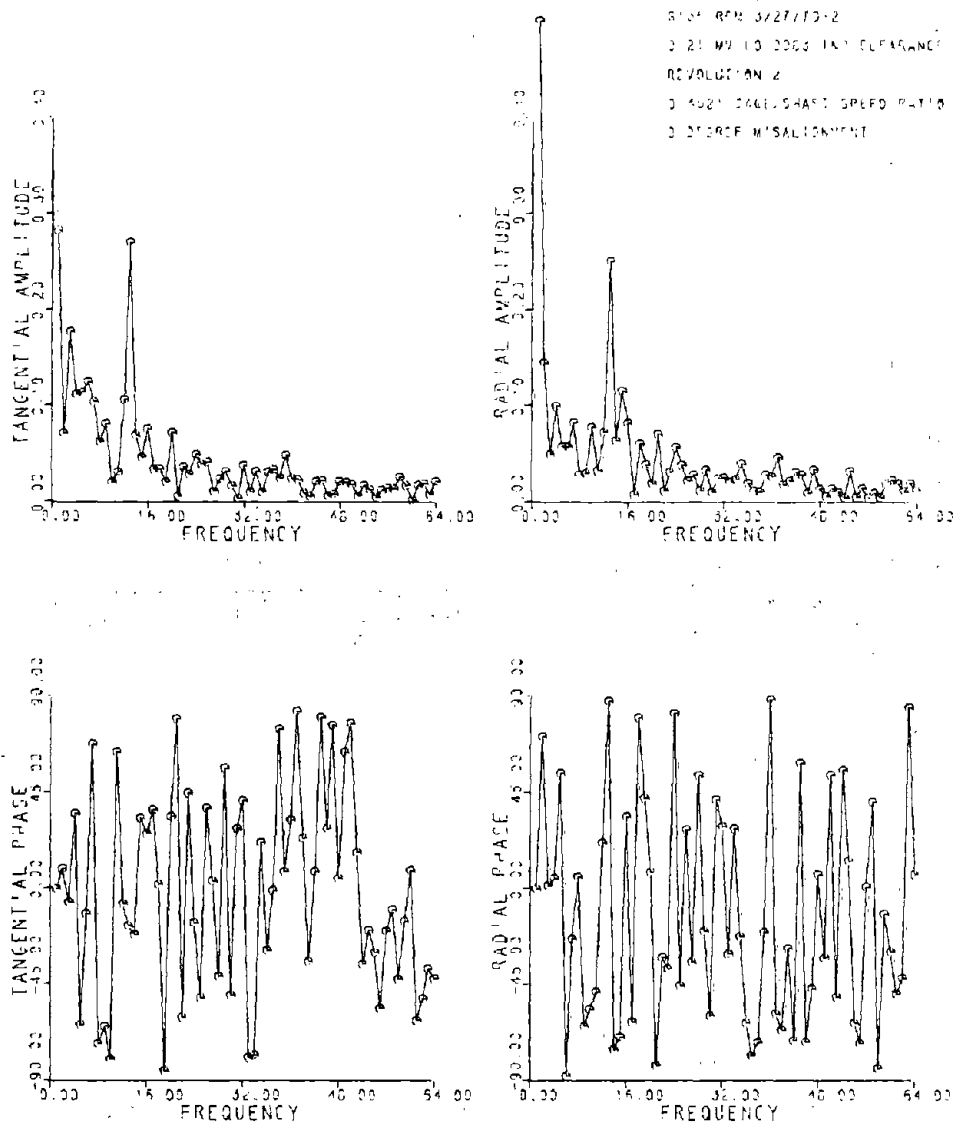


Figure 8bF. Fast Fourier Transform of Data in Figure 8b

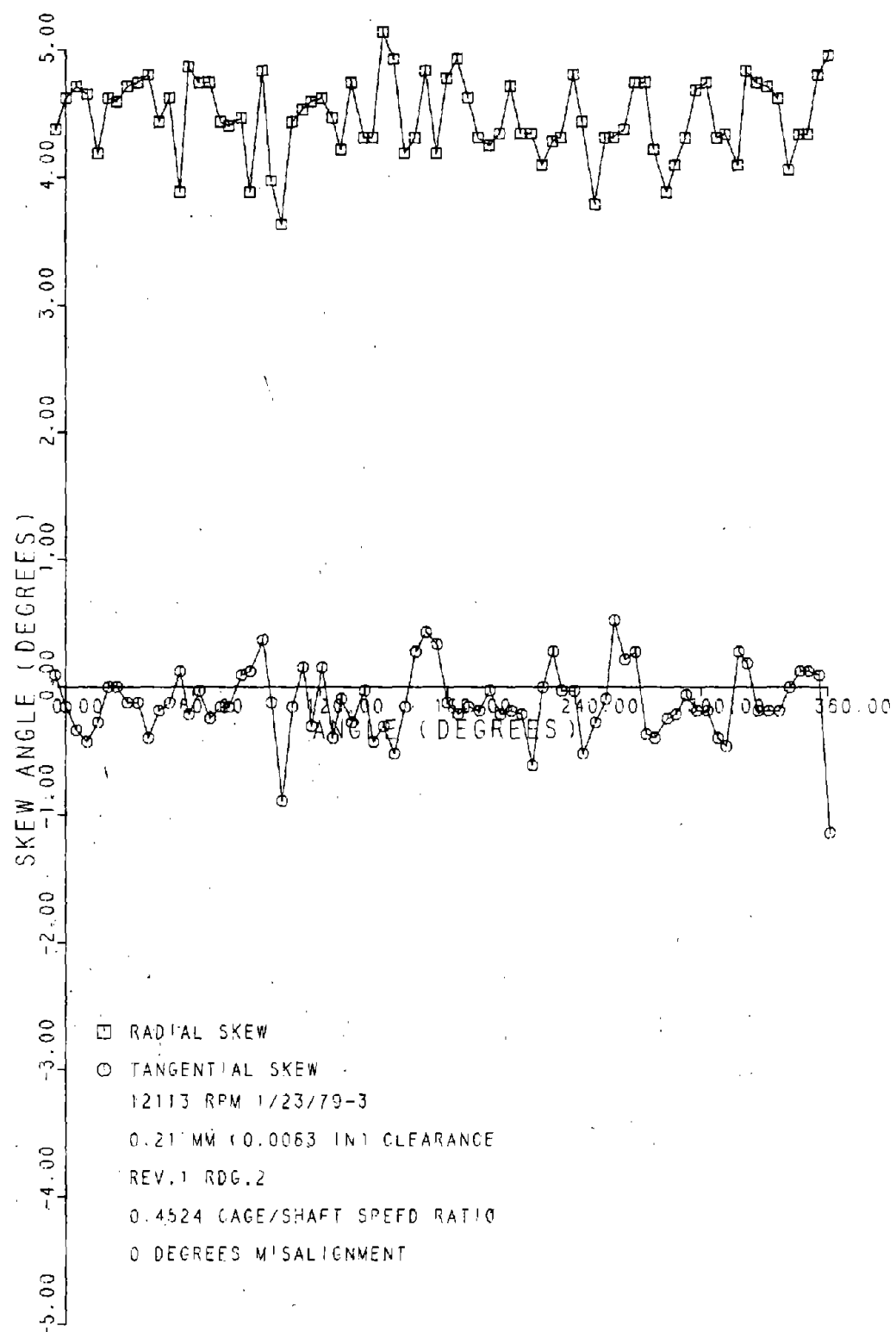


Figure 8c Roller Skew, 0.21 mm Clearance
Bearing, 0° Misalignment

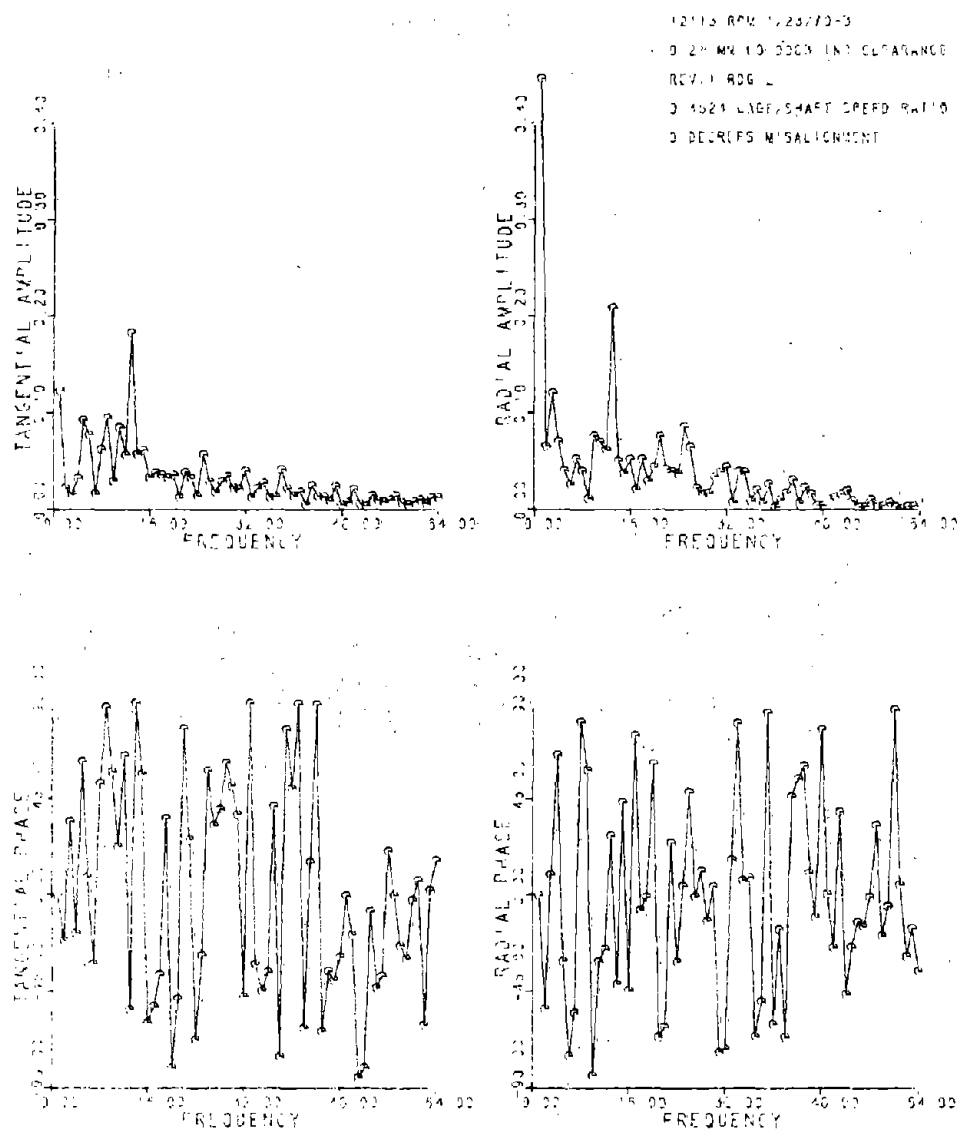


Figure 8cF Fast Fourier Transform of Data in Figure 8c

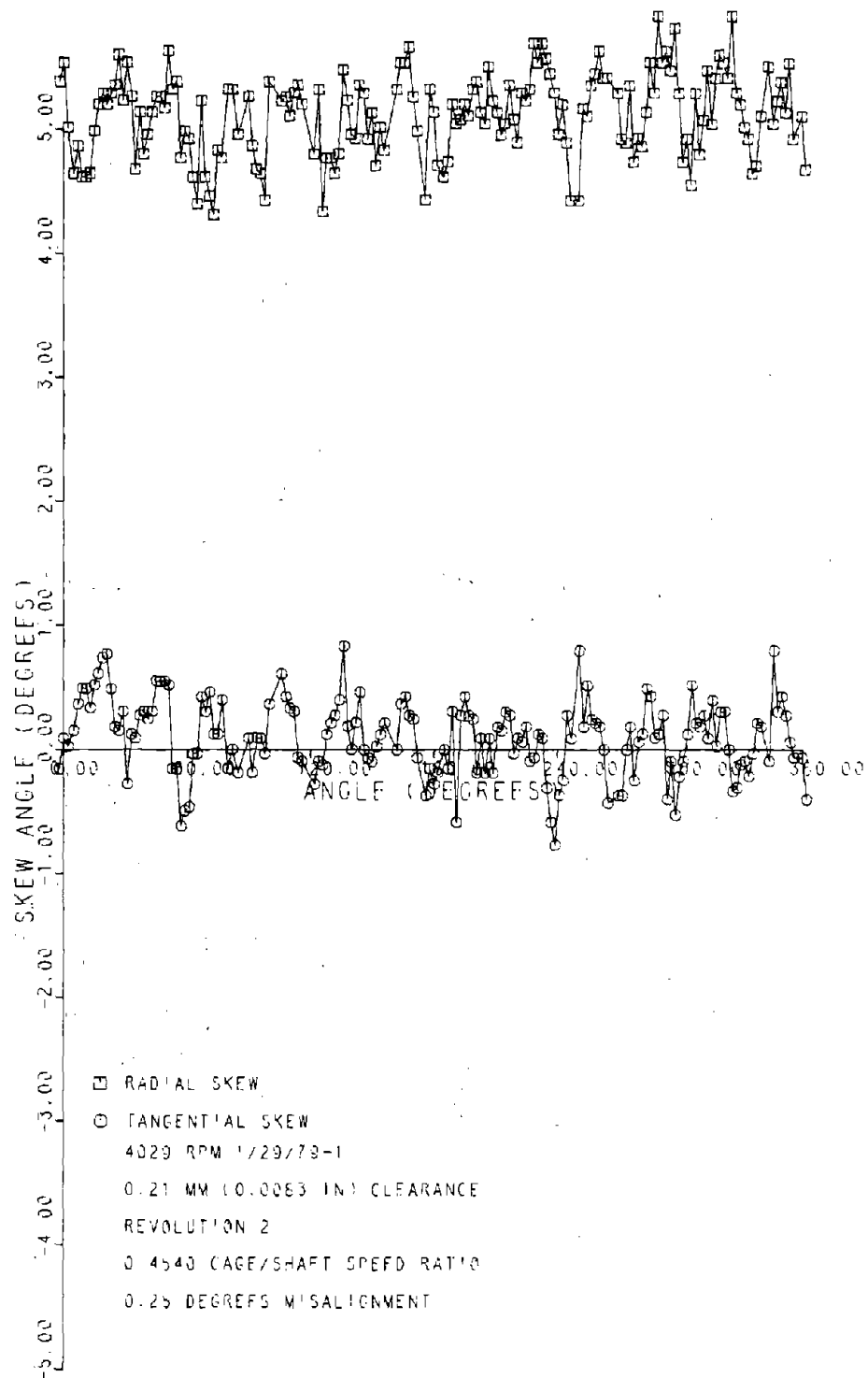
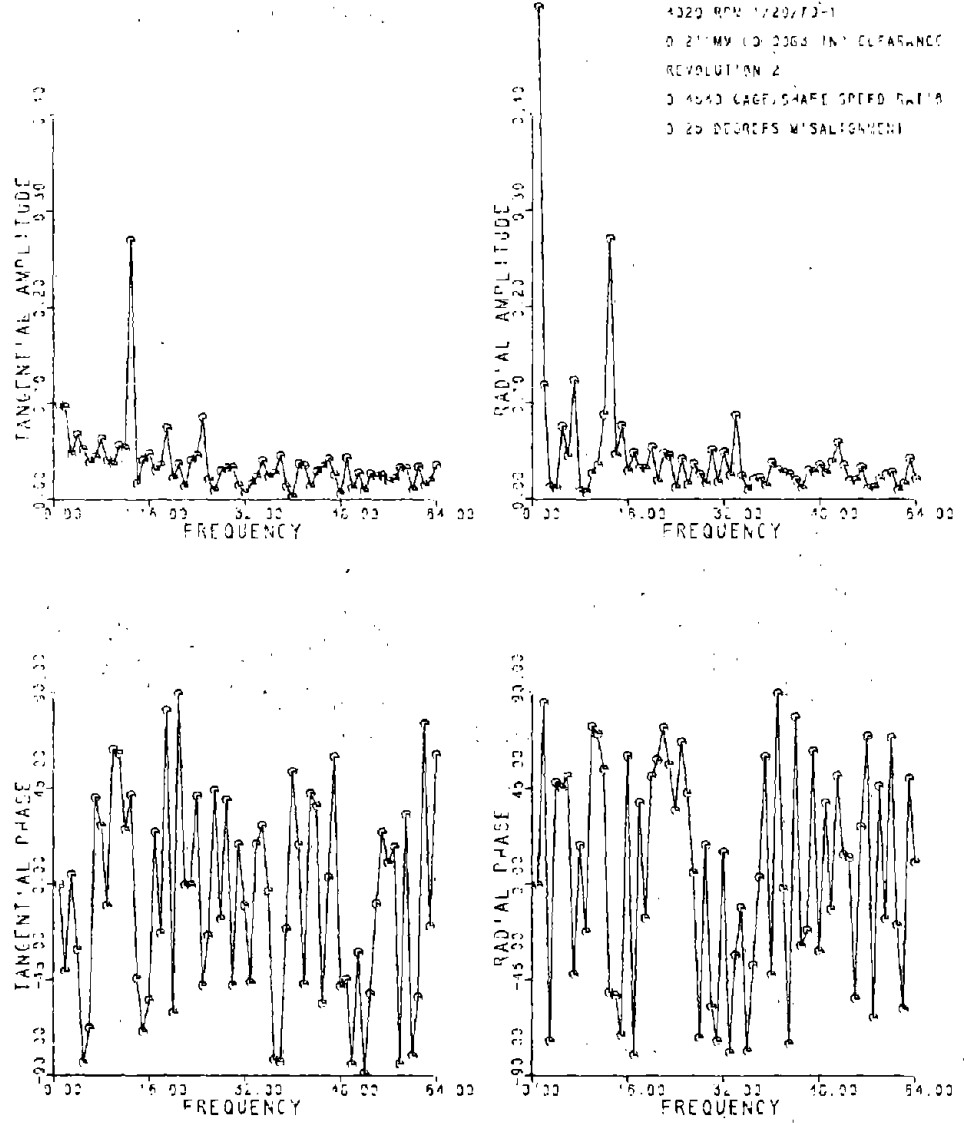


Figure 9a Roller Skew, 0.21 mm Clearance
Bearing, 0.25° Misalignment



ORIGINAL PAGE IS
 OF POOR QUALITY

Figure 9aF Fast Fourier Transform of Data in Figure 9a

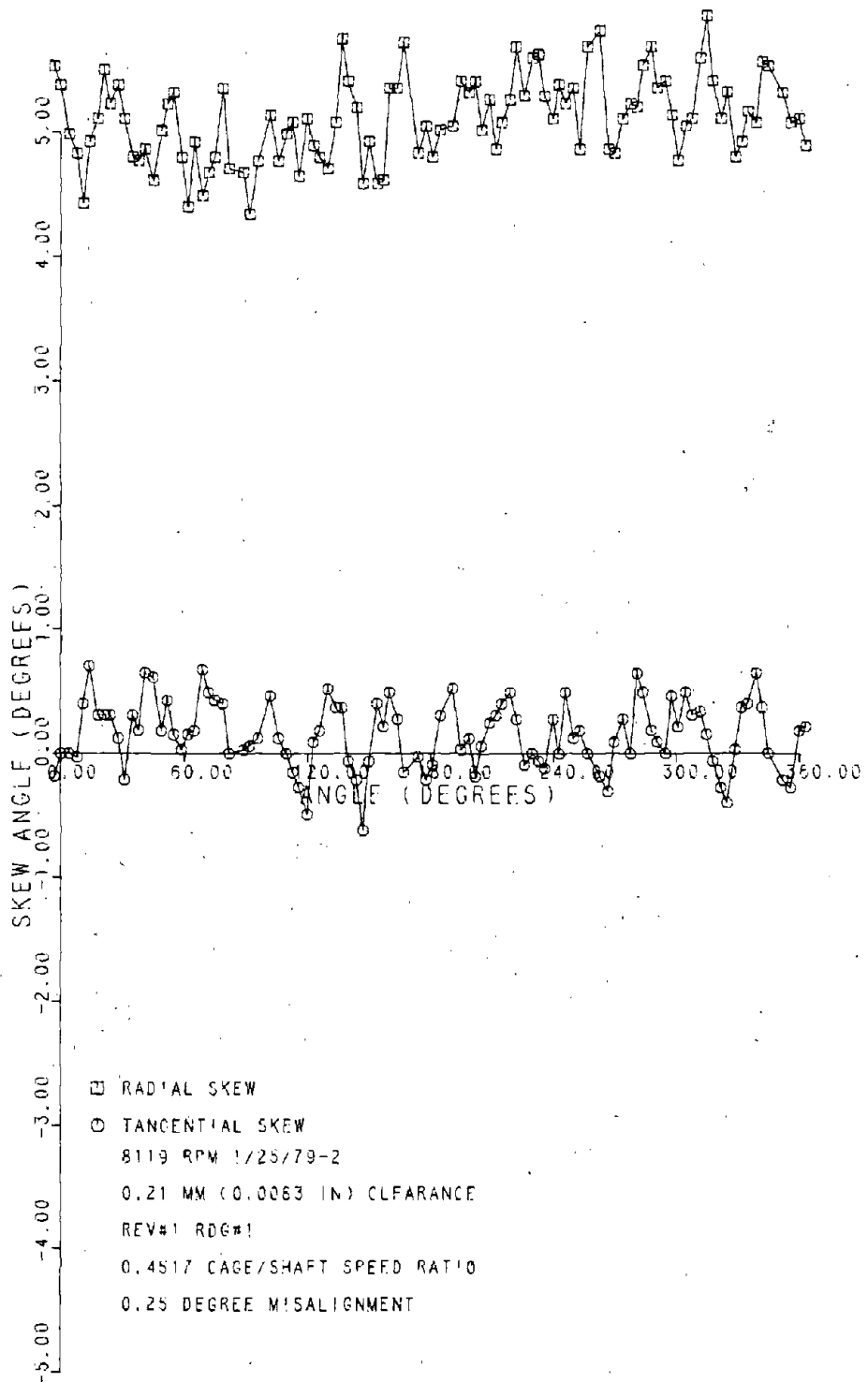


Figure 9b Roller Skew, 0.21 mm Clearance
Bearing, 0.25° Misalignment

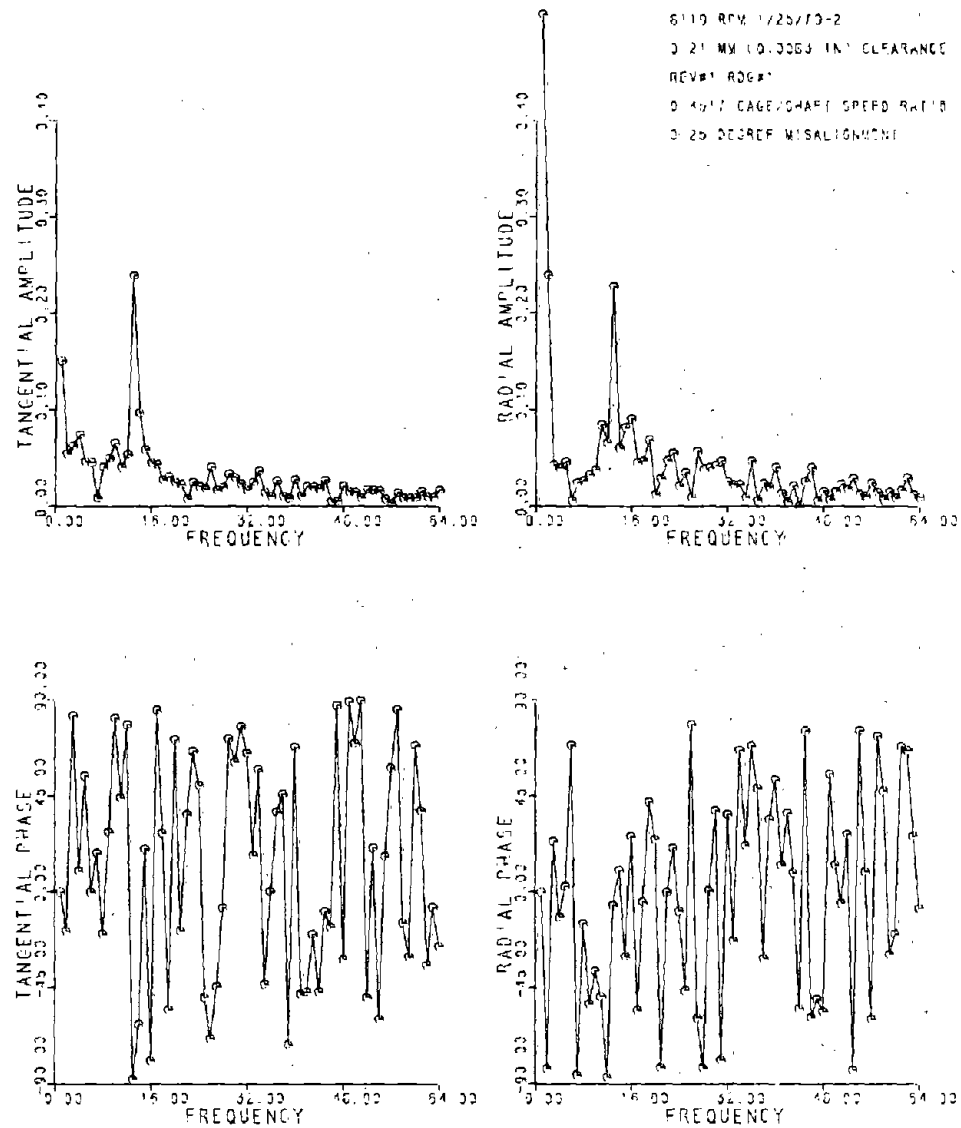


Figure 9bF Fast Fourier Transform of Data in Figure 9b

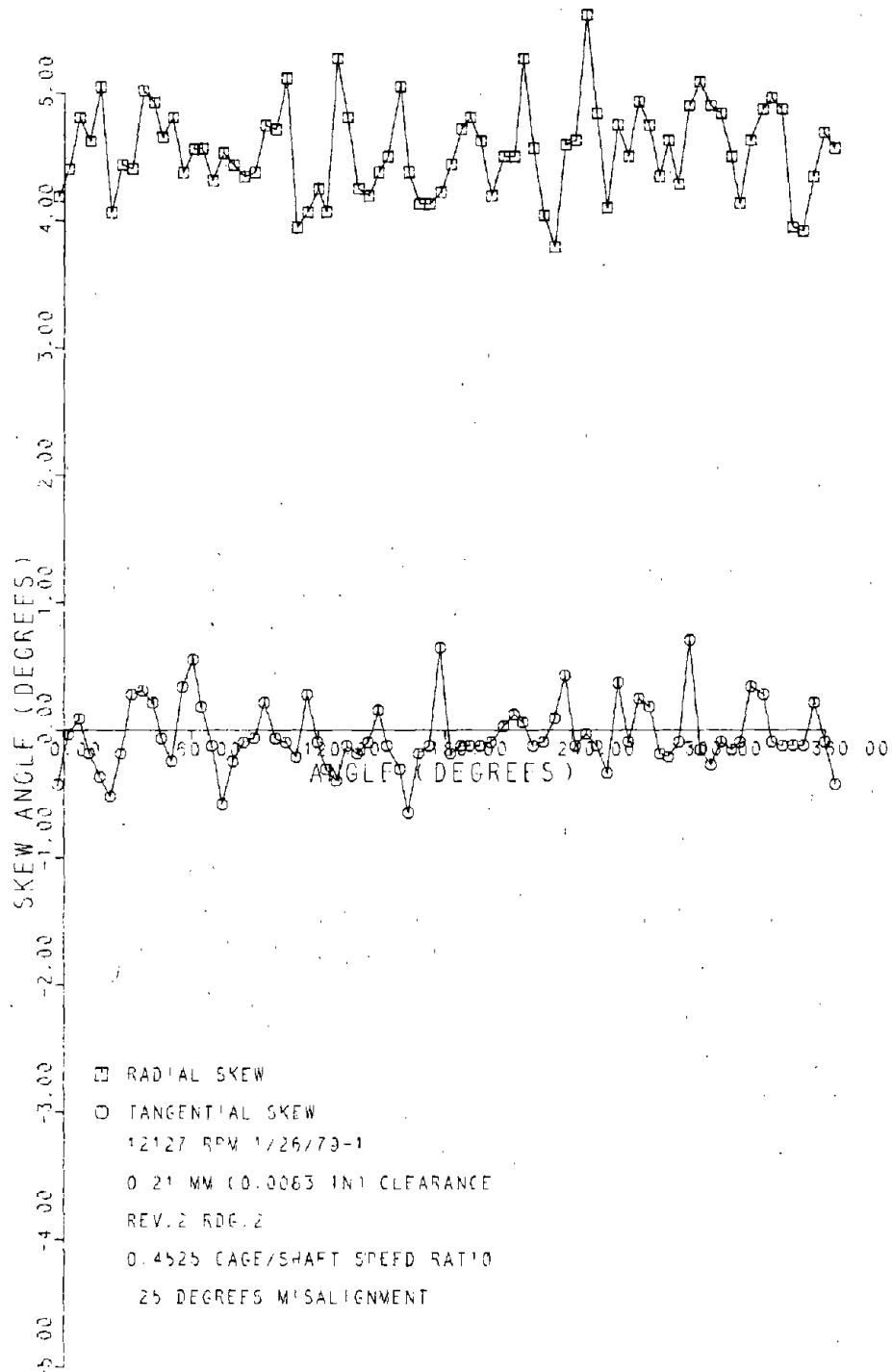


Figure 9c Roller Skew, 0.21 mm Clearance
Bearing, 0.25° Misalignment

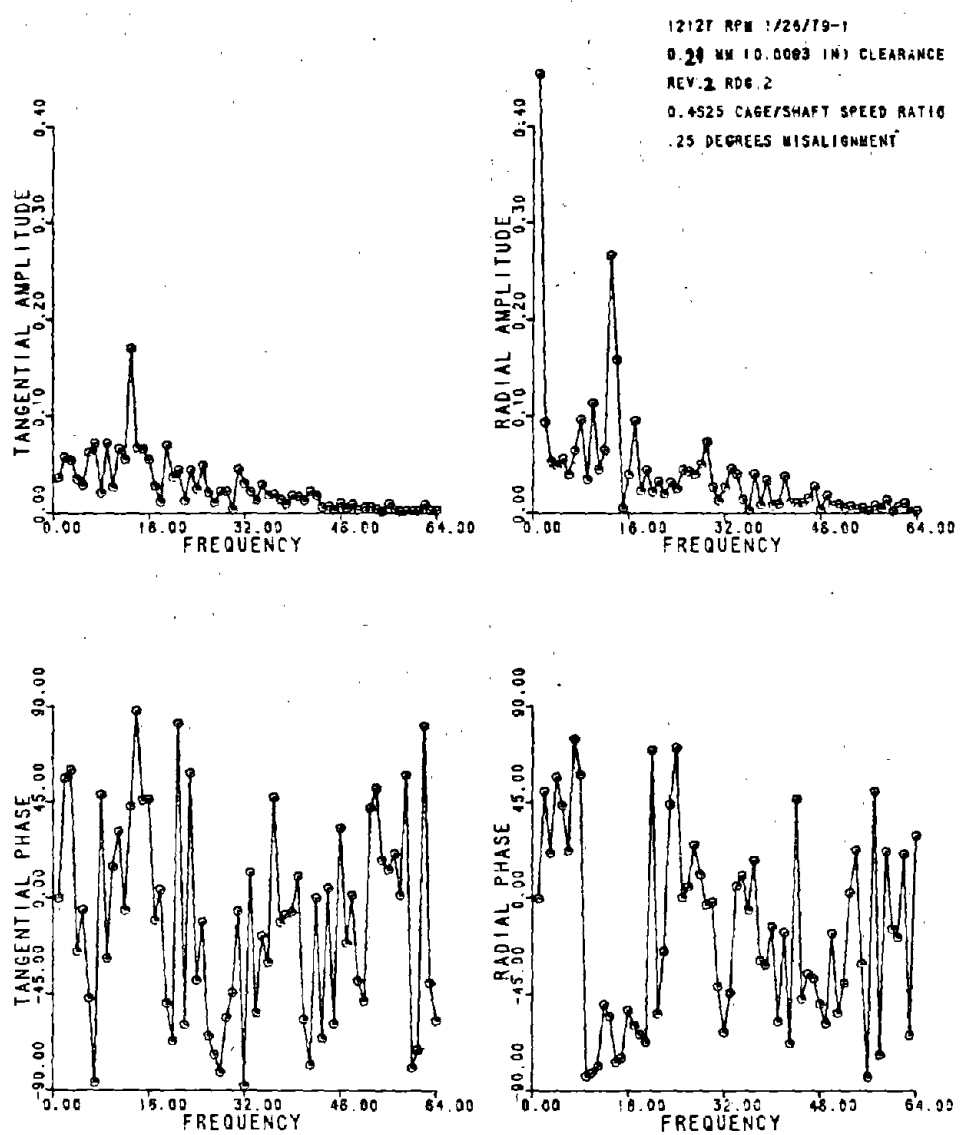


Figure 9cF Fast Fourier Transform of Data in Figure 9c

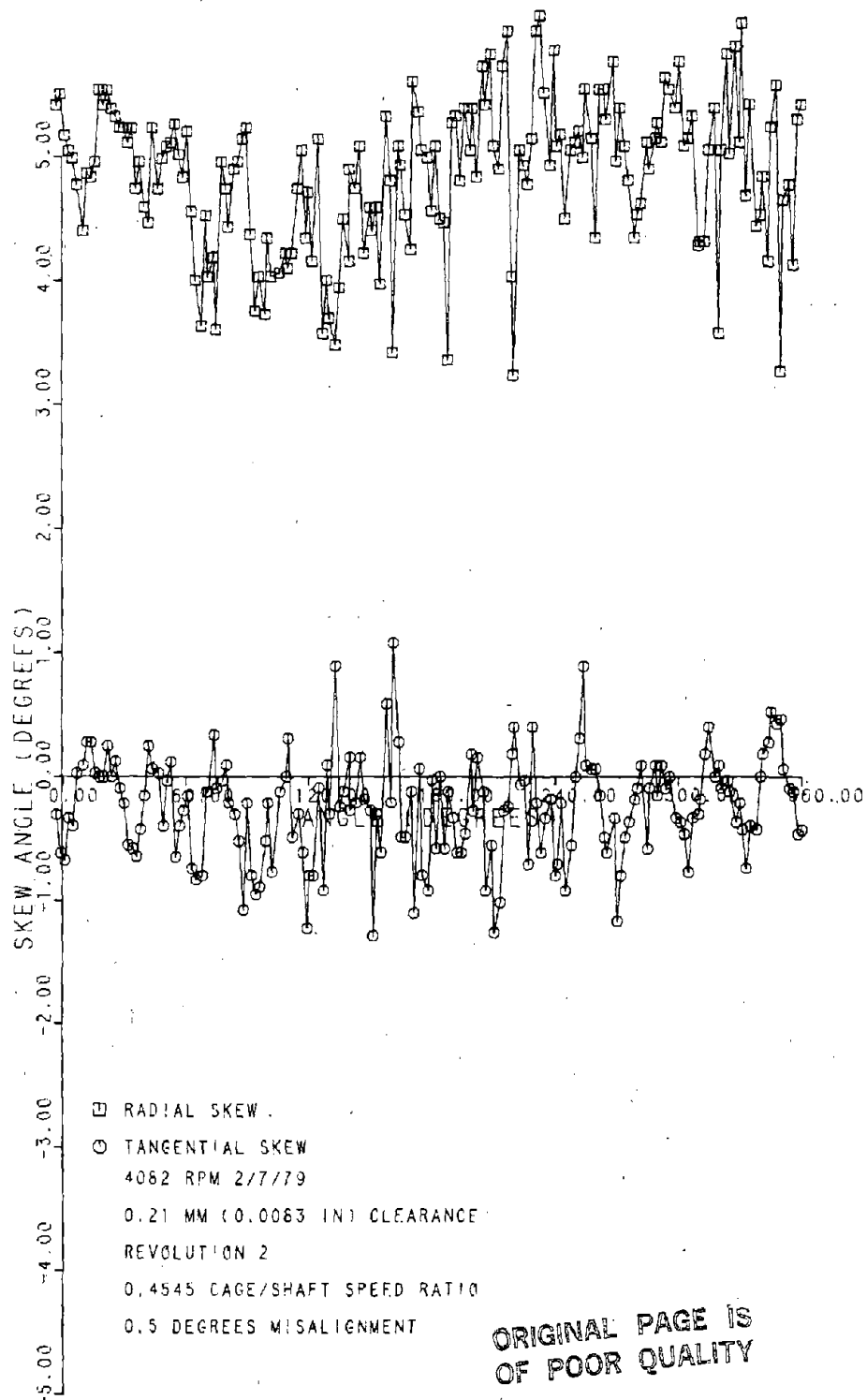


Figure 10a. Roller Skew, 0.21 mm Clearance
 Bearing, 0.50° Misalignment

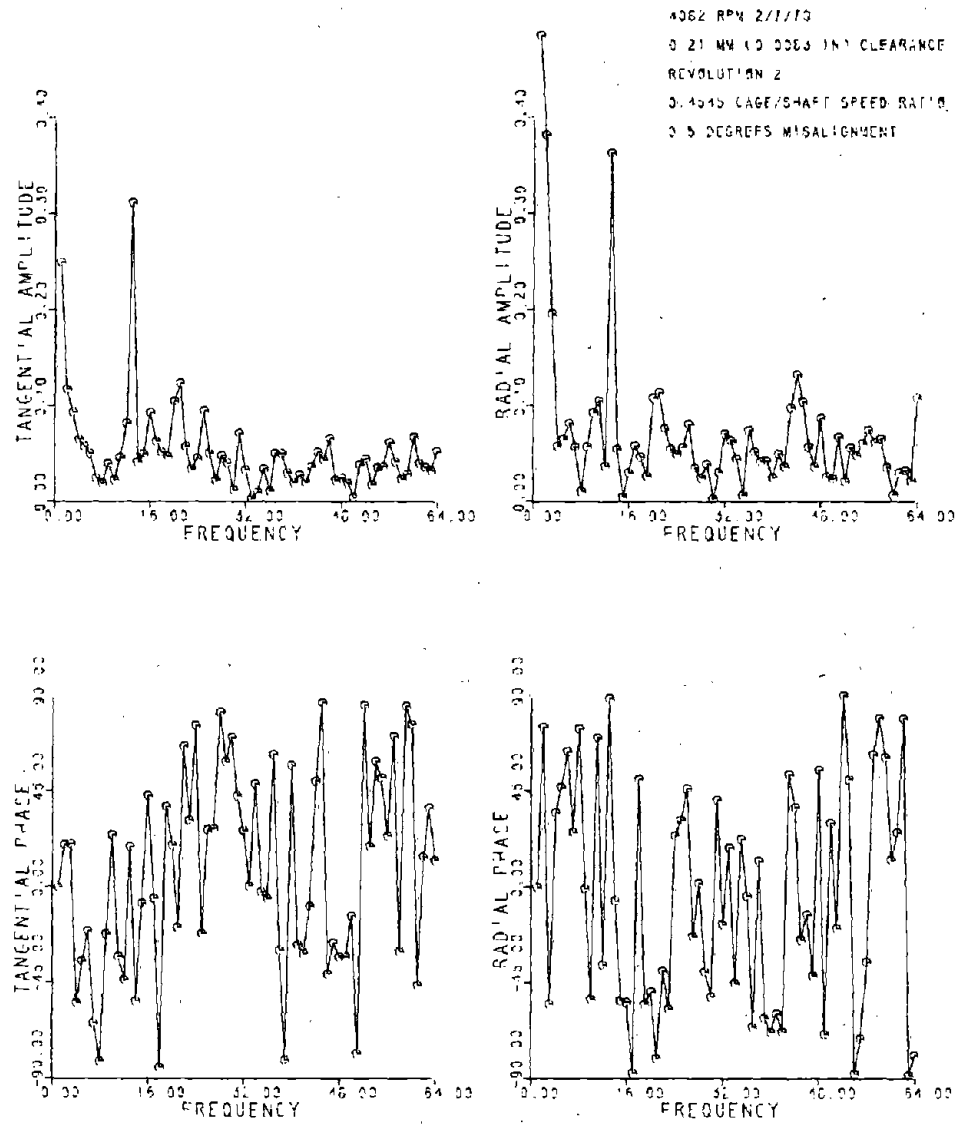


Figure 10aF Fast Fourier Transform of Data in Figure 10a

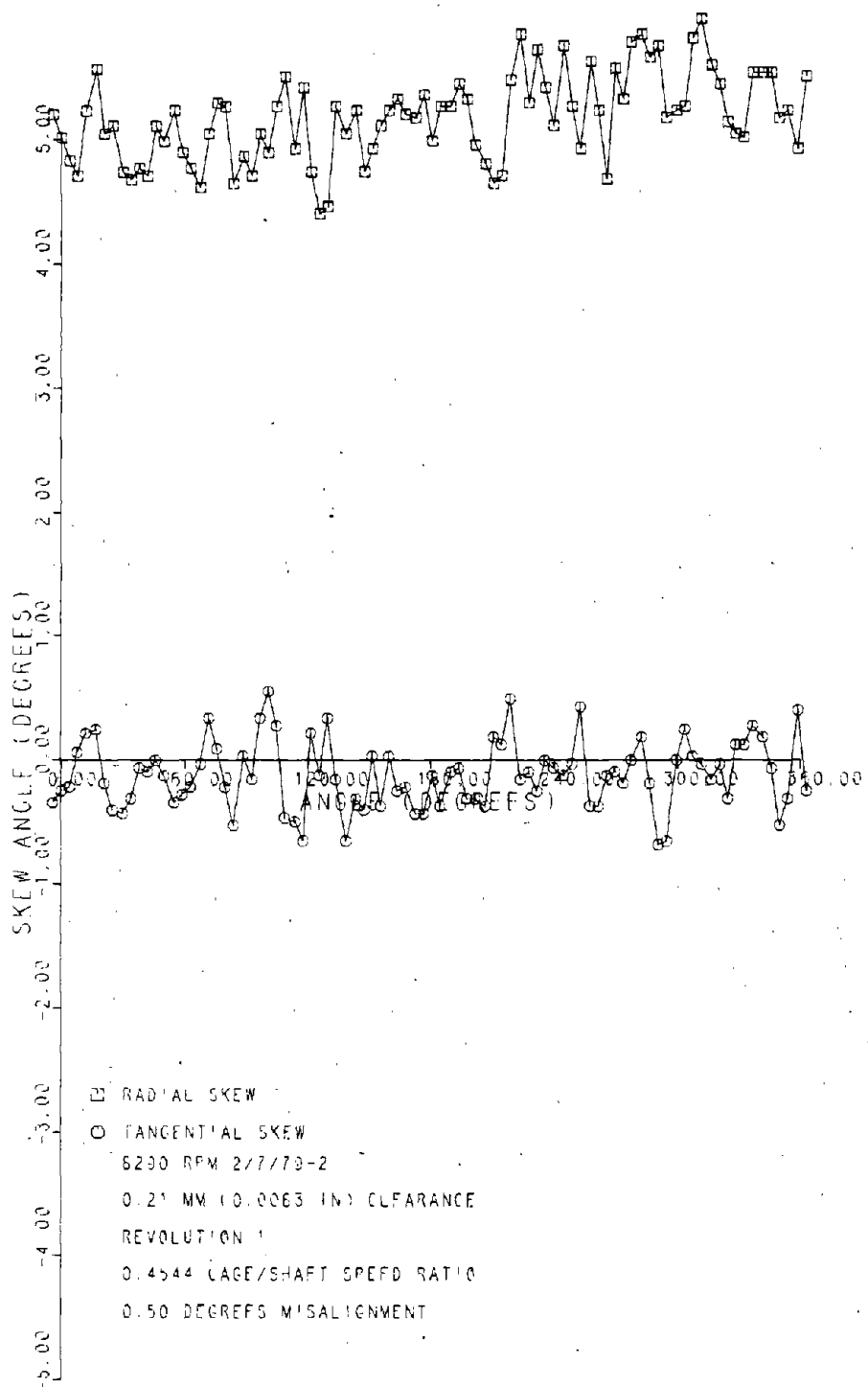


Figure 10b-1 Roller Skew, 0.21 mm Clearance
Bearing, 0.50° Misalignment

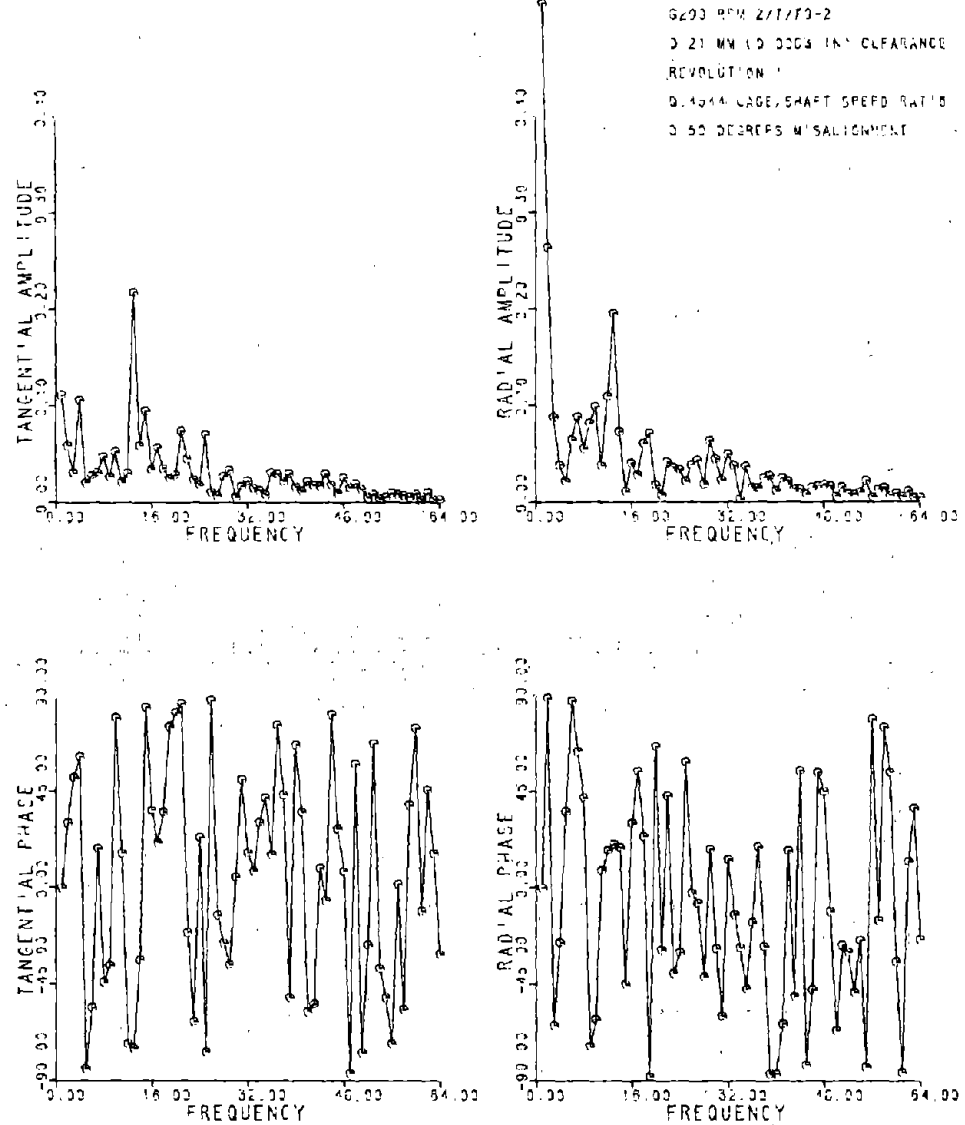


Figure 10b-1F Fast Fourier Transform of Data in Figure 10b-1

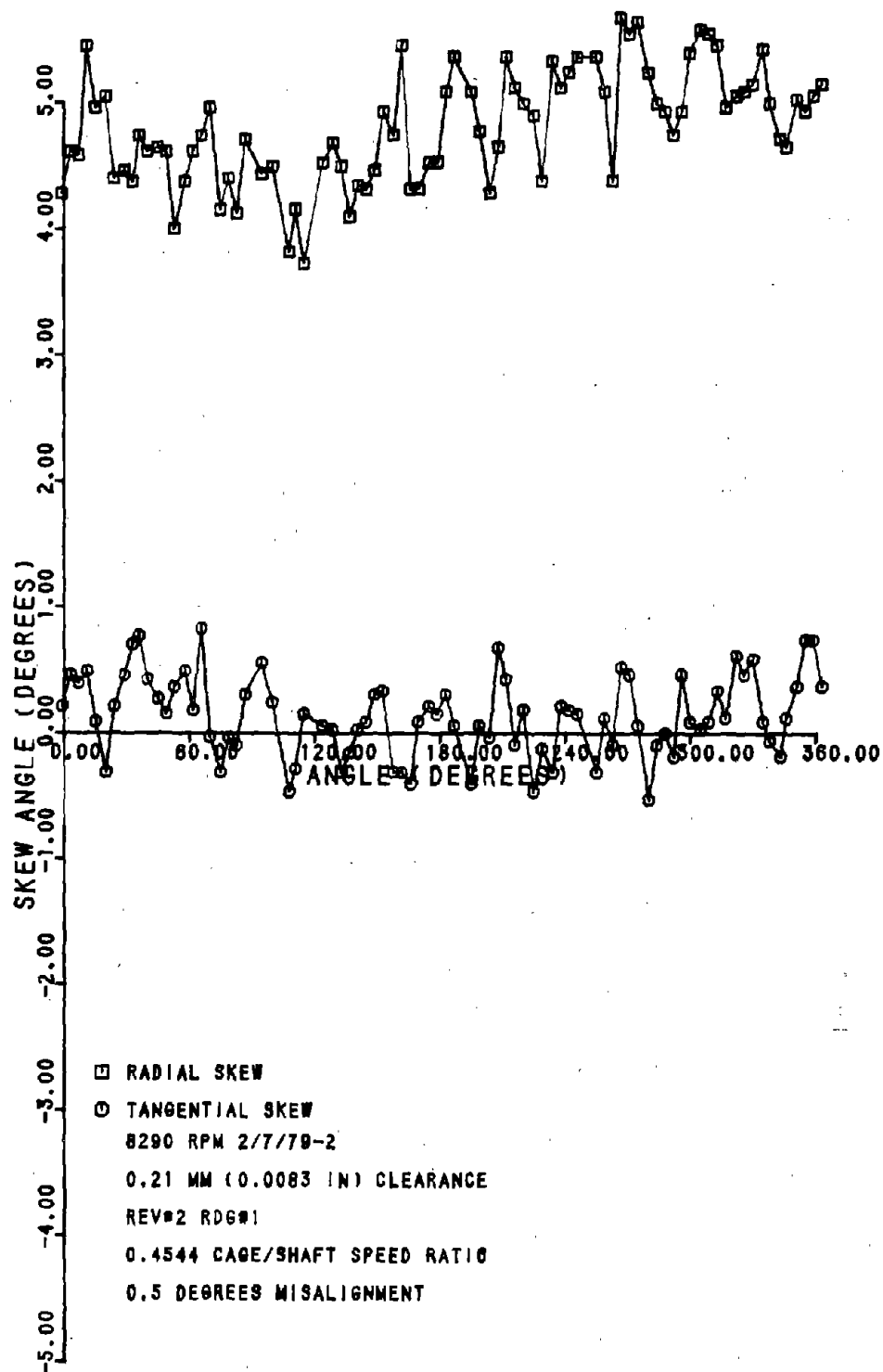
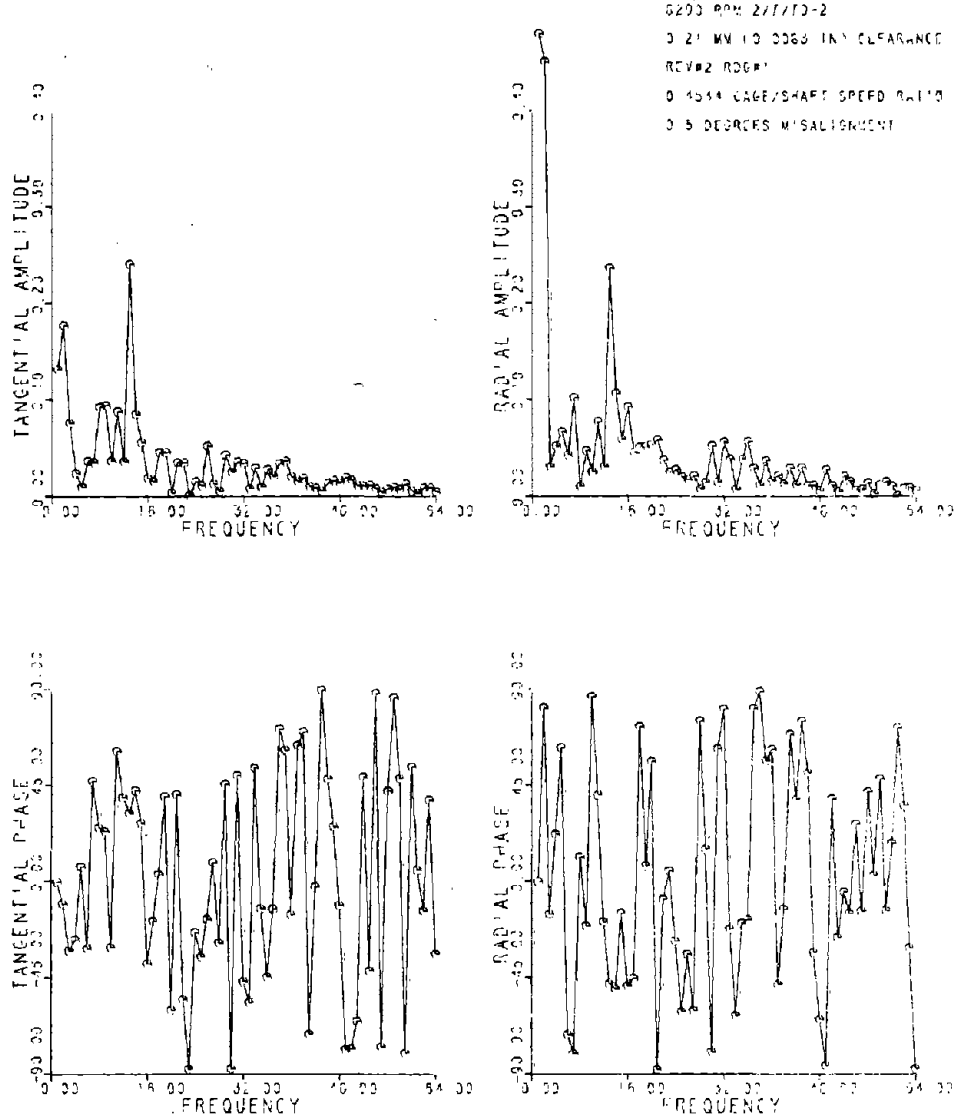


Figure 10b-2 Roller Skew, 0.21 mm Clearance
Bearing, 0.50° Misalignment



ORIGINAL PAGE IS
 OF POOR QUALITY

ORIGINAL PAGE IS
 OF POOR QUALITY

Figure 10b-2F Fast Fourier Transform of
 Data in Figure 10b-2

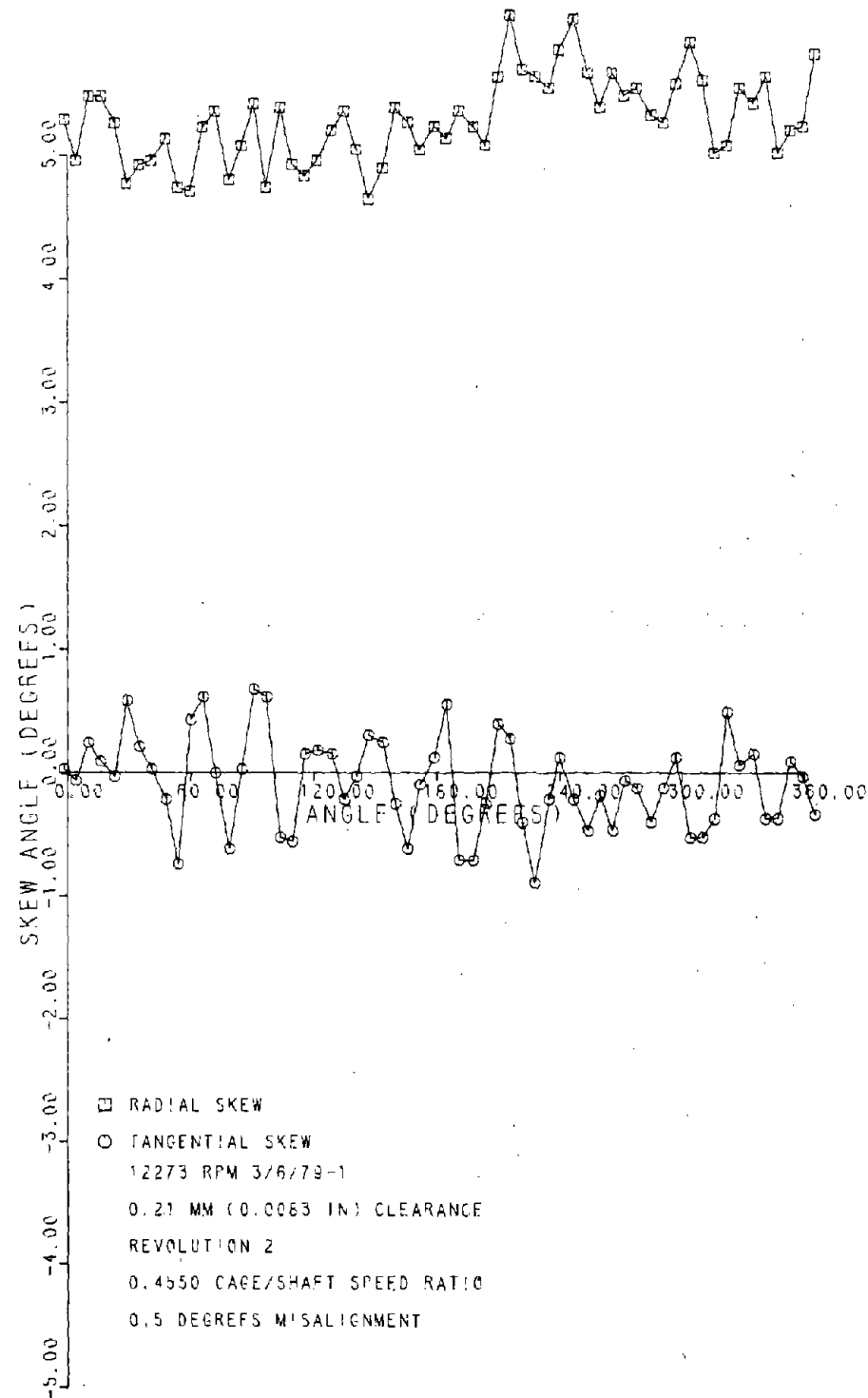


Figure 10c-1 Roller Skew, 0.21 mm Clearance
Bearing, 0.50° Misalignment

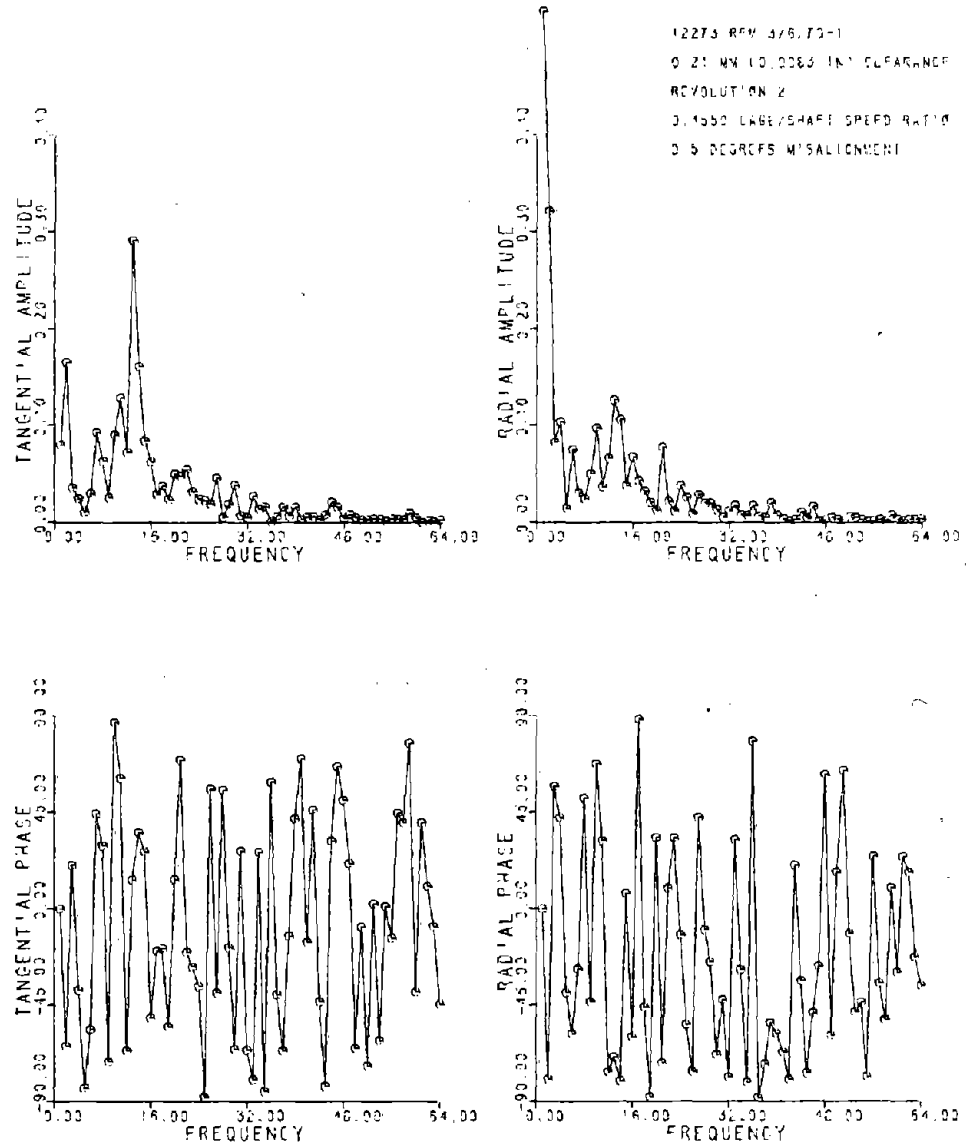


Figure 10c-1F Fast Fourier Transform of Data in Figure 10c-1

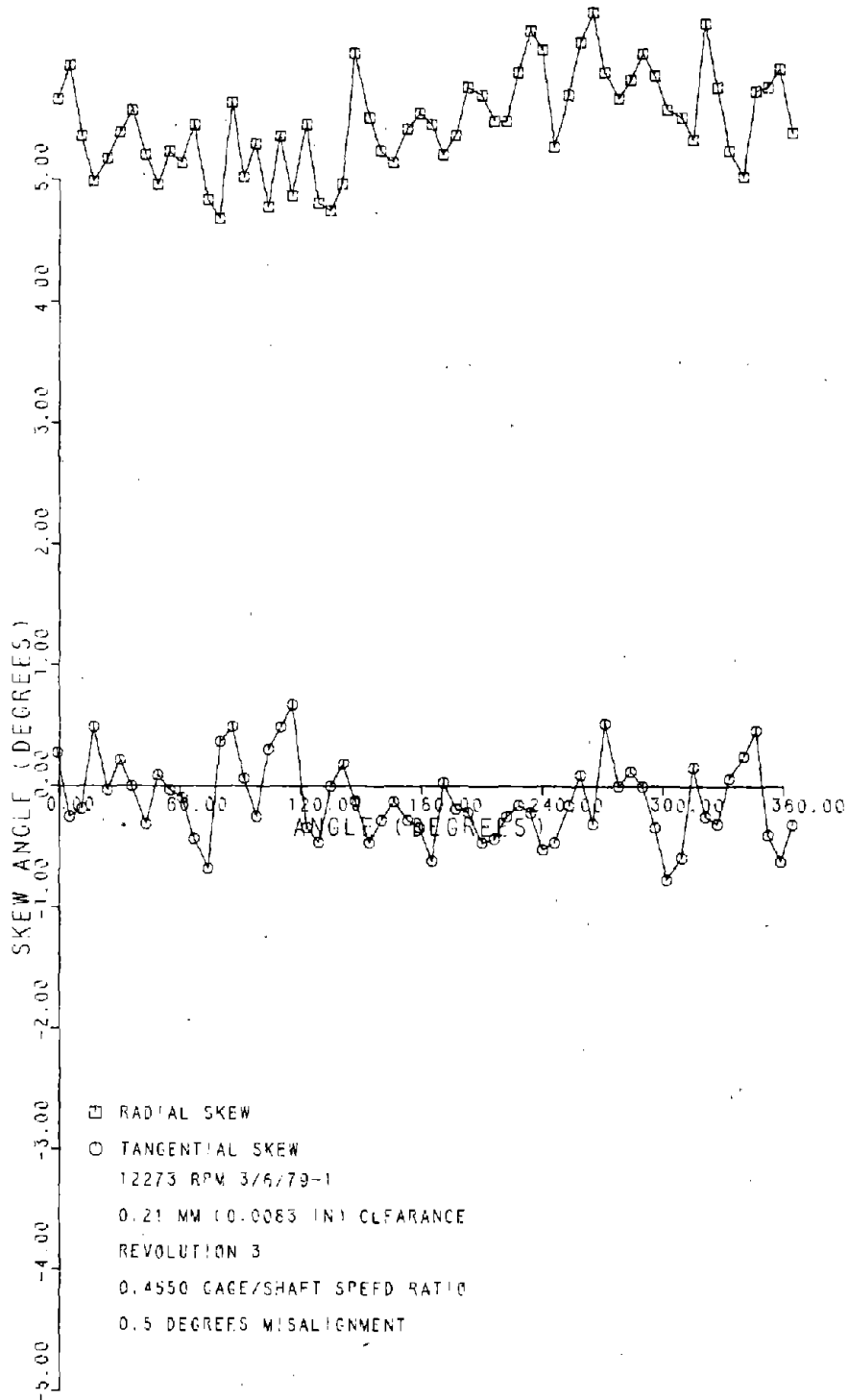


Figure 10c-2 Roller Skew, 0.21 mm Clearance
Bearing, 0.50° Misalignment

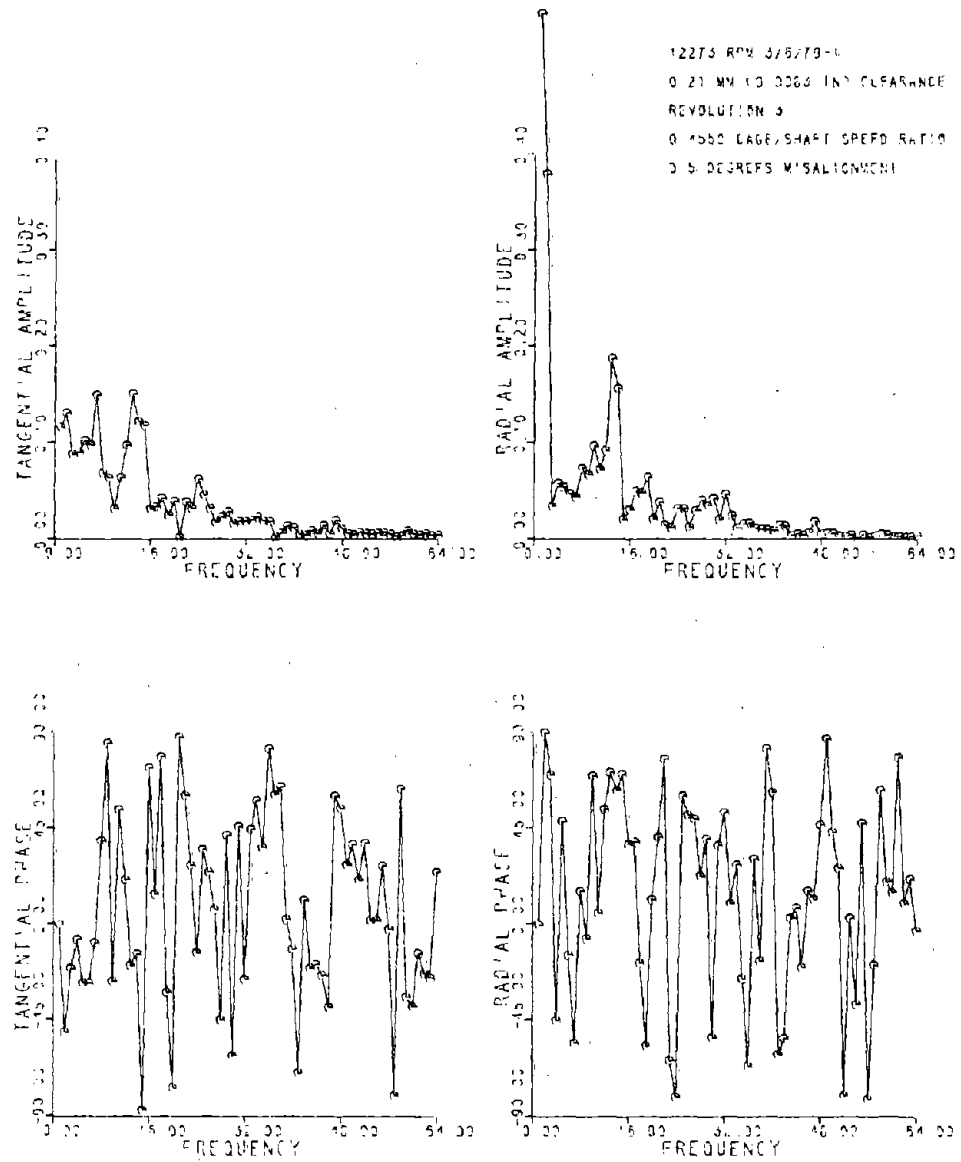


Figure 10c-2F Fast Fourier Transform of Data in Figure 10c-2

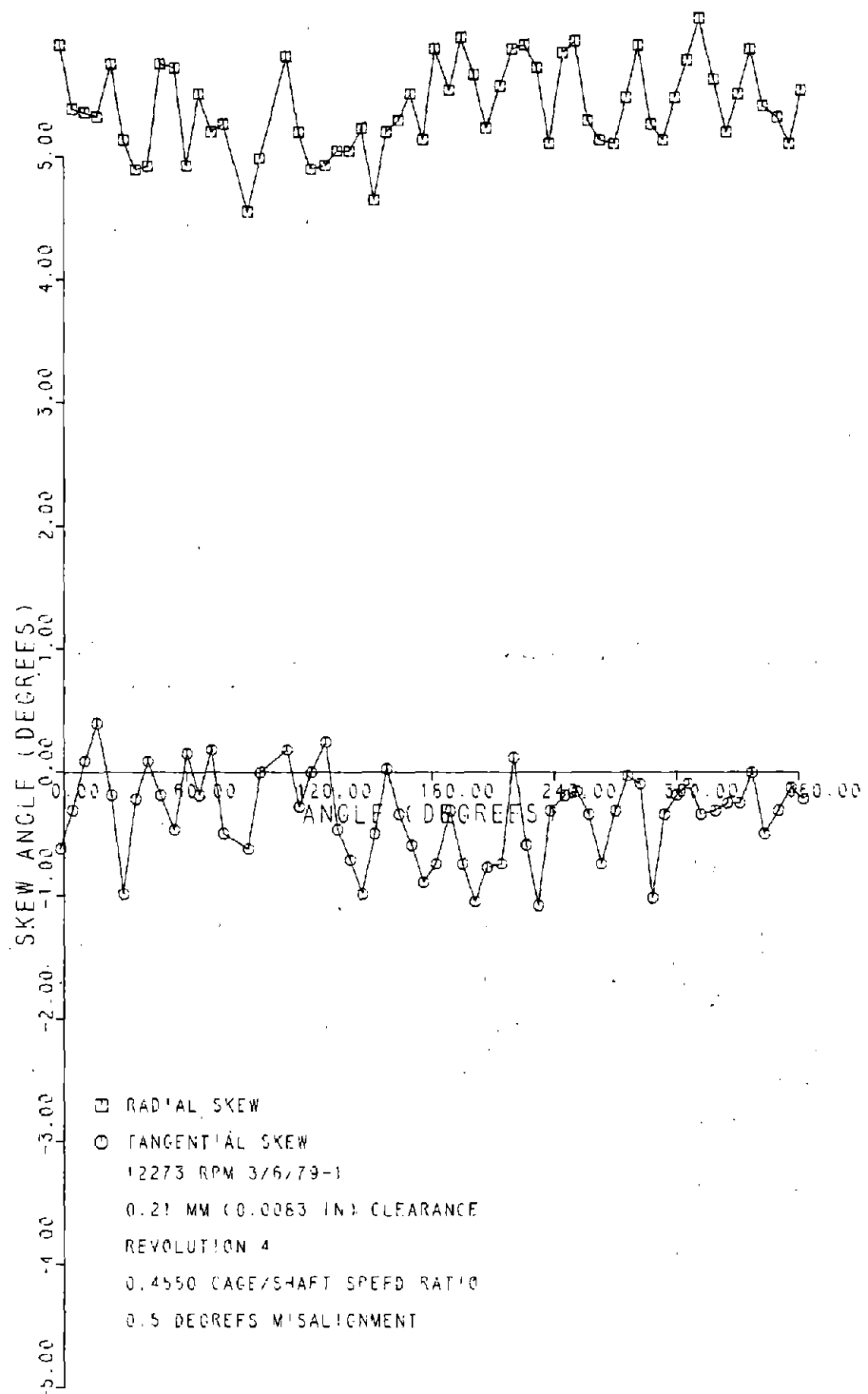
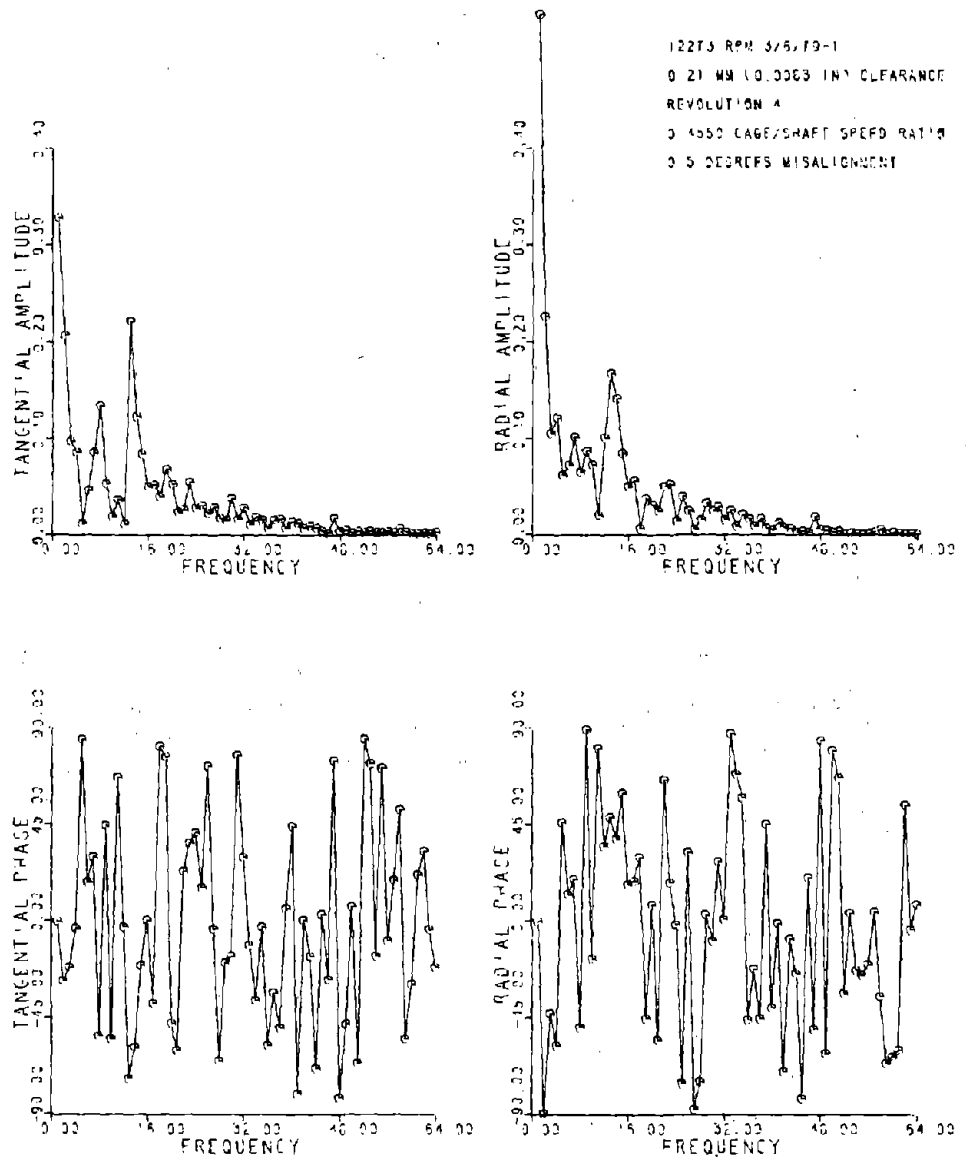


Figure 10c-3 Roller Skew, 0.21 mm Clearance
Bearing, 0.50° Misalignment



ORIGINAL PAGE IS
 OF POOR QUALITY

Figure 10c-3F Fast Fourier Transform of
 Data in Figure 10c-3

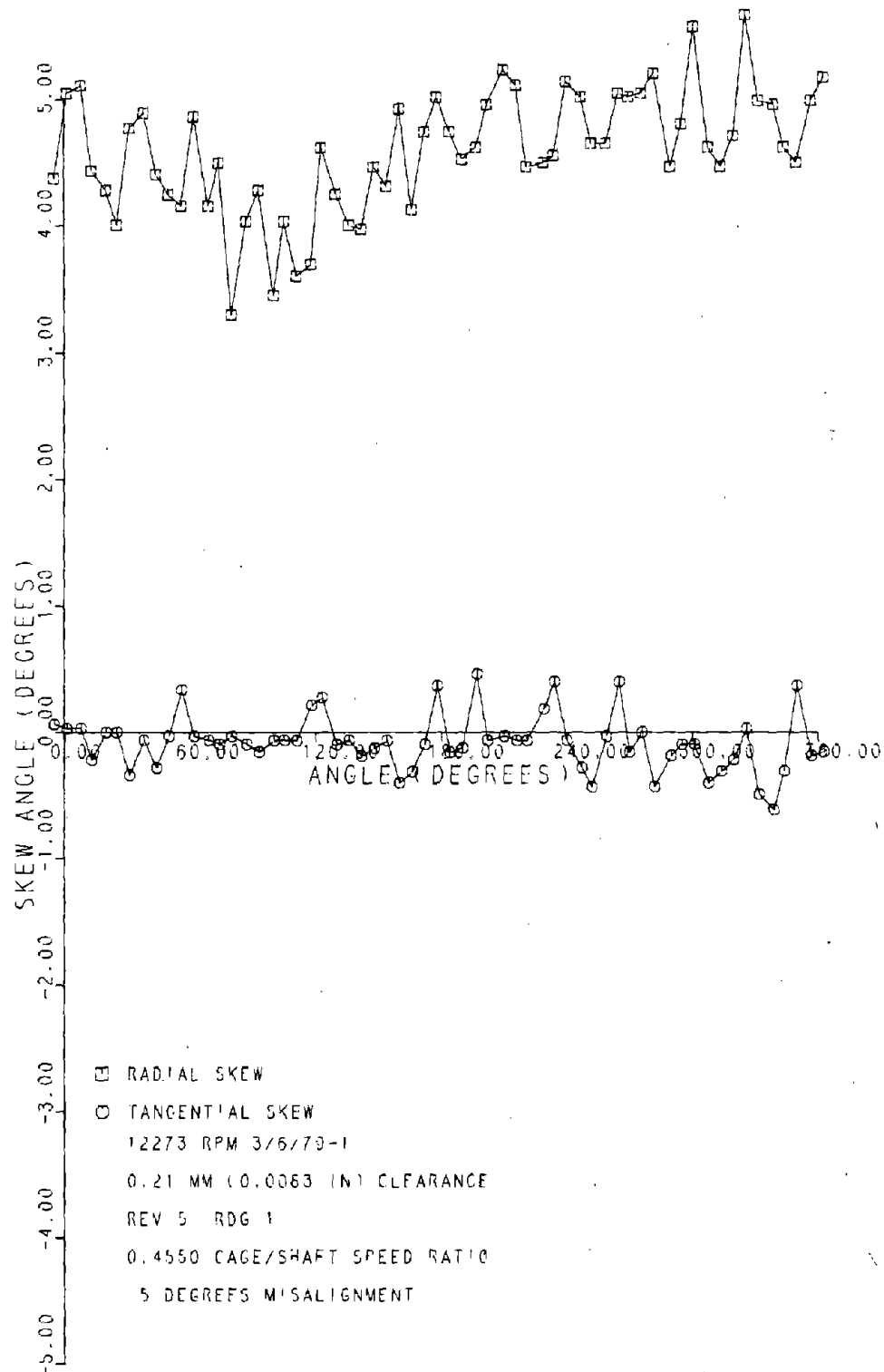


Figure 10c-4 Roller Skew, 0.21 mm Clearance
Bearing, 0.50° Misalignment

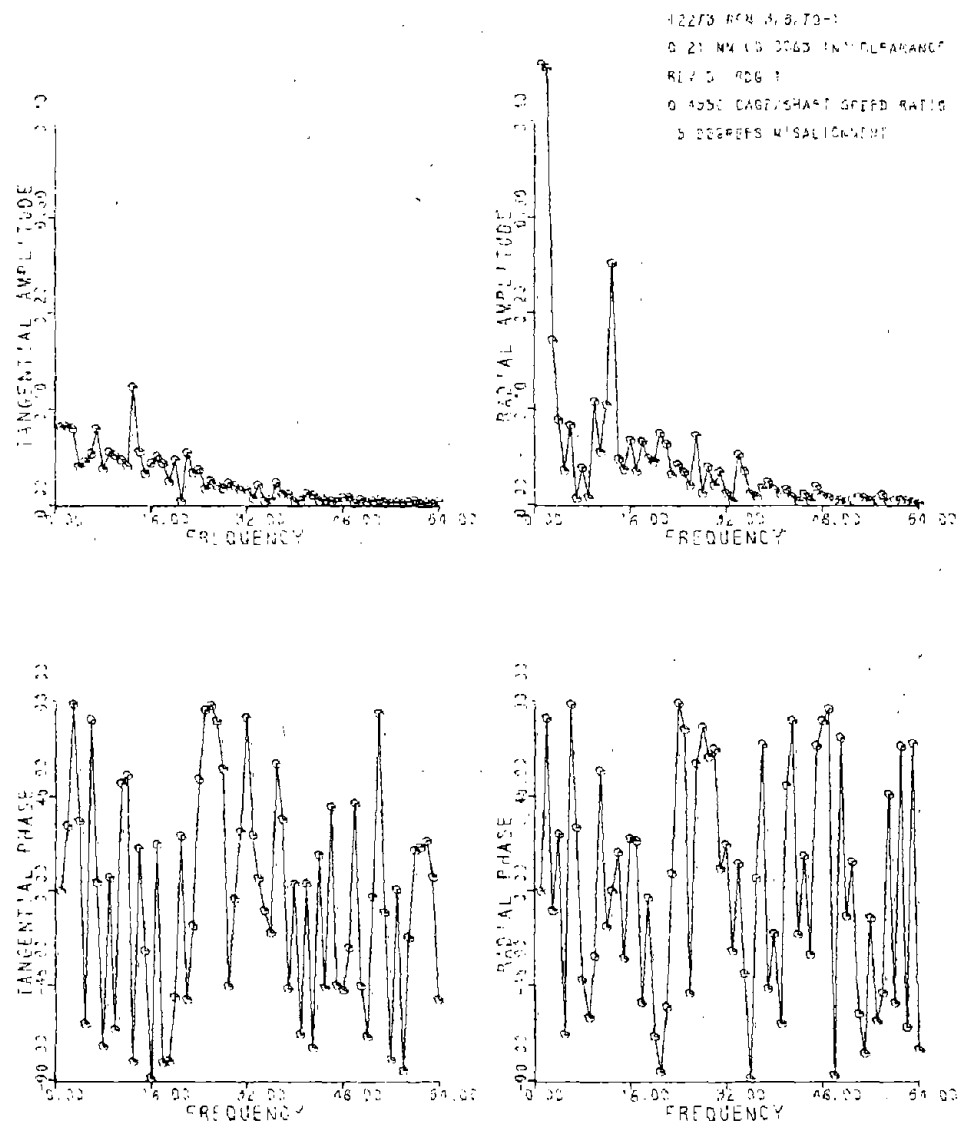


Figure 10c-4F Fast Fourier Transform of Data in Figure 10c-4

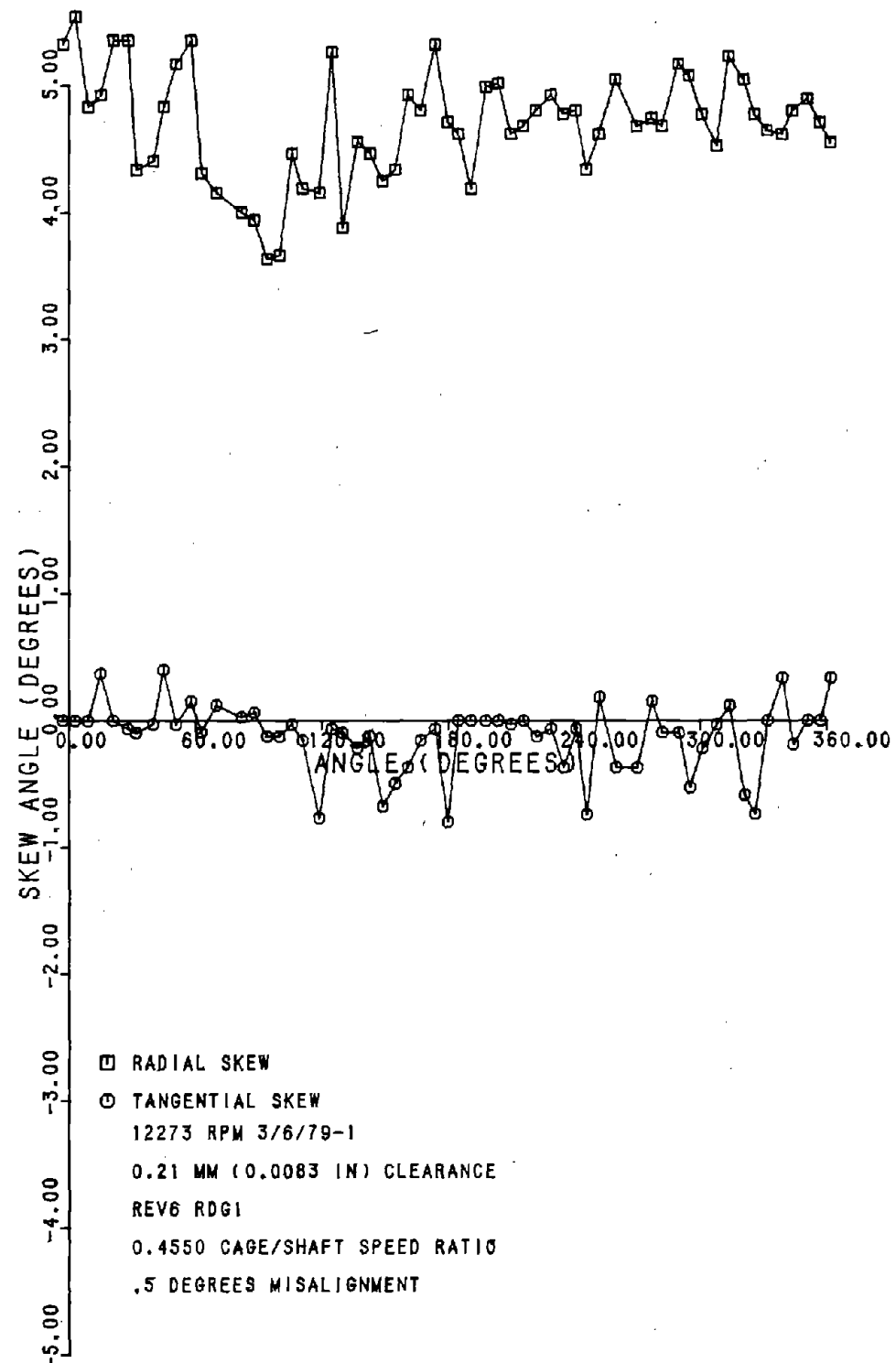
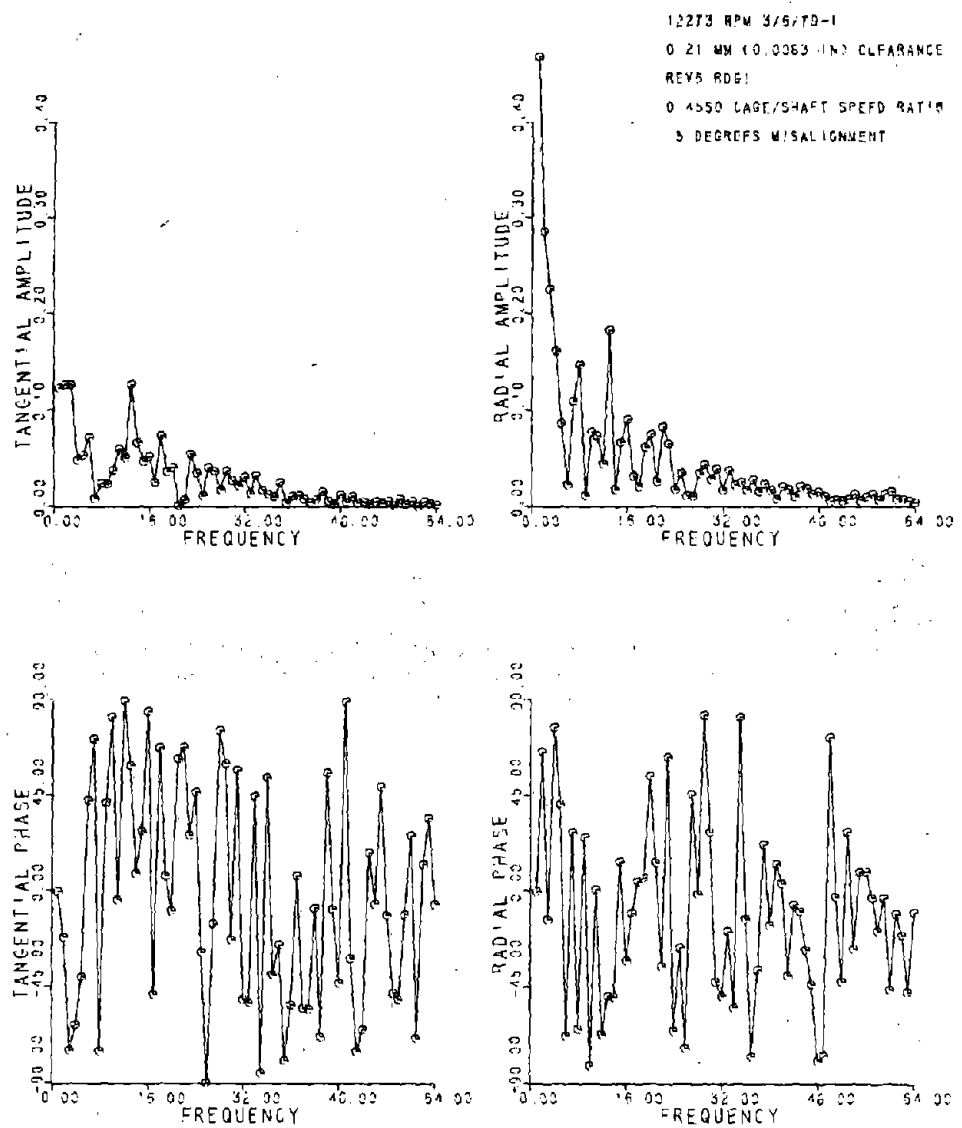


Figure 10c-5 Roller Skew, 0.21 mm Clearance Bearing, 0.50° Misalignment



ORIGINAL PAGE IS
 OF POOR QUALITY

Figure 10c-5F Fast Fourier Transform of
 Data in Figure 10c-5

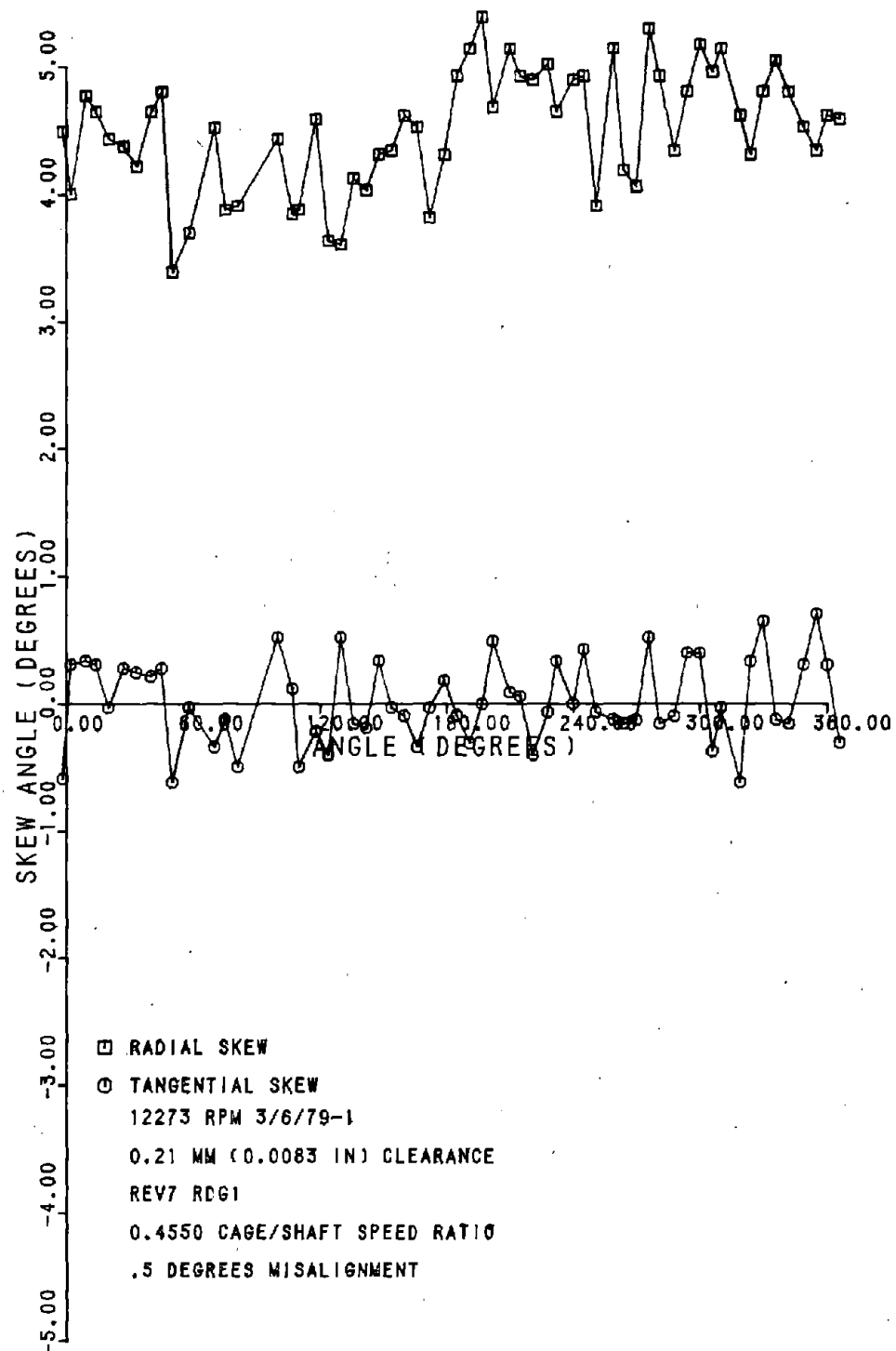


Figure 10c-6 Roller Skew, 0.21 mm Clearance
Bearing, 0.50° Misalignment

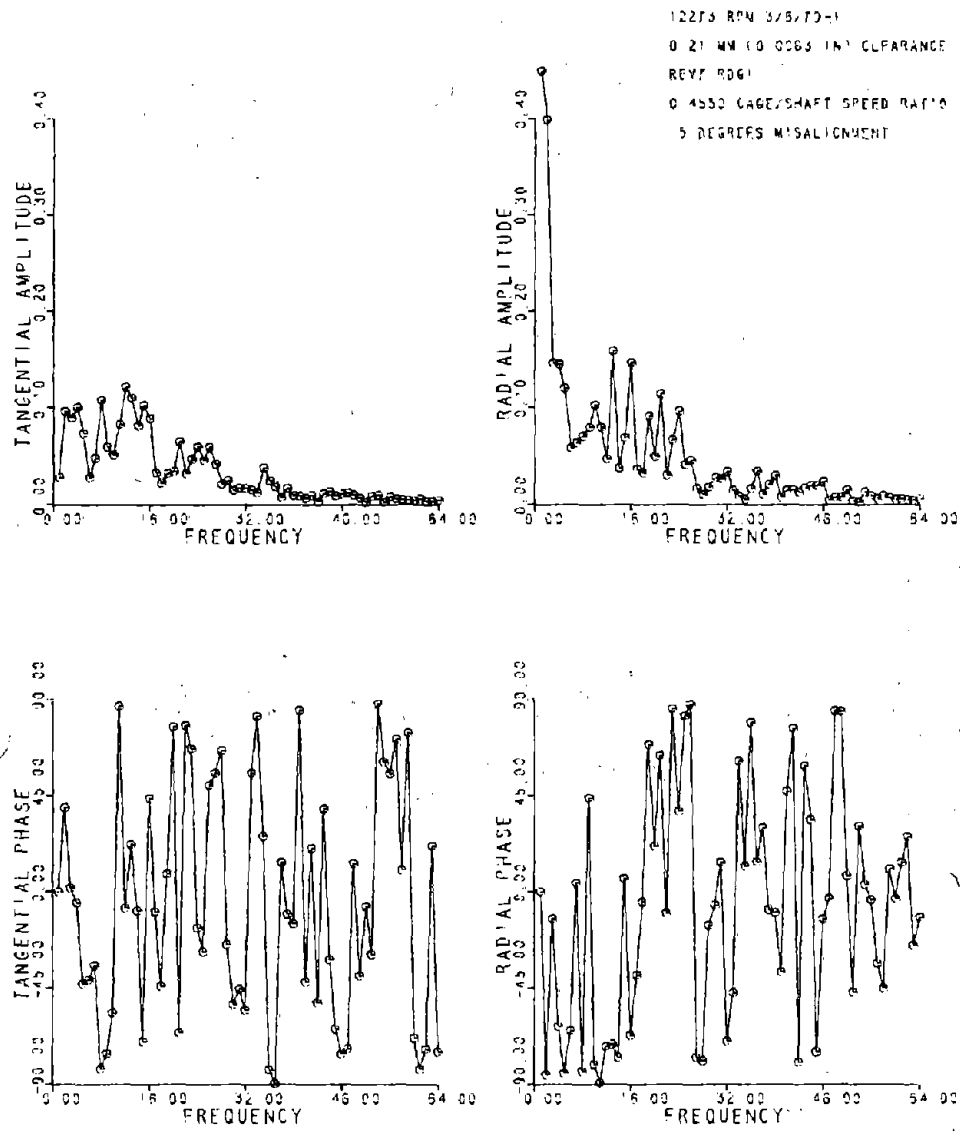


Figure 10c-6F Fast Fourier Transform of Data in Figure 10c-6

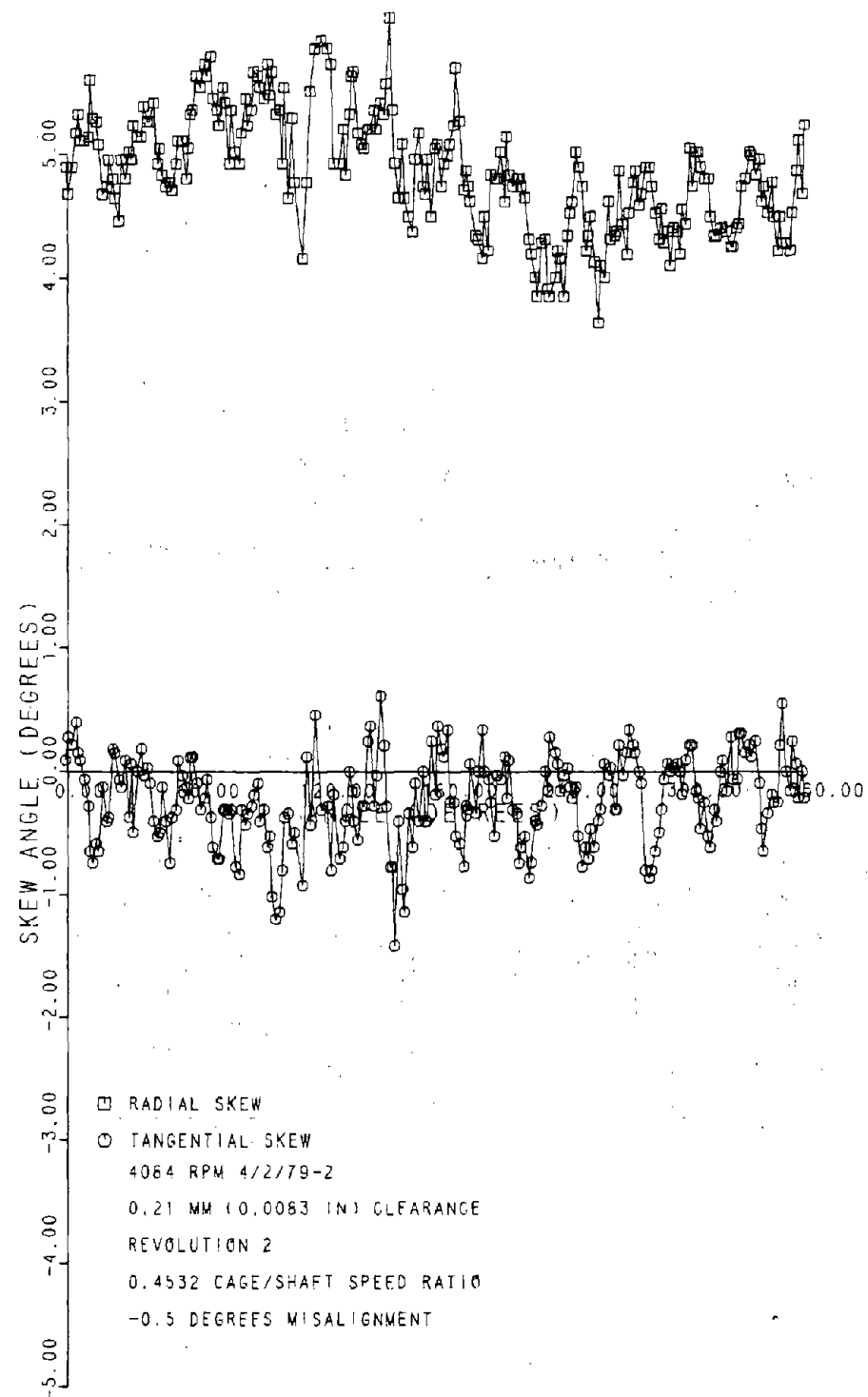


Figure 11a Roller Skew, 0.21 mm Clearance
Bearing, -0.50° Misalignment

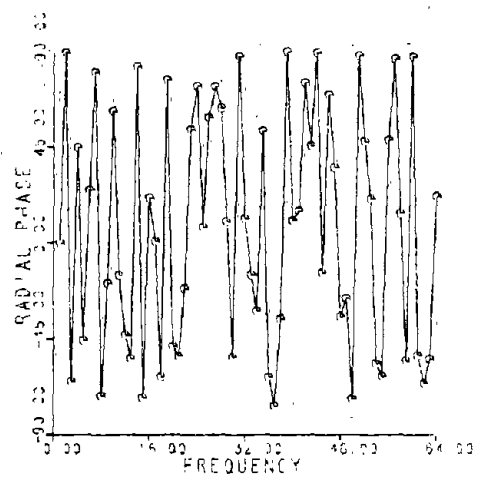
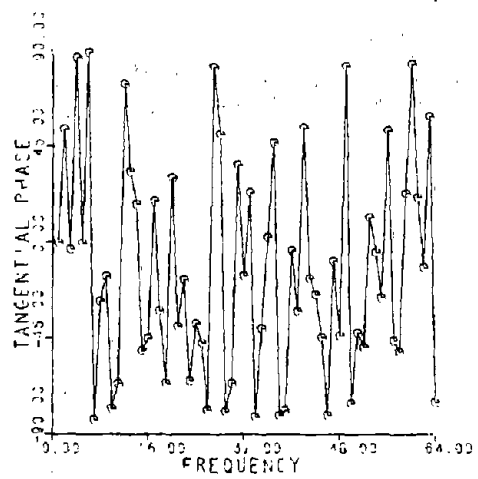
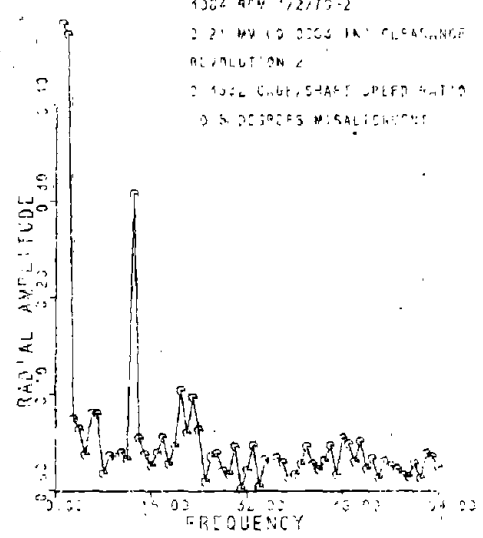
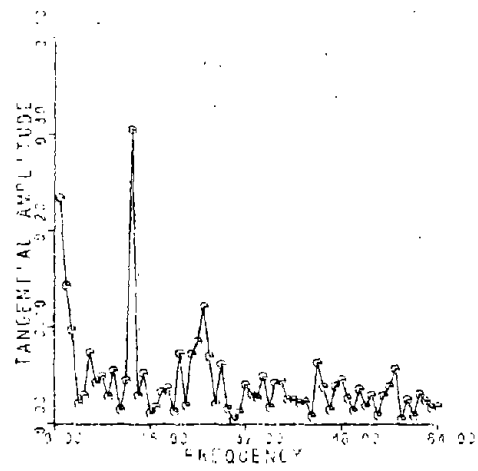


Figure 11aF Fast Fourier Transform of Data in Figure 11a

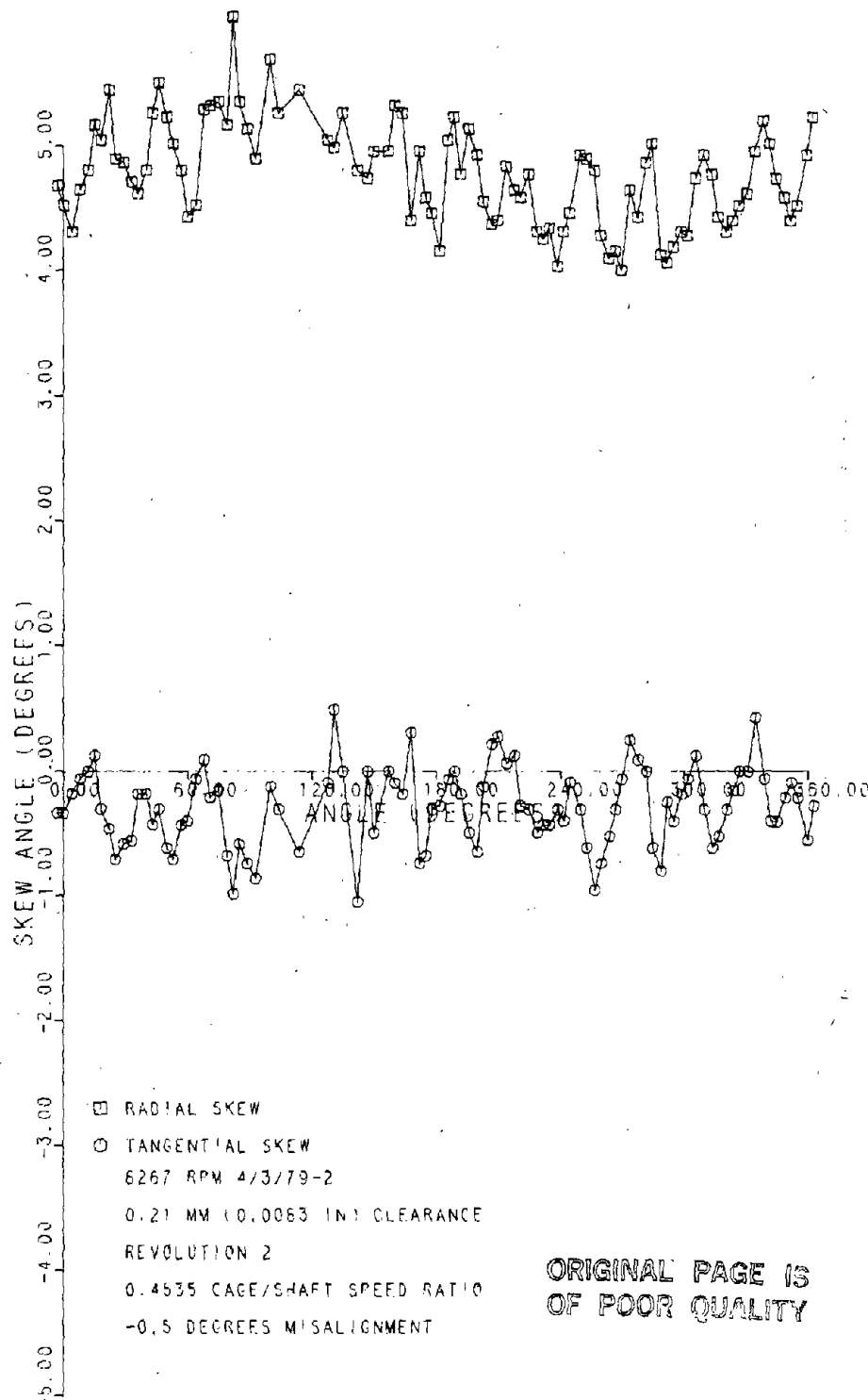


Figure 11b-1 Roller Skew, 0.21 mm Clearance
Bearing, -0.50° Misalignment

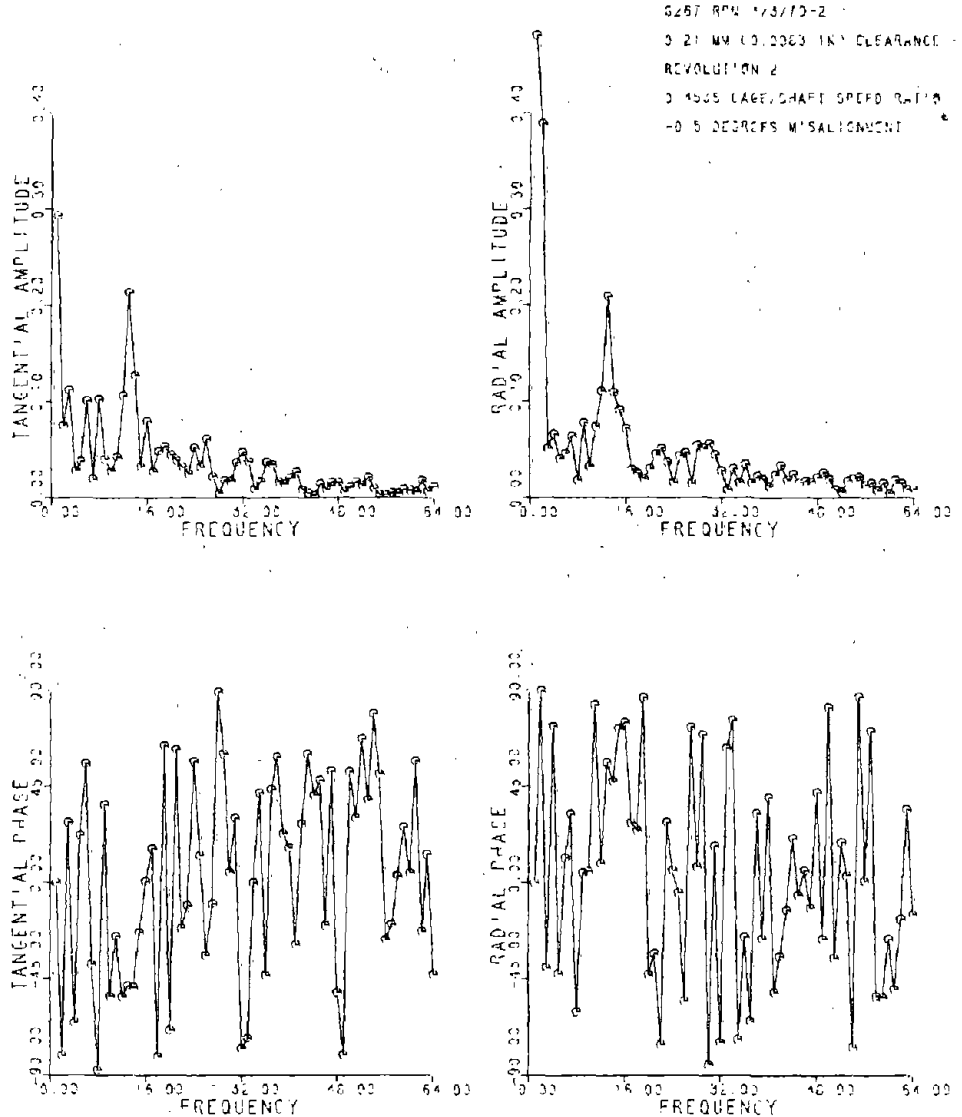


Figure 11b-1F Fast Fourier Transform of Data in Figure 11b-1

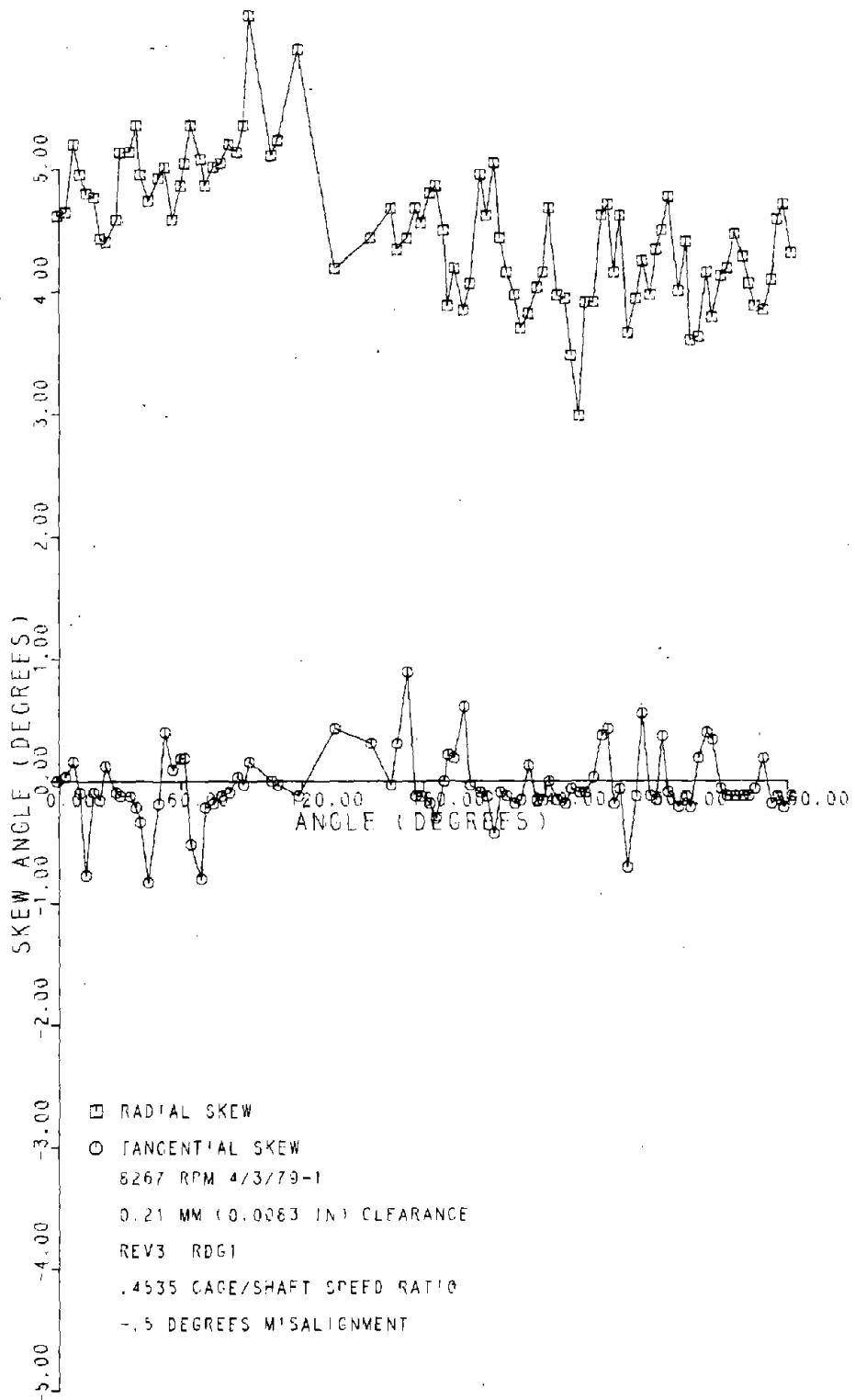


Figure 11b-2 Roller Skew, 0.21 mm Clearance
Bearing, -0.50° Misalignment

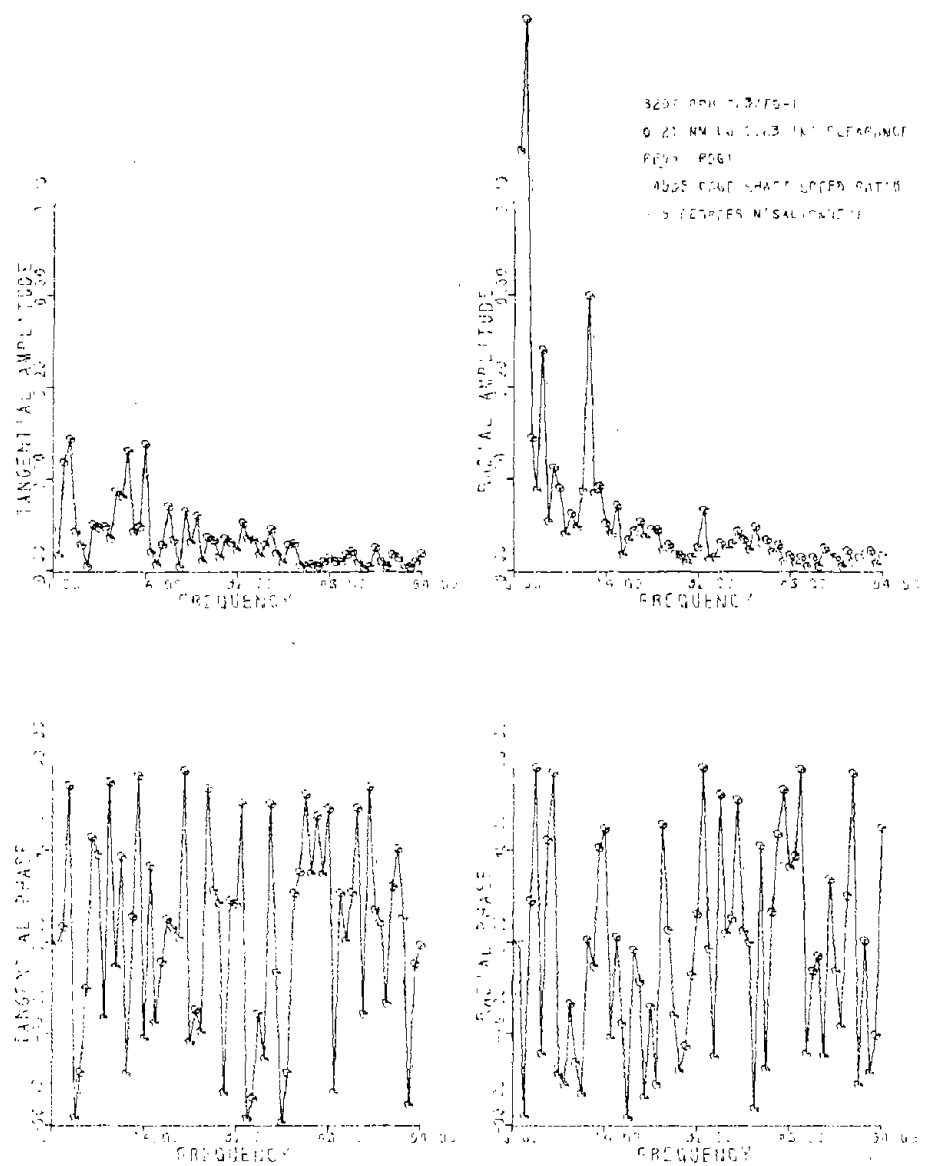


Figure 11b-2F Fast Fourier Transform of Data in Figure 11b-1

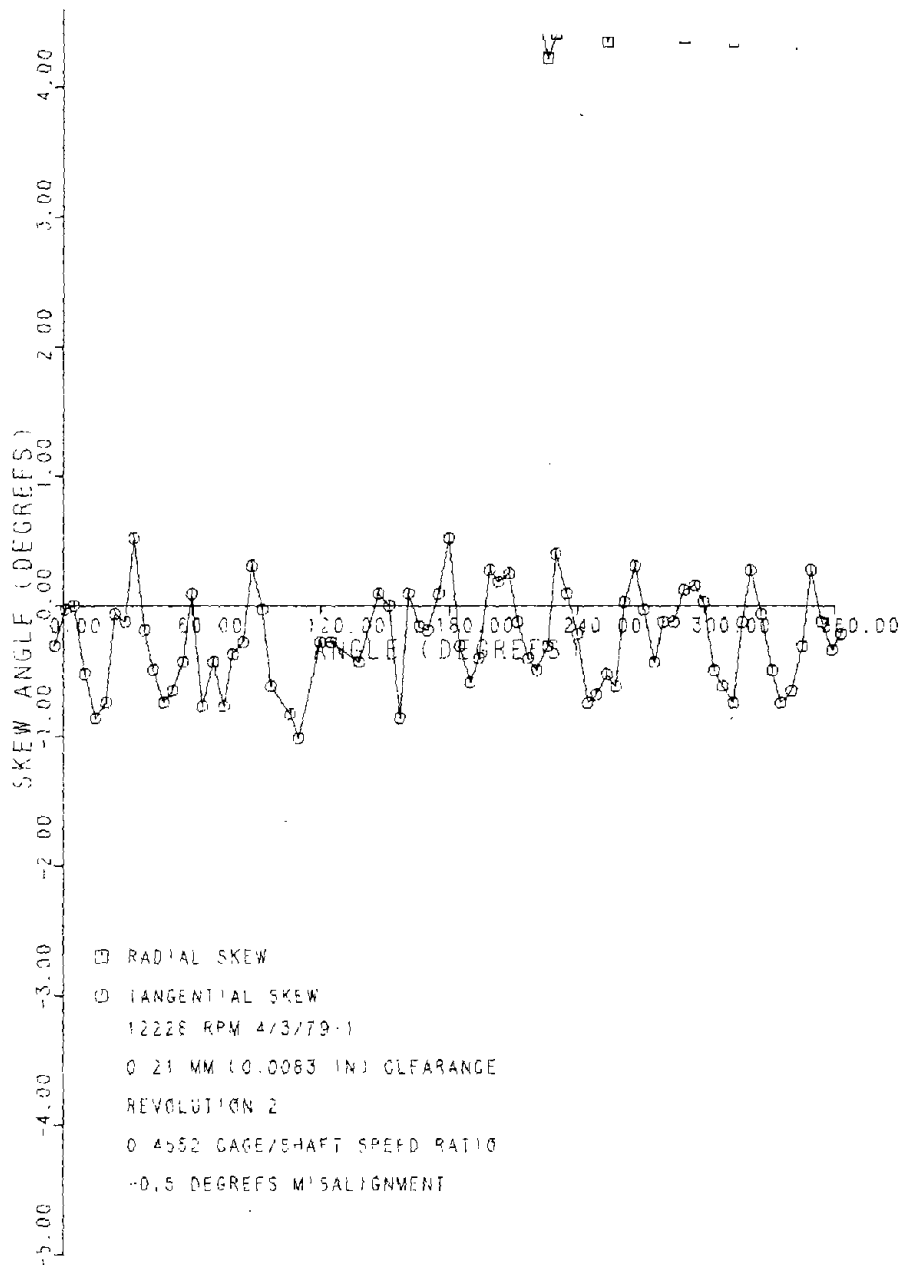


Figure 11c-1 Roller Skew, 0.21 mm Clearance
Bearing, -0.50° Misalignment

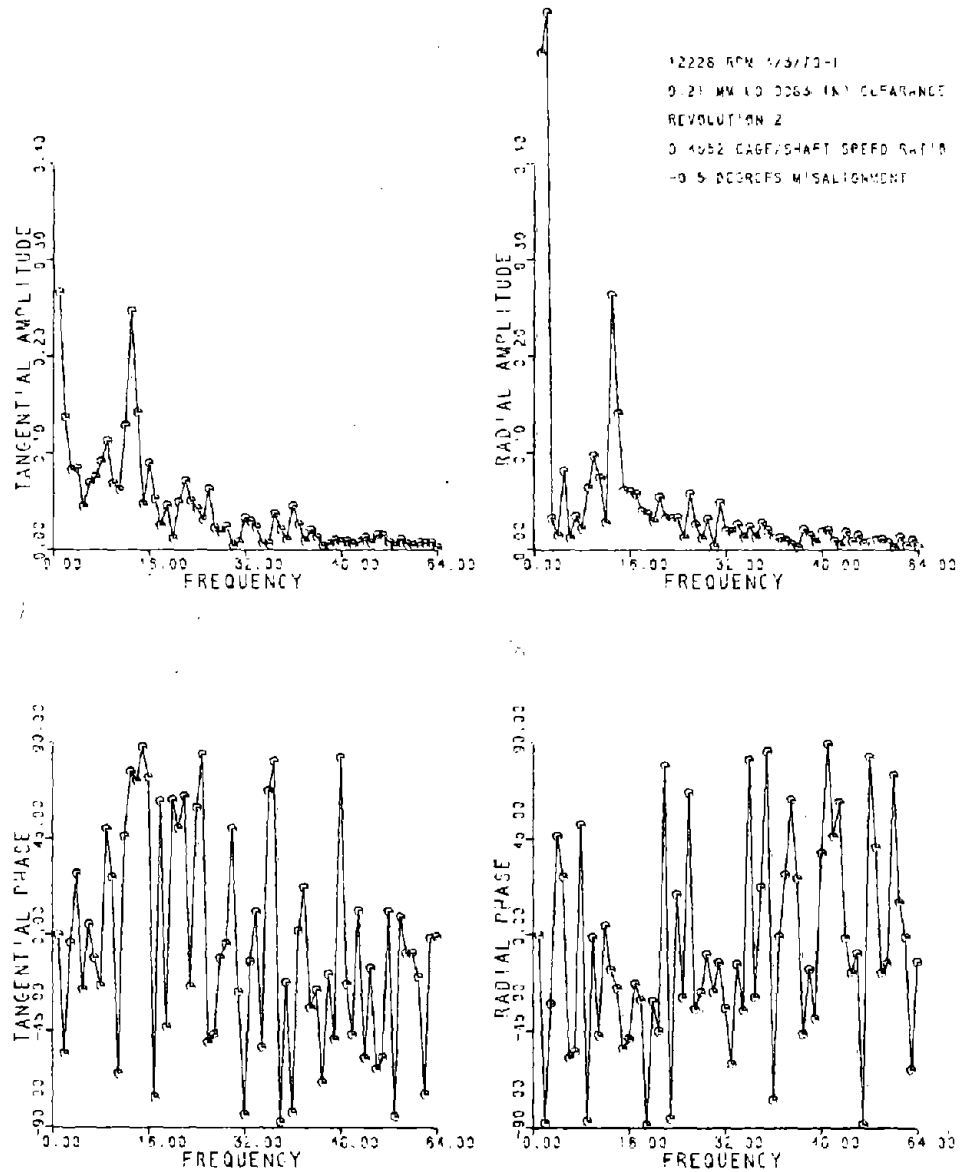


Figure 11c-1F Fast Fourier Transform of Data in Figure 11c-1

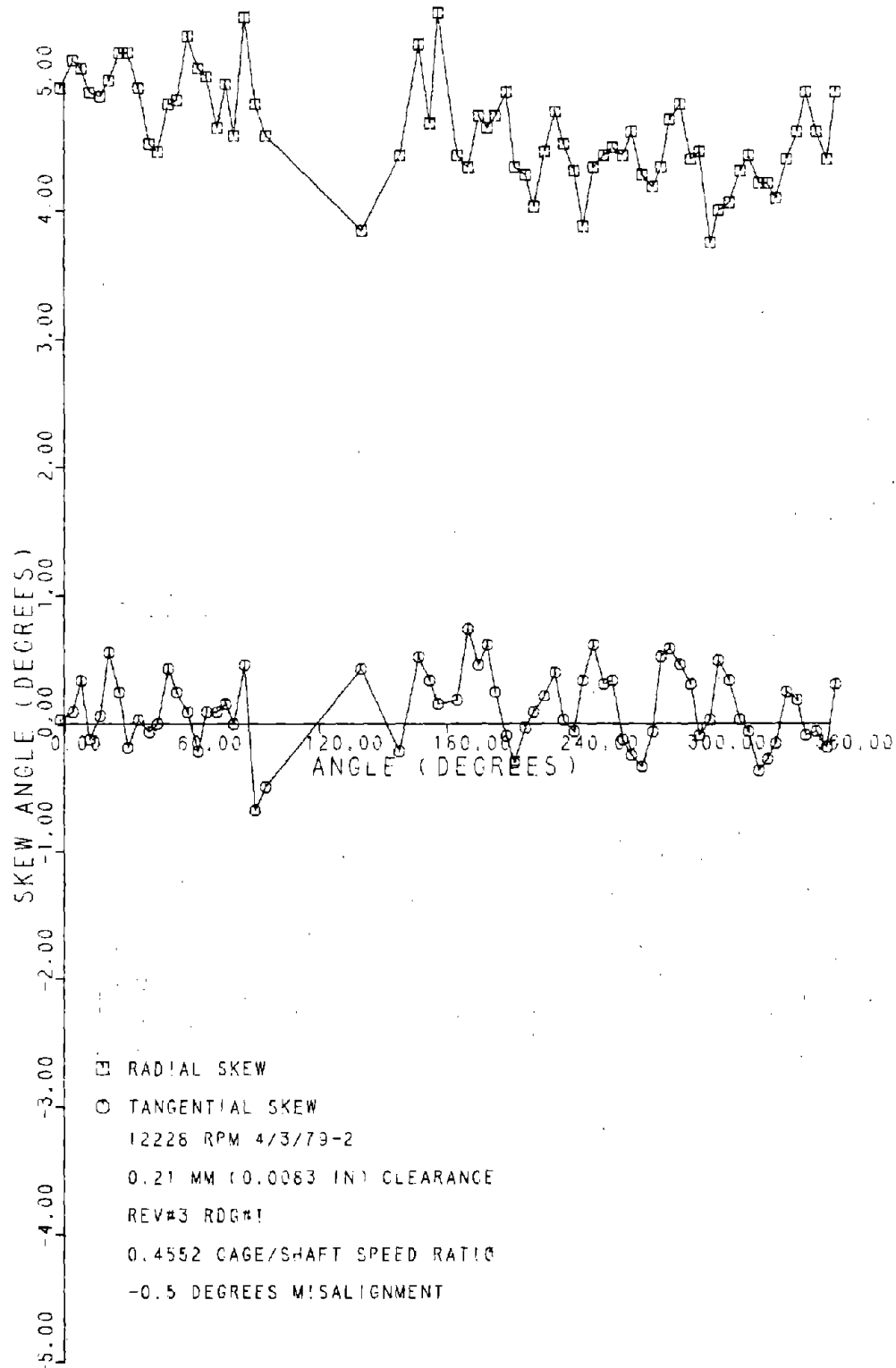


Figure 11c-2 Roller Skew, 0.21 mm Clearance Bearing, -0.50° Misalignment

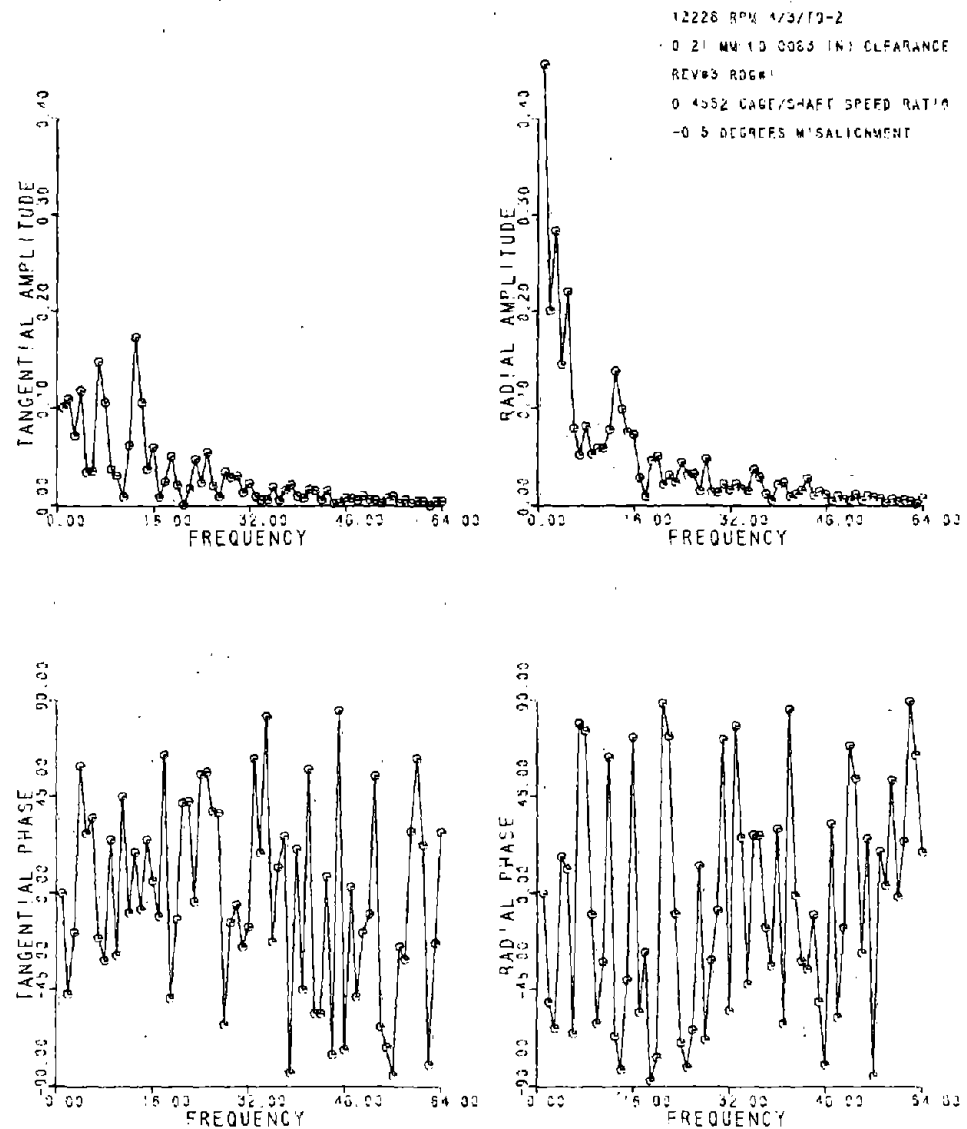


Figure 11c-2F Fast Fourier Transform of Data in Figure 11c-2

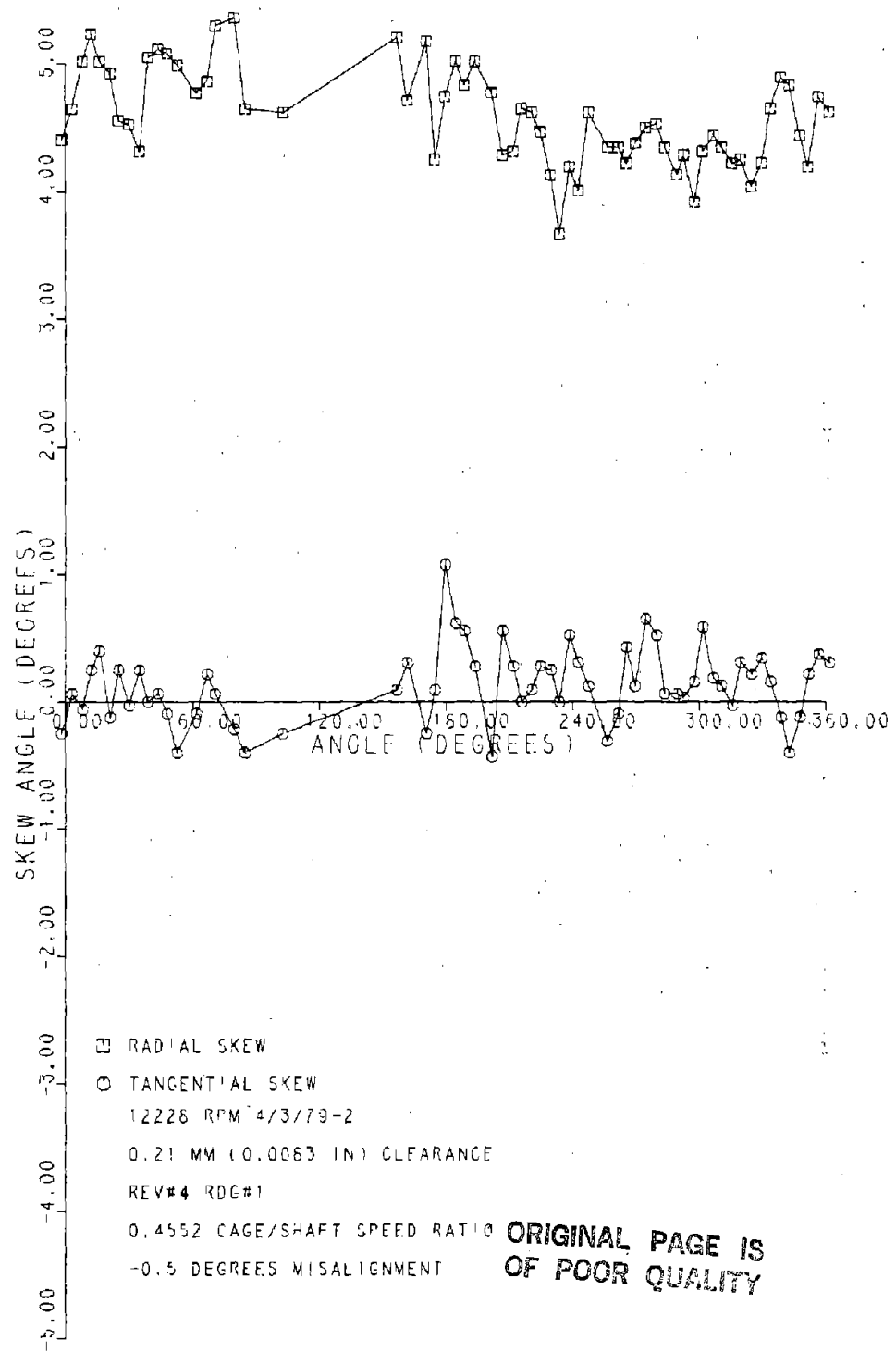


Figure 11c-3 Roller Skew, 0.21 mm Clearance
Bearing, -0.50° Misalignment

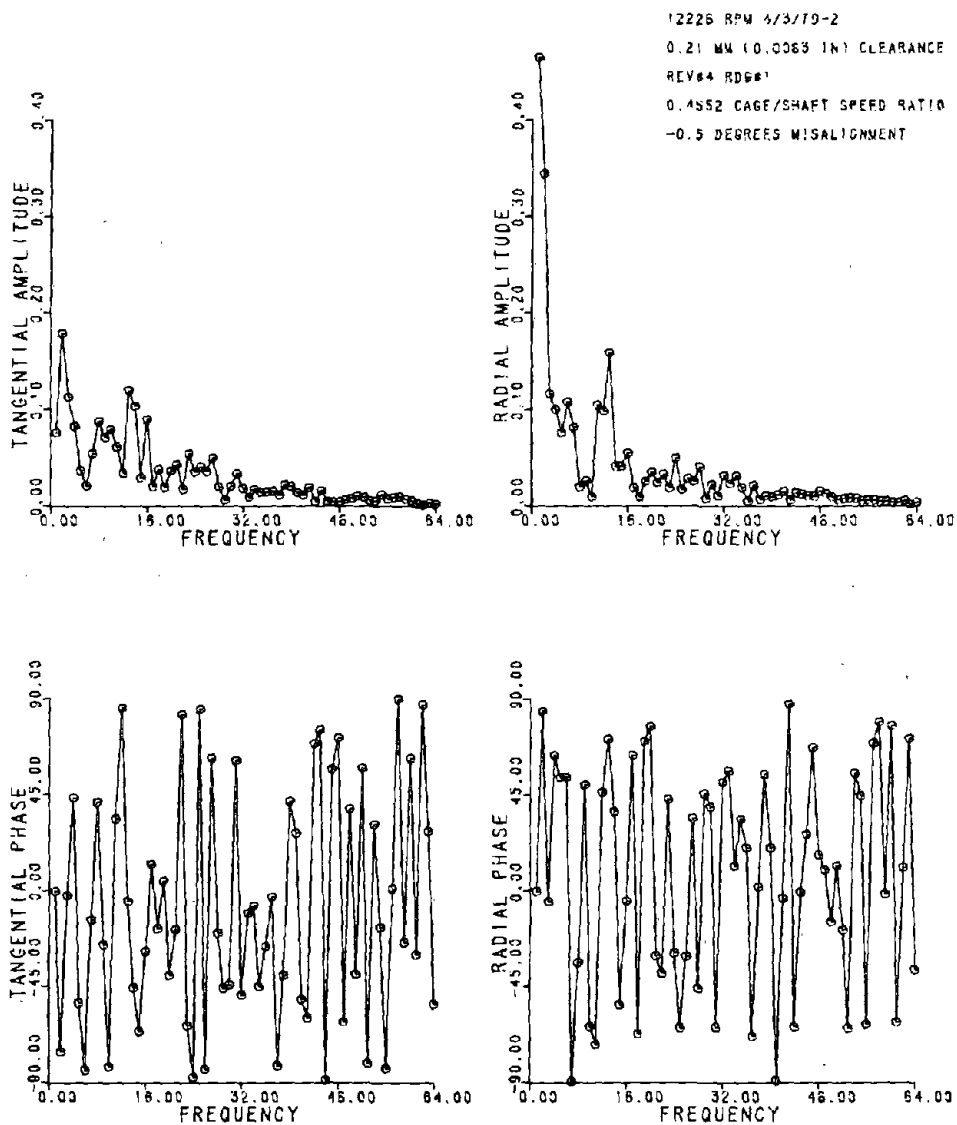


Figure 11c-3F Fast Fourier Transform of Data in Figure 11c-3

Table I

Roller Bearing Specifications

Inner Race

Bore Dia.	mm (in)	118	(4.6457)
Raceway Dia.	mm (in)	131.66	(5.1834)
Flange Dia.	mm (in)	137.47	(5.4122)
Width	mm (in)	26.92	(1.060)
Groove Width	mm (in)	14.59	(.5746)
Flange Angle		0 degree	

Outer Race

Outer Dia.	mm (in)	164.49	(6.4760)
Raceway Dia.	mm (in)	157.08	(6.1842)
Width	mm (in)	23.9	(.942)

Rollers

Diameter	mm (in)	12.65	(.4979)
Length - overall	mm (in)	14.56	(.5733)
effective	mm (in)	13.04	(.5133)
flat	mm (in)	8.40	(.3307)
Crown Radius	mm (in)	622.3	(24.5)
End Radius	mm (in)	inf.	
Number		28	

Cage

Land Dia.	mm (in)	137.95	(5.4312)
Axial Pocket Clearance	mm (in)	.020	(.0008)
Tangential Pocket Clearance	mm (in)	.221	(.0087)
Single Rail Width	mm (in)	4.6	(.18)

Clearance

Serial No. A2284	mm (in)	0.18	(0.0073)
Serial No. A2279	mm (in)	0.21	(0.0083)

Table 2. - Summary of Test Conditions and Data
[PWA 541043]

(a) Serial No. A2284 - 0.18 mm (0.0073 in.) Clearance

Misalignment Degrees	Speed RPM	Case Figure	Exact Speed RPM	Date, Film Set	Cage to Shaft Speed Ratio	Slip %	Rev 2 Rdg 2	
							0.4537	0.6
0	4000	4a	4 055	4/19/79-1	0.4537	0.6	Rev 2	Rdg 2
0	8000	4b	8 229	4/30/79-1	0.4545	0.4	Rev 1	
0	12000	4c	12 161	4/30/79-2	0.4493	1.5	Rdg 3	
0.25	4000	5a	4 135	6/1/79-2	0.4529	0.7	Rev 1	Starts 57°
0.25	8000	5b-1	8 169	5/31/79-1	0.4531	0.7	Rev 1	Starts 12°
		5b-2	8 169	5/31/79-1	0.4531	0.7	Rev 2	Rdg 2
0.25	12000	5c-1	12 346	6/1/79-2	0.4538	0.5	Rev 1	Rdg 1
		5c-2	12 346	6/1/79-1	0.4541	0.5	Rev 2	
0.5	4000	6a	4 020	6/8/79-1			Rev 1	Rdg 1
0.5	8000	6b-1	8 137	6/8/79-2	0.4545	0.4	Rev Starts	193°
		6b-2	8 137	6/8/79-2	0.4545	0.4	Rev Starts	0°, inc.
0.5	12000	6c-1	12 238	6/8/79-3	0.4557	0.1	Rev 1	
		6c-2	12 238	6/8/79-3	0.4557	0.1	Rev 2	Rdg 1
		6c-3	12 238	6/8/79-3	0.4541	0.5	Rev 3	Rdg 1
-0.5	4000	7a-1	4 247	6/11/79-2	0.4541	0.5	Rev 1	
		7a-2	4 247	6/11/79-2	0.4541	0.5	Rev 2	Rdg 1
-0.5	8000	7b-1	8 390	8/6/79-2	0.4545	0.4	Rev 1	Rdg 1
		7b-2	8 390	8/6/79-2	0.4545	0.4	Rev 2	Rdg 1
-0.5	12000	7c-1	12 181	6/11/79-4	0.4547	0.3	Rev 1	Starts 114°
		7c-2	12 181	6/11/79-4	0.4547	0.3	Rev 2	Rdg 1

Table 2. - Summary of Test Conditions and Data
[PWA 541043]

(b) Serial No. A2279 - 0.21 mm (0.0083 in.) Clearance

Misalignment Degrees	Speed RPM	Case RPM	Figure	Exact Speed RPM	Date, Film Set	Cage to Shaft Speed Ratio	Slip %	Rdg 2	
								Rev 2	After misaligned
0	4000	8a	8a	4 000	1/23/79-1	0.4537	0.6	Rev 2	Rdg 2
0	8000	8b	8b	8 136	3/27/79-2	0.4521	0.9	Rev 2	After misaligned
0	12000	8c	12 113	1/23/79-3	0.4524	0.8	Rev 1	Rdg 2	
0.25	4000	9a	4 029	1/29/79-1	0.4540	0.5	Rev 2		
0.25	8000	9b	8 119	1/25/79-2	0.4517	1.0	Rev 1	Rdg 1	
0.25	12000	9c	12 127	1/26/79-1	0.4525	0.8	Rev 2	Rdg 2	
0.5	4000	10a	4 082	2/7/79-1	0.4545	0.4	Rev 2		
0.5	8000	10b-1	8 290	2/7/79-2	0.4544	0.4	Rev 1		
0.5	12000	10b-2	8 290	2/7/79-2	0.4544	0.4	Rev 2	Rdg 1	
0.5	10c-1	12 273	3/6/79-1	0.4550	0.3	Rev 2			
0.5	10c-2	12 273	3/6/79-1	0.4550	0.3	Rev 3			
0.5	10c-3	12 273	3/6/79-1	0.4550	0.3	Rev 4			
0.5	10c-4	12 273	3/6/79-2	0.4549	0.3	Rev 5			
0.5	10c-5	12 273	3/6/79-2	0.4549	0.3	Rev 6			
0.5	10c-6	12 273	3/6/79-2	0.4549	0.3	Rev 7			
-0.5	4000	11a	4 084	4/2/79-2	0.4532	0.7	Rev 2		
-0.5	8000	11b-1	8 267	4/3/79-2	0.4535	0.8	Rev 2		
-0.5	12000	11c-1	12 228	4/3/79-1	0.4552	0.2	Rev 2		
-0.5		11c-2	12 228	4/3/79-1	0.4552	0.2	Rev 3		
-0.5		11c-3	12 228	4/3/79-1	0.4552	0.2	Rev 4		

1. Report No. NASA CR-3381	2. Government Accession No.	3. Recipient's Catalog No	
4. Title and Subtitle ROLLER SKEWING MEASUREMENTS IN CYLINDRICAL ROLLER BEARINGS		5. Report Date January 1981	6. Performing Organization Code
7. Author(s) Lester J. Nypan		8. Performing Organization Report No. None	10. Work Unit No.
9. Performing Organization Name and Address California State University, Northridge Northridge, California 91330		11. Contract or Grant No. NSG-3065	13. Type of Report and Period Covered Contractor Report
12. Sponsoring Agency Name and Address National Aeronautics and Space Administration Washington, D.C. 20546		14. Sponsoring Agency Code	
15. Supplementary Notes Lewis Technical Monitor: Harold H. Coe Final Report			
16. Abstract Measurements of roller skewing in a 118 mm bore roller bearing operating at shaft speeds to 12,000 rpm are reported. High speed motion pictures of a modified roller were taken through a derotation prism to record skewing as the roller moved through loaded and unloaded regions of the bearing. Subsequent frame by frame measurement of the photographic film provided information on roller skewing. Radial and tangential skew amplitudes of 0.4 to 0.5 degrees were observed with 0.5 degree misalignment.			
17. Key Words (Suggested by Author(s)) Roller bearings; Roller skewing; Misalignment; Skew angle; Cylindrical		18. Distribution Statement Unclassified - unlimited Subject Category 37	
19. Security Classif. (of this report) Unclassified	20. Security Classif. (of this page) Unclassified	21. No. of Pages 104	22. Price* A06

NIOSH



PB97-124606

Posthearing Comments to DOL

**POSTHEARING COMMENTS OF THE
NATIONAL INSTITUTE FOR OCCUPATIONAL SAFETY AND HEALTH
ON THE
OCCUPATIONAL SAFETY AND HEALTH ADMINISTRATION
PROPOSED RULE ON INDOOR AIR QUALITY**

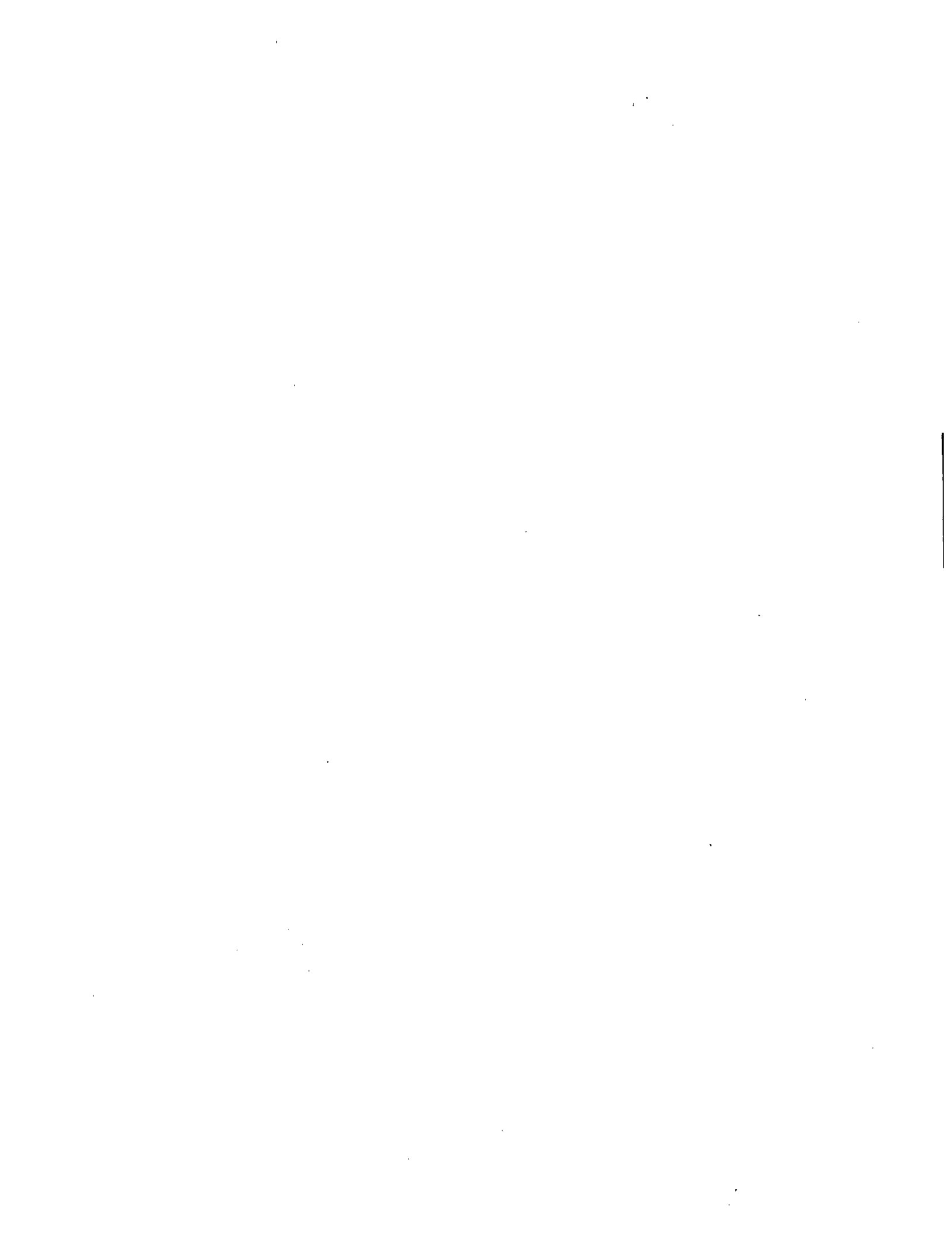
**29 CFR Parts 1910, 1915, 1926, 1928
Docket No. H-122**

**U.S. DEPARTMENT OF HEALTH AND HUMAN SERVICES
Public Health Service
Centers for Disease Control and Prevention
National Institute for Occupational Safety and Health**

9/1/95



REPORT DOCUMENTATION PAGE	1. REPORT NO.	2.	3. Recipient's Accession No.
4. Title and Subtitle NIOSH Testimony on Indoor Air Quality by L. Rosenstock, September 1, 1995		5. Report Date 1995/09/01	6.
7. Author(s) NIOSH		8. Performing Organization Rept. No.	
9. Performing Organization Name and Address NIOSH		10. Project/Task/Work Unit No.	
		11. Contract (C) or Grant(G) No. (C) (G)	
12. Sponsoring Organization Name and Address		13. Type of Report & Period Covered	
		14.	
15. Supplementary Notes			
<p>16. Abstract (Limit: 200 words) In response to requests for information made at the OSHA hearing on indoor environmental quality (IEQ), these posthearing comments were submitted. NIOSH has conducted at least 12 workplace evaluations where a previous IEQ investigation found environmental deficiencies. In one case the recommendations had not been implemented, and in three the follow up reports did not specify whether the recommendations had been followed. In the other eight cases some or all of the recommendations had been implemented. In five of these cases an improvement in environmental conditions was noted and in at least four of these, health complaints had decreased. There were 105 health hazard evaluation (HHE) reports of office buildings that NIOSH has analyzed as a group. Previous NIOSH HHE summaries provide no useful information on any associations between health problems and environmental tobacco smoke. In general, requests for evaluations of nonindustrial environments have generally involved health or comfort problems for which the causes were not understood. Even when workers complained of acute health effects of ETS during the course of a HHE, this information may or may not have been included in the study, and the summaries tallied only the primary problem in each building.</p>			
<p>17. Document Analysis a. Descriptors</p> <p>b. Identifiers/Open-Ended Terms NIOSH-Publication, NIOSH-Author, NIOSH-Testimony, Indoor-air-pollution, Tobacco-smoke, Cigarette-smoking, Ventilation-systems, Air-quality-control, Control-technology, Respiratory-system-disorders, Office-workers, Rosenstock-L</p> <p>c. COSATI Field/Group</p>			
18. Availability Statement		19. Security Class (This Report)	21. No. of Pages 9
		22. Security Class (This Page)	22. Price



LIST OF ABBREVIATIONS

AC	Mechanical ventilation with air-conditioning
CO ₂	Carbon dioxide
CPS II	American Cancer Society Cancer Prevention Study II
ETS	Environmental tobacco smoke
FY	Fiscal year
GEE	Generalized estimating equations
HHE	Health hazard evaluation
HVAC	Heating, ventilating and air-conditioning
IARC	International Agency for Research on Cancer
IEQ	Indoor environmental quality
MECH	Mechanical ventilation without air-conditioning
NAT	Natural ventilation
NIOSH	National Institute for Occupational Safety and Health
OSHA	Occupational Safety and Health Administration

These posthearing comments are submitted by the National Institute for Occupational Safety and Health (NIOSH) in response to requests for information made at the Occupational Safety and Health Administration (OSHA) hearing on indoor air quality on September 28, 1994.

1. **Mr. Rex Tingle from the AFL-CIO asked if NIOSH conducted any followup investigations on the approximately 1500 non-industrial health hazard evaluations (HHEs) conducted for indoor environmental quality (IEQ) complaints, and what percentage of corrections impacted the IEQ problem?**

NIOSH has conducted at least 12 evaluations at workplaces where a previous NIOSH IEQ investigation had found environmental deficiencies (see Table 1). Six were at schools, four were in office buildings, and two were in other facilities. Intervals between the evaluations ranged from 1 month to 4 years. These follow-up evaluations were generally done at the request of the employer or a representative of employees, in some cases because employees still had health or comfort complaints, and in others to assess the effectiveness of the control measures. These 12 cases are therefore not necessarily representative of the outcomes of IEQ HHEs in general.

In one of the cases, the recommendations from the first investigation were not implemented, and environmental deficiencies and complaints persisted. In three others, the follow-up reports did not specify whether the recommendations had been followed. In the remaining eight cases, some or all of the recommendations were implemented. In five of these cases, there was some improvement in environmental conditions, and in at least four of these five, health complaints decreased. In the three cases in which environmental conditions did not improve, health complaints were unchanged in one and were not assessed in the other two.

Table 1
Follow-Up Investigations of NIOSH IEQ HHEs

HHE #	Company	Type of Facility	Interval Between Evaluations	Recommendations Followed	Improvement in Environment	Decrease in Health Complaints
89-183-2101	Andrew Jackson Jr. High School	School	1 year	Yes	Yes	Yes
93-011-2309 94-0129-2397	Tri-County North Schools	School	1 year	Yes	Yes	Yes
92-362-2385 94-338	Kingwood Elementary School	School	1 year	Yes	No	No
89-046 89-117	Patton Elementary School	School	1 year	Unknown	No	No
87-323 90-202-2116	Shamokin Area Elementary Center	School	1 month	Unknown	Partial	Yes
91-143-2136 92-107-2227	Western Primary School	School	3 years	Yes	Partial	Yes
80-122-1117 86-045-1681	101 Marietta Tower	Government Offices	3 years	No	No	No
91-263 92-247	Department of Labor & Human Resources	Government Offices	1 year	Yes	No	Unknown
84-370 89-014	Internal Revenue Service	Government Offices	4 years	Yes	Partial	Yes
88-130 90-059	Henley Chemicals	Commercial Offices	2 years	Unknown	Yes	No
84-531 86-459	Norristown State Hospital	Office Area in Hospital	1½ years	Yes	No	Unknown
86-333 89-209	Marshall University	Laboratory Building	3 years	Yes	Yes	Unknown

Following the completion of the IEQ HHEs that resulted from the CBS newscast, NIOSH conducted a questionnaire survey of the HHE requesters to assess the usefulness of on-site IEQ evaluations. Fifty percent of respondents at visited sites thought that IEQ at their workplace had improved, compared to 22% of respondents at non-visited sites, where NIOSH responded to the HHE request by sending a copy of the *EPA/NIOSH Building Air Quality Guide*.

2. **Mr. Rex Tingle from the AFL-CIO asked if NIOSH was planning on submitting the HHE reports from the 104 office buildings investigated?**

There are 105 HHE reports of office buildings that NIOSH has analyzed as a group. These are a subset of the 160 HHEs conducted following the CBS newscast. The reports are listed in Attachment 1 and are being submitted to the OSHA docket as part of Attachment 2. See comment 7. below.

3. **Mr. Grossman requested that NIOSH submit the "New Zealand" meta-analysis report.**

The report [Kawachi MB et al. (1989), Deaths from lung cancer and ischaemic heart disease due to passive smoking in New Zealand, NZ Med J 102:337-340] is included as Attachment 3.

4. **Mr. Sirridge asked if the Phillip Morris statement that "2% of the IEQ complaints investigated by NIOSH were related to cigarette smoking" was a correct description of the findings in the NIOSH report, *Indoor Air Quality - The NIOSH Experience*.**

Previous NIOSH HHE summaries [Melius 1984; Seitz 1990] provide no useful information on any associations between health problems and environmental tobacco smoke. Perhaps most important, these summaries do not assess relationships between workplace exposures to ETS and either cancer or heart disease, the health effects relevant to the proposed OSHA rule eliminating ETS exposure in the workplace. Nor do they provide useful information about acute health effects of ETS. There are three major reasons for this.

First, requests to NIOSH for HHEs in non-industrial environments have generally involved health or comfort problems for which the causes were not understood. When ETS exposure was perceived as the cause, workers may have thought (correctly) that NIOSH would have little to offer. Indeed, even when someone would contact NIOSH about ETS in the workplace, NIOSH personnel would generally not have encouraged the caller to make a formal HHE request if that were the sole complaint. Among the 283 HHEs included in the first summary [Melius 1984], 6 (2%) of the requests mentioned ETS as an exposure of concern. Even though, at that time, most HHE requests resulted in a site visit, two of the six requests to evaluate ETS were closed without a site visit. Among the 2247 HHEs closed since that time, 139 (6.2%) of the requests mentioned ETS. Therefore,

during the period covered by the first summary, the number of requests to evaluate ETS exposure likely under-represented, by at least a third, the actual occurrence of this problem. (The proportion of IEQ HHE requests involving complaints of ETS exposure had increased by the time of the second summary [Seitz 1990], but since that report grouped ETS with other air contaminants, specific findings for ETS comparable to those in the first summary are not available.)

Second, even when workers complained of acute health effects from ETS during the course of a HHE, this information may or may not have been recorded by investigators, as these earlier investigations were not standardized and the investigator may not have considered such complaints as noteworthy. At the time most of the HHEs included in the summaries were done, the health implications of ETS exposure were not fully appreciated, the expectation of a smoke-free workplace was less common, and the need for more stringent control of worker exposure to ETS was less well recognized.

Third, even if ETS complaints were recorded by the NIOSH investigator, the summaries tallied only the primary problem (as defined by the HHE investigators or authors of the summaries) in each building. Therefore, inadequate ventilation, poor thermal comfort, or other identifiable exposures were more likely to have been considered the "primary" IAQ problem, even if ETS were also present. This hierarchical single-cause attribution scheme precluded the counting of "secondary" problems.

Prior to 1981, ASHRAE recommended a minimum outside air supply rate of 15 cfm per person (with no consideration of smoking in the building). In 1981, ASHRAE recommended 20 cfm per person for areas where smoking was allowed and 5 cfm per person for non-smoking areas. (The latter was discontinued in 1989 and the 20-cfm guideline applied to all areas except smoking lounges, which requires 60 cfm per person.) Thus, during the 1980's, when most of the NIOSH HHEs summarized by Melius [1994] and Seitz [1990] were conducted, many buildings had ventilation systems designed (before 1981) to meet the 15-cfm guideline but not the 20-cfm guideline. So when NIOSH investigators found a worksite that allowed smoking but had less than 20 cfm per person outside air, the likely conclusion (at the time) was that inadequate ventilation was the problem, not the smoking that invoked the need for the higher ventilation rate. If no workers "complained" of ETS, and maybe even if they did, smoking was still considered by many (including NIOSH investigators) to be a "normal" office activity and therefore not an IAQ "problem."

In summary, it would be incorrect and very misleading to state that "tobacco smoke was a source of claimed discomfort in only two percent of all buildings investigated" by NIOSH ("OSHA's Proposed Rule on Indoor Air Quality Not Based on Best Available Evidence," statement released by John C. Lenzi, Phillip Morris U.S.A., September, 1994]. This is because buildings in which ETS was considered by affected workers to be the only IAQ problem were less likely to have a HHE in the first place, and because the many workplaces with inadequate ventilation would likely have had this classified as the primary problem, even if ETS were the most prominent air contaminant.

The two percent figure cited above is not, and was not intended to be, an accurate index of the health effects or discomfort related to ETS. This is clearly shown by questionnaire data from 105 recent IEQ HHEs; 51% of the survey participants reported that they were "sensitive" to tobacco smoke. For all these reasons, then, the previous summaries of NIOSH IEQ HHEs provide no useful information about the acute or chronic health effects due to ETS exposure in the workplace and are therefore not relevant to the ETS part of the proposed rule.

5. **Mr. Rupp asked how NIOSH reconciles the statement regarding the International Agency for Research on Cancer (IARC) on page 18 of the NIOSH Current Intelligence Bulletin #54: *Environmental Tobacco Smoke in the Workplace - Lung Cancer and Other Health Effects*, with IARC Volume 38, *Tobacco Smoking*?**

NIOSH states on page 18 of *Current Intelligence Bulletin (CIB) #54: Environmental Tobacco Smoke in the Workplace - Lung Cancer and Other Health Effects* (June 1991):

"The International Agency for Research on cancer [IARC 1986] stated that epidemiologic studies have demonstrated an increased risk of lung cancer for nonsmoking spouses of smokers."

This statement is based on the Summary in IARC Volume 38, *Tobacco Smoking* (page 308) in which IARC states: "Several epidemiological studies have reported an increased risk of lung cancer in nonsmoking spouses of smokers, although some others have not." This is followed by the statement on page 314:

"The observations on nonsmokers that have been made so far are compatible with either an increased risk from 'passive' smoking or an absence of risk."

and the conclusion on page 314:

"Knowledge of the nature of sidestream and mainstream smoke, of the materials absorbed during 'passive' smoking, and of the quantitative relationships between dose and effect that are commonly observed from exposure to carcinogens, however, lead to the conclusion that passive smoking gives rise to some risk of cancer."

The NIOSH statement on page 18 of the CIB is consistent with the conclusion of IARC on page 314.

6. Mr. Rupp inquired about the basis for concluding that the Brownson [1992] study is appropriately categorized as having positive findings?

The Brownson et al. study [Am J Pub Hlth 82(11):1525-1530, 1992] found an elevated risk of lung cancer for women who have never smoked and have been exposed for >40 pack-years as a result of smoking among all household members (OR=1.3; 95% CI 1.0, 1.8) or spouses only (OR=1.3; 95% CI 1.0, 1.7). Consistent relative risks were found when the time-weighted product of pack-years and average hours exposed per day was calculated. The study concluded that exposure to high levels of environmental tobacco smoke in adulthood increases the risk of lung cancer in nonsmokers by approximately 30%.

7. Mr. Weinberg asked if NIOSH was intending to submit to the docket the 160 completed HHEs conducted following the CBS newscast?

The 160 HHEs are submitted as Attachment 2.

Submission of 4 reports

NIOSH has enclosed four reports (Attachment 4) relevant to indoor air quality. The following are abstracts of the reports:

- NIOSH has been conducting non-industrial indoor environmental HHEs since 1971. In fiscal year 1992 (FY'92), the percentage of this type of evaluation request reached 44% of the total received (181). Due to a large number of indoor environmental requests in FY'93 (814), NIOSH conducted a project that resulted in the accumulation

of a large amount of building and environmental data. Evaluations were conducted in 105 office buildings and an indoor environmental database was created. The data and reported results from these evaluations showed that the predominant building deficiencies found were those related to heating, ventilating and air-conditioning (HVAC) design, operation, and maintenance, and overall facility maintenance [Crandall 1995].

- NIOSH evaluated the prevalence of symptoms in 80 IEQ evaluations conducted in office buildings in 1993-1994 [Malkin 1995]. Using a standardized, self-administered questionnaire, symptom prevalences of 18 symptoms and 4 subsequently defined symptoms' groups were calculated using three different definitions: (1) on the day of the evaluation, (2) at least once a week during the preceding 4 weeks, and (3) at least once a week during the preceding 4 weeks and having the symptom improving when the employee left the workplace. Prevalences of the most commonly reported symptoms, using the last definition, were: tired or strained eyes (33%); dry itching or irritated eyes (30%); unusual tiredness, fatigue or drowsiness (26%); headache (25%); tension, irritability or nervousness (23%); and stuffy or runny nose, or sinus congestion (22%). All 18 symptoms were more likely to be reported by females, and 40% of female respondents reported experiencing at least one upper respiratory symptom (sore or dry throat, stuffy/runny nose or sinus congestion, or sneezing) at least once a week that improved when they left work.
- The relationship between environmental factors, personal and questionnaire variables, and symptom prevalence in 80 office buildings included in the National Institute for Occupational Safety and Health (NIOSH) Health Hazard Evaluation (HHE) program was investigated [NIOSH 1995]. Environmental data including information about the building's heating, ventilation, and cooling (HVAC) system and work areas; CO₂, temperature, and relative humidity readings; and symptom and workplace data, were collected in each building using a standardized checklist and symptom questionnaire. Both environmental and health data were available for the 80 office buildings, from which a total of 2,435 employee health questionnaires were available. To assess how severely employees were affected by symptoms, symptom groups were defined corresponding to organ systems involved. Two symptom groups were used in this analysis: multiple lower respiratory symptom group and multiple atopic symptom group. Diagnosis of asthma after coming to work in the office building was also analyzed.

The relationship between health outcome and environmental and personal variables was assessed by logistic regression, generalized estimating equations (G.E.E), and relative risk regression. All models were adjusted for sex and age. Results from the logistic, G.E.E., and relative risk models were generally very similar. For

environmental variables, relative risks for multiple lower respiratory symptoms varied between .4 (for the presence of fabric wall covering) to 3.1 for debris inside the HVAC air intake. Relative risks varied between .3 (for outdoor air intake within 25 feet of a cooling tower) and 2.3 (for presence of suspended ceiling panels) for atopic symptoms, and between .5 (for daily surface dusting) and 2.5 (for renovation including new drywall) for asthma diagnosed after coming to work in the building. High relative risks for all health outcomes were found for variables in the personal and questionnaire categories. Although results from only those environmental or personal variables thought to be most highly associated with health outcomes are presented, the association between multiple environmental variables in the same building indicate that consideration should be given to the entire HVAC system and work environment in the building as well as to single variables.

Changes in odds ratios and relative risks over measured values for indoor CO₂ concentration, relative humidity, and temperature were also determined for three health outcome and a general symptom grouping (Brooks). Relative humidity was not associated with any health outcome, and indoor temperature was only associated with the Brooks symptom group. Odds ratios for multiple lower respiratory symptoms and atopic symptoms approximately doubled over the 5%-95% measured value range when indoor CO₂ concentrations was considered, and when indoor temperature was considered for the Brooks group. Odds ratio for asthma diagnosed after coming to work increased less than 50% over the same range of CO₂ concentrations.

The analysis is useful for determining factors, both in the HVAC system and building environment, which may be strongly associated with development of health outcomes in the office environment.

- European epidemiologic studies have consistently found health symptoms in office workers to be increased in air-conditioned buildings relative to naturally ventilated buildings. Because this had not been studied in the U.S., the California Healthy Building Study was designed to assess the relationship of ventilation system type to office worker symptoms in a set of U.S. buildings selected without regard to worker complaints [Mendell 1995]. This paper presents an updated analysis.

Study buildings were public office buildings in San Francisco Bay Area counties which satisfied certain criteria. Criteria included having one of three ventilation types: natural ventilation (NAT), mechanical ventilation without air-conditioning (MECH), and mechanical ventilation with air-conditioning (AC). Questionnaire data and building information were collected and multiple logistic regression was used to assess relations between ventilation type and work-related symptoms, defined either as specific symptoms or as symptom groups, adjusting for potential confounding by

personal, job, and workplace factors. The 12 buildings studied included 3 NAT, 3 MECH, and 6 AC, none of which allowed smoking in work spaces. A total of 880 completed questionnaires (response rate 85%) were received. Higher adjusted prevalences of most work-related symptoms and symptom groups were associated with both MECH and AC, relative to NAT. The highest adjusted prevalence odds ratios were found for dry or itchy skin [MECH 6.0 (95% confidence interval=1.6-22); AC 6.0 (1.7-21)], lower respiratory symptoms [MECH 2.9 (0.7-11); AC 4.0 (1.1-15)], multiple mucous membrane symptoms [MECH 3.3 (1.2-9.5); AC 3.4 (1.3-9.1)], and multiple lower respiratory symptoms [MECH 2.9 (1.0-8.0); AC 2.8 (1.1-7.6)]. Available evidence suggested that reporting bias was unlikely to explain these findings. This study provides further evidence that work-related symptoms among office workers are increased in association with unidentified factors in some mechanically ventilated or air-conditioned buildings. Research to identify these factors should include assessment of contaminants emitted by ventilation systems.

Submission of Data File

The data set used for the NIOSH [1995] analysis is included in Attachment 5. This data set contains records for 2406 workers in 80 office buildings. A description of all variables in the data set is included in Attachment 6. The development of the data set from observational survey checklists, environmental data, and questionnaire responses is described in NIOSH [1995].

The binary file CBSIEQ.SD2 is formatted for use in SAS V.6.10 and is included with this submission to OSHA. Because of the large size of the SAS file (2435 observations of 477 variables each, requiring approximately 9 megabytes of disk storage), the SAS file is being provided in an archived format using the shareware program PKZIP V.2 (PKWare Technologies, Inc.).

Enclosures and/or attachments that are not included are available free of charge from the NIOSH Docket Office (513/533-8450).

